ผลของระดับการกำจัดหมู่อะซิทิลและน้ำหนักโมเลกุลของไคโทซานและการเตรียมบีดที่มีต่อการควบคุมการปลดปล่อยยา

นางกฤษณา ศิรเลิศมุกุล

วิทยานิพนธ์นี้เป็นส่วนหนึ่งของการศึกษาตามหลักสูตรปริญญาวิทยาศาสตร์ดุษฎีบัณฑิต
สาขาวิชาวัสดุศาสตร์ ภาควิชาวัสดุศาสตร์
คณะวิทยาศาสตร์ จุฬาลงกรณ์มหาวิทยาลัย
ปีการศึกษา 2546

ISBN 974-17-4915-5

EFFECTS OF DEGREE OF DEACETYLATION AND MOLECULAR WEIGHT OF CHITOSAN AND BEAD PREPARATION ON THE CONTROLLED DRUG RELEASE

Mrs.Krisana Siraleartmukul

A Dissertation Submitted in Partial Fulfillment of the Requirements
for the Degree of Doctor of Philosophy in Materials Science
Department of Materials Science
Faculty of Science
Chulalongkorn University
Academic year 2003

ISBN 974-17-4915-5

Thesis Title	EFFECTS OF DEGREE OF DEACETYLATION AND MOLECULAR WEIGHT OF CHITOSAN AND BEAD PREPARATION ON THE CONTROLLED DRUG RELEASE
By	Ms Krisana Siraleartmukul
Field of Study	Materials Science
Thesis Advisor	Associate Professor Werasak Udomkichdecha, Ph.D.
Thesis Co-advisor	Associate Professor Supot Hannongbua, Ph.D.

Accepted by the Faculty of Science, Chulalongkorn University in Partial Fulfillment of the Requirements for the Doctor's Degree

..... Dean of the Faculty of Science
(Professor Piamsak Menasveta, Ph.D.)

THESIS COMMITTEE

..... Chairman
(Associate Professor Saowaroj Chauyjulchit)

..... . Thesis Advisor
(Associate Professor Werasak Udomkichdecha, Ph.D)

..... Thesis Co-advisor
(Associate Professor Supot Hannongbua, Ph.D)

..... Member
(Assistant Professor Mongkol Sukwattanasinitt, Ph.D.)

..... Member
(Assistant Professor Vimolvan Pimpan, Ph.D.)

..... Member
(Narueporn Sutanthavibul, Ph.D.)

..... Member
(Associate Professor Suwalee Chandrakrachang)

กฤษณา ศิรเลิศมุกุล : ผลของระดับการกำจัดหมู่อะซิทิลและน้ำหนักโมเลกุลของไคโทซานและการเตรียมบีดที่มีต่อการควบคุมการปลดปล่อยยา (EFFECTS OF DEGREE OF DEACETYLATION AND MOLECULAR WEIGHT OF CHITOSAN AND BEAD PREPARATION ON THE CONTROLLED DRUG RELEASE) อ.ที่ปรึกษา: รศ.ดร. วีระศักดิ์ อุดมกิจเดชา, อ.ที่ปรึกษาร่วม: รศ.ดร. สุพจน์ หารหนองบัว. 102 หน้า.ISBN974-17-4915-5.

วัตถุประสงค์ของการศึกษานี้เพื่อศึกษาผลของระดับการกำจัดหมู่อะซิทิลและน้ำหนักโมเลกุลของไคโทซานต่อการแสดงพฤติกรรมการปลดปล่อยยาต้นแบบคือไดโคลฟีแนคโซเดียม (ดีเอส) และผลของการเตรียมไคโทซานบีดในรูปแบบต่าง ๆ ได้แก่ บีดขนาด 500 ถึง 1000 ไมครอน ไมโครพาร์ ติเกิ้ล ขนาดเฉลี่ย 37 ไมครอน และมัลติเลเยอร์บีด จากการใช้ไคโทซานบีดที่ระดับการกำจัดหมู่อะซิทิล 70% และ 91% และขนาดน้ำหนักโมเลกุล 150,000, 400,000 และ 600,000 ดาลตัน ในการควบคุมการปลดปล่อยยาดีเอสโดยวิธีรับประทาน ในสารละลายฟอสเฟตบัฟเฟอร์พีเอช 6.8 พบว่าอัตราการปลดปล่อยยาดีเอสจากเมทริกซ์บีดมีค่าลดลงอย่างชัดเจนเมื่อเทียบกับไมโครพาร์ติเคิล และพบว่าการเพิ่มระดับของการกำจัดหมู่อะซิทิลและขนาดโมเลกุล มีผลให้อัตราการปลดปล่อยยามีค่าเพิ่มขึ้นเล็กน้อย โดยเปอร์เซนต์การปลดปล่อยยาดีเอส ในบีด ที่ 75% มีค่าน้อยกว่าไมโครพาร์ติเกิ้ลที่ 85% เล็กน้อย

ในการเตรียมไคโทซาน-อัลจิเนต มัลติเลเยอร์บีดเพื่อศึกษาพฤติกรรมการปลดปล่อยยาดีเอส ได้ลักษณะมัลติเลเยอร์บีดที่มีชั้นเคลือบ 3 ชั้นคือ อัลจิเนต/ไคโทซาน/อัลจิเนต พบการปลดปล่อยลดลงเหลือเพียง 5-39%

จากการศึกษาพฤติกรรมการซอลเวทของน้ำล้อมรอบโมเลกุลไคโทซานมอนอเมอร์ และไคโทซานเตตระเมอร์ โดยวิธีมอนติ คาร์โล และวิธีโมเลกุลาไดนามิกส์ ซิมุเลชัน ในโมเลกุลไคโทซานมอนอเมอร์ให้ผลการศึกษาไม่ต่างกันเมื่อใช้ฟังก์ชันศักย์ แอบ อินิชิโอ ที่พัฒนาขึ้นใหม่และฟอร์สฟิวส์โพเทนเชียล กล่าวคือ พบชั้นซอลเวชั่นแรกปรากฏที่ระยะ 4.6 อังสตอรม ประกอบด้วยน้ำที่ล้อมรอบ 7 โมเลกุล ส่วนโมเลกุลไคโทซานเตตระเมอร์ ผลที่ได้จากการจำลองโมเลกุลตามวิธีโมเลกุลาร์ไดนามิกส์ พบว่า ออกซิเจนอะตอมที่เป็นจุดเชื่อมต่อระหว่างโมเลกุลในสายโซ่มีการซอลเวทของน้ำล้อมรอบอะตอมน้อยมาก เมื่อเทียบกับออกซิเจนอะตอมที่หมู่ไฮดรอกซิล และหมู่เอมีน

ภาควิชา วัสดุศาสตร์ ลายมือชื่อนิสิต .....

สาขาวิชา วัสดุศาสตร์ ลายมือชื่ออาจารย์ที่ปรึกษา.....

ปีการศึกษา 2546 ลายมือชื่ออาจารย์ที่ปรึกษาร่วม .....

4273803023: MAJOR MATERIALS SCIENCE
KEY WORD: CHITIN / CHITOSAN / CONTROLLED RELEASE / MULTILAYER
KRISANA SIRALEARTMUKUL: EFFECTS OF BASIC PROPERTIES OF CHITOSAN AND BEAD PREPARATION ON THE CONTROLLED DRUG RELEASE. THESIS ADVISOR: ASSOC.PROF. WERASAK UDOMKICHDECHA, Ph.D., THESIS CO-ADVISOR: ASSOC.PROF. SUPOT HANNONGBUA, Ph.D. 102 pp. ISBN 974-17-4915-5.

The major objective of this study is to investigate the influence of degree of deacetylation (%DD) and molecular weight (MW) of chitosan on a release behavior of diclofenac sodium (DS) from the chitosan matrix. In addition, an effect of drug delivery vehicle design of chitosan beads with diameter in the range of 500-1000 μm, chitosan microparticles with mean sized diameter 37 μm and chitosan beads coated with multilayers thin film were also taken into consideration.

Beads of chitosan with %DD of 70 and 91 and the MW of 150,000, 400,000 and 600,000 Daltons were prepared. Bead size was not affected by %DD and MW. A phosphate buffer with pH 6.8 was chosen as a media for DS release study. This condition mimics small intestinal fluid found in human digestive system.

The highest DS loading efficiency was 83% and the highest DS released after 8 hr of 75%, take place at MW = 400,000 Daltons. DS releasing rate in 91%DD chitosan bead was slightly higher than that of 70%DD. The DS releasing rate increased slightly with the increase in chitosan molecular weight. Design of drug carrier plays also important role in determining the DS releasing rate. The maximum DS released after 8 hr from the chitosan bead at 75% was slightly lower than that from the chitosan microparticles at 85%. The chitosan bead coated with 3 alternating layers of alginate-chitosan-alginate, reduced the maximum DS released to only 5-39%.

A solvation behavior of chitosan monomer and tetramer units in aqueous solution was studied using computer simulations, Monte Carlo (MC) and Molecular Dynamic (MD) methods. For chitosan monomer, the newly develop *ab initio* fitted and the force field potential yielded almost identical results. The first solvation layer was observed at a distance of 4.6 Å, with the corresponding coordination number of 7 water molecules. For the chitosan tetramer, the MD results, however, indicate that the solvation at the oxygen atom in the hydroxy and amine groups is much higher than that at oxygen atom in the glycosidic linkage.

Department Materials Science Student's signature…….
Field of study Materials Science Advisor's signature……
Academic year 2003 Co-advisor's signature……...

ACKNOWLEDGEMENTS

The author wishes to express her hearty gratitude to her advisor Assoc. Prof. Dr. Werasak Udomkichdecha for his encouragement, valuable guidance and suggestions with patience, good sense of humor and continuous support throughout this work. The author is highly indebted for his valuable time.

She wishes to express her utmost appreciation and gratitude to her co-advisor Assoc. Prof. Dr. Supot Hannongbua for his inspiration and encouragement to achieve the best. The author is highly indebted for the time and suggestions he has shared in helping hers to bring out the best of this work.

The author would like to express his deep gratitude to Assoc. Suwalee Chandrakrachang who always provide me the useful guidance, suggestion, encouragement and understanding and also patiently practiced my technical skill during the study.

Sincere thanks and deep concern to Dr.Tawan Rimsonnean and Mr. Khatcharin Siriwong for their willingness to participate and technical advice in part of molecular modeling and likes to extend her sincere thanks to Dr. Pranee Lertsuttiwong for her valuable guidance and constructive ideas

Gratefully thanks to Assoc. Prof. Saowaroj Chauyjulchit, Assist. Prof. Dr. Mongkol Sukwattanasinitt, Assist. Prof. Dr. Vimolvan Pimpan, and Dr. Narueporn Sutanthavibul for their substantial advice as thesis committee. And the author is very much thankful to all her friends and staff at Metallurgy and Materials Science Research Institute for their friendly help.

The author wishes to dedicate this piece of work to her beloved parents, and her family for their understanding, inspiration and love.

CONTENTS

Pages

Pages

Pages

LIST OF FIGURES

Pages

Pages

Pages

LIST OF TABLES

Pages

LIST OF ABBREVIATIONS

%	percentage
μm	micrometer
Å	aunstrom
cps	centripoises
DD	degree of deaectylation
DDS	drug delivery system
DS	diclofenac sodium
g	gram
GI tract	Gastrointestinal Tract.
h	hour
kDa	kilodalton
HDD	chitosan with 92%DD
HMW	chitosan with 600,000
LDD	chitosan with 70%DD
LMW	chitosan with 150,000
min	minutes
ml	mililiter
MMW	chitosan with 400,000
MW	molecular weight
^{o}C	degree centrigate
pH	power of hydrogen ion or the negative logarithm (base ten)
SD	standard deviation
sec	second
SEM	scanning electron microscopy
EDS	energy-dispersive x-ray spectrometer
w/v	weight/volumn
w/w	weight/weight

CHAPTER 1

INTRODUCTION

1.1 Rationale

In recent years, much attention has been paid to the oral sustained release drug delivery systems. Matrices are considered to be the simplest and cheapest method for production such systems. Of the several possible routes of introducing controlled release medication into the body, the oral administration of single dose medicinal is one of the simplest and safest, since it does not pose the sterility problem and the risk of damage at the site of administration is also minimal. However, an oral controlled release formulation is subjected to frequently changing environments during transit through the gastrointestinal tract as it passes from the strongly acidic to the weakly alkaline medium in the lower part of the small intestine. The variable absorbing surfaces over the length of the GI tract adds further constraint to the design of oral dosage forms (Smith, 1992). The key point with traditional drug administration is that the blood level of the active agent should be remained between a maximum value, which may represent a toxic level, or a level at which undersized side effects might occur and minimum value, below which the drug is not longer effective. In controlled drug delivery systems designed for long-term administration, the drug level in the blood remains constant, between the desired maximum and minimum, for an extended period of time. Figure 1.1 shows the level of drug in blood plasma of consumable drugs with sudden-release and constantly controlled-release styles.

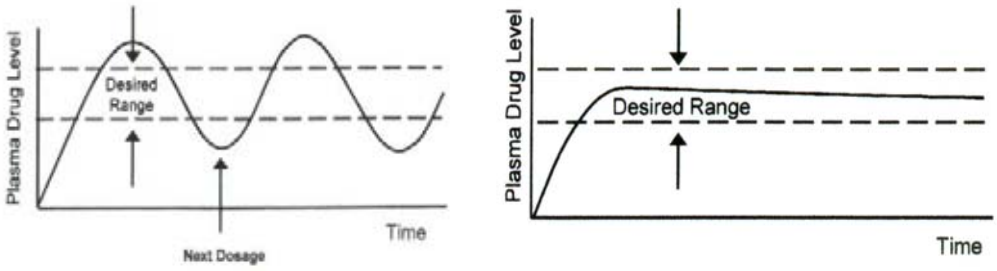

a **b**

Figure 1.1 Drug level in blood plasma: (a) traditional dosing of tablets or injections and (b) controlled drug delivery dose.

The ideal drug delivery should be inert, biocompatible, mechanically strong, comfortable for the patient, capable of achieving high drug loading, simple to administer and easy to fabricate and sterilize. A range of materials has been employed to control the release of drugs and other active substances. One of the major research interests is focused on the encapsulation or incorporation of drug molecules (active substances) in biodegradable and biocompatible polymers. The most frequently used natural polymers recently use algal polysaccharides such as alginate, carageenan, starch and agarose (Murano, 1998). Among these biopolymers, chitosan was found to be an efficient compound to be applied for controlled drug delivery of various drugs. (Dodance, 1998).

1.2 Chitosan

Chitosan is a chitin derivative form obtained by deacetylation reaction of chitin (Figure 1.2) and displays in form of cationic polymer with non-toxic and easily bioabsorbable (Shepherd, 1997). Moreover, chitosan has antacid and antiulcer activities that prevent or weaken drug irritation in stomach (Felt, 1998). Chitosan has been used as matrices device in form of beads and microparticles for

controlled release, chitosan matrix formulations appear to float and gradually swell in acid medium or at low pH range (hydrogel) with gel forming (Kubota, 1993). In earlier research, the incorporation of drugs to the polymer matrices can be done through the various techniques depends upon the physicochemical properties of the drug molecules and the polymers. For chitosan, it has been established that the drug can be entrapped in the matrices beads or microparticles during the formation and absorbed after the formation.

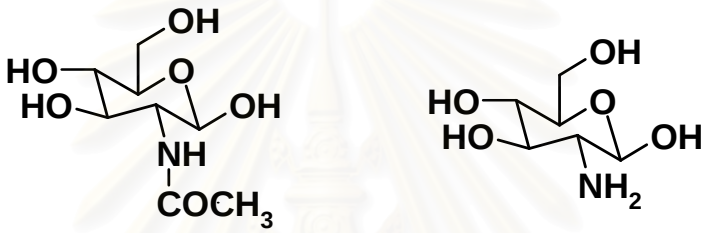

(a) **(b)**

Figure 1.2 Chemical structure of (a) chitin and (b) chitosan

This research focuses on the matrices-beads devices having sodium diclofenac as a model drug and chitosan which is biocompatible as a supported polymer. The samples were prepared in form of beads and microparticles. Effect of physical properties of chitosan such as degree of deacetylation, and molecular weight on drug release were investigated. In addition, releasing rate was also studied when the beads were coated by the chitosan-alginate thin film.

1.3 Objectives

The overall objective of this study is to explore the use of chitosan for controlled drug delivery. Effect of degree of deacetylation and molecular weight of chitosan was varied in the preparation of beads, microparticles and bead-coated. The

method of matrices production, swelling behavior and drug release profile were evaluated.

In addition, computer simulations, Monte Carlo (MC) and Molecular Dynamics (MD) methods, were also performed to investigate solution and orientation of solvent molecule around chitosan.

1.4 Layout of dissertation

After brief introduction of drug delivery system and the role of chitosan and its application in Chapter 1, theoretical background was presented in Chapter 2. Then, the methodology, results and discussion were given in Chapter 3 and 4, respectively. In the last chapter, conclusion was summarized.

CHAPTER 2

LITERATURE REVIEWS

2.1 Chitin and Chitosan

2.1.1 Structure of chitin and chitosan

Chitin, a β-(1-4)-linked 2-acetamido-D-glucopyranan, is the second most abundant biopolymer on earth (Majeti and Kumar, 2000). *N*-deacetylation of chitin with enzyme (Shigehiro, 1999) or alkaline solution (Sandford, 1987) produces chitosan, which is cationic biopolymer. The non-toxic, biodegradable and biocompatible properties of chitin and chitosan provide much potential for many food, pharmaceutical and biotechnology applications (Shepherd, 1997, Majeti, 2000). Enzymatic or acid hydrolysis of chitin or chitosan produced oligosaccharides consisting of a β-(1-4)-linked *N*–acetyl-D-glucosamine (2-acetamido-2-deoxy-D-glucose; GluNac) and glucosamine (2-amino-2-deoxy-D-glucose; GlcN). These *N*-acetyl-chito-oligosaccharides and chito-oligosaccharides have various biological properties (Kurita, 1998, Shigehiro, 1996).

Chitosan is a principle derivative of chitin obtained by deacetylation reaction in concentrated alkaline solution to remove acetyl groups from *N*-acetyl glucosamen sugar, which is a part of chitin, at the degree of deacetylation more than 50%. Chemical structures of chitin and chitosan are very similar to that of cellulose, which is chains of saccharide, however, with nitrogen atoms in the composition. If nitrogen atoms are in form of acetamide, it is called chitin, and if nitrogen atoms are in form of amino, it is called chitosan. Normally, polymer chains of chitin and chitosan contain

both chitin and chitosan as a copolymer as shown in Figure 2.1. The difference between chitin and chitosan lies in the degree of deacetylation, in percents.

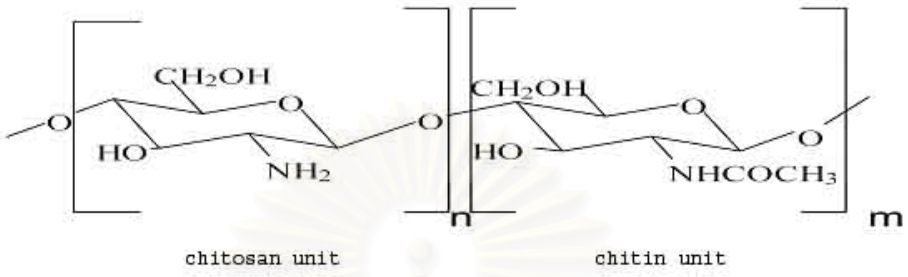

Figure 2.1 A copolymer structure of a chitosan molecule.

Chitin and chitosan show very useful properties in biotechnology in which they are used as biomaterial, due to their biodegradability and biocompatibility. Apart from that, they are also used as chelating agents in which they can selectively bind desirable materials or several metal ion. Chelation has been applied to areas of food preparation, health care, water improvement and pharmaceutics (Illum, 1998). Chitosan can be formed into many shapes, such as bead, membrane and fiber, etc. There are three chemical functional groups of chitosan (Figure 2.2), as referred to its applications: 1) amino group 2) acetamite at position C-2 and 3) hydroxyl at position C-3 (secondary alcohol) and C-6 (primary alcohol).

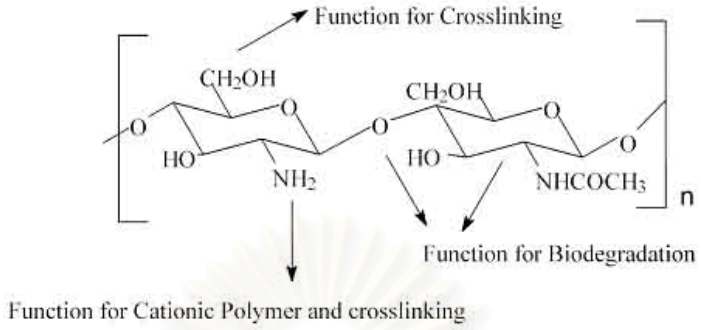

Figure 2.2 Chemical functional groups in chitin and chitosan structures.

2.1.2 Biodegradability and biocompatibility of chitin and chitosan

Many studies have shown that chitin and chitosan are biodegradable and biocompatible polymers, and that they degrade in vivo mainly through their susceptibility to enzymatic hydrolysis mediated by lysozyme, which is ubiquitous in human body; however, this action has been determined to be depend on factors including pH, type of chitin or chitosan, and chitosan preparation method (Marit, 1993) determined that chitosan is most susceptible to hydrolysis by lysozyme at pH 5.2 , and the optimum rang of pH values has been determined to be between pH 5.2 and 8.0 (Shigemasa, et al. 1993).

2.1.3 Application of chitin and chitosan

Chitosan with a large molecular weight, exhibits a positive charge, and demonstrates film forming ability and gelation characteristics. The material has been extensively used in many industies, foremost as a flocculant in the clarification of waste water in Japans (Kumar, 1999). It can also be used as a chelating agent for

harmful metals for detoxification of hazardous waste (Mitani, 1995) and for agricultural purposes such as a fungicide in protection of crops and the coating materials. In addition, chitosan has been exploited in the cosmetic industry and the dental industry (Illum, 1998).

Table 2.1 Applications and functions of chitin and chitosan (Shigehiro, 1996).

Compounds	Functions	Applications
Chitosan	Polyelectrolyte and chelating agent	1. Coagulant flocculating agents and cationic sludge dewatering for polluted wastewater. 2. Recovery of acidic proteins, uranuim, specific metal ions, and radioactive isotopes in waste water or sea. 3. Ion exchanger for chromatography. 4. Food processing and dyeing additives.
Chitin, chitosan and derivatives	Molding or casting	Beads, fibers, nonwoven fabrics, films, gels and sponges.
Chitin and chitosan	Industrial reagents	Oligosaccharides, carboxymethyl chitin, N-acetyl glucosamine etc.
Chitin and chitosan	Viscous property	Thickness for paining etc.
Chitosan	Biocompatability and digestibilty	Biomedical materials (absorbable surgical suture, sustained release of drug.
Chitin and chitosan	Wound healing	Burn and skin lesion dressing materials for human and animals. Wounded tissue-dressing materilas for plants.
Chitosan	Hypochloesterlemic action	Reduce the cholesterol level by binding (Slimming agent)
Chitosan and some other derivatives	Blood anticoagulant, antithrombogenic, and homeostatic activities	Biomedical uses (heparinoids, contact lens etc.)
Chitin and chitosan	Microbial flora improvement	1 Environment ad ecological improvements in the soil and hydrosphere. 2. Improvement of microbial flora in intestines.
Chitin, chitosan and some other derivatives	Enhancement and preservation of the biological self defense function	1. Agricultural materials 2. Health-preserving foods for human, fishes and animals. 3. Cosmetic ingredients for hair and skin cares.

2.1.4 The use of chitosan as pharmaceutical excipient

In recent years, chitosan has been introduced as a material in the nutritional supplement market, especially as a weight loss aid and cholesterol lowering agent. The mechanism behind this apparent effect of chitosan has been suggested to be its effect on lipid transport mechanism in the gut, where in free fatty acids, cholesterol, bile salts and other components form mixed micelles that comprise an essential step in the fat absorption process (Koseva, 1999).

Table 2.2 show the list of some important applications of chitosan as a excipient in pharmaceutical.

Table 2.2 Chitosan as a Pharmaceutical Excipient (IIIum, 1998)

Conventinal formulations
Direct compression tablets
Controlled release matrix tablets
Wet granulation
Gels
Films
Emulsions
Wetting agent
Coating agent
Microspheres and microcapsules
Novel applications
Bioadhesion
Transmucosal drug transport
Vaccine delivery
DNA delivery

Chitosan has been extensively examined in the pharmaceutical industry for its potential in the development of controlled release drug delivery systems. This is due to its unique polymeric cationic character and its gel and film forming properties.

Chitosan gel beads/microspheres and microcapsules

The term “microcapsules” is here loosely defined as spherical particles in the size range of 50 nm to 2 mm containing a core substance. “Microspheres” are, in a strict sense, spherically empty particles (Yao, 1995). However, the terms microcapsules and microspheres are often used synonymously. In addition, some related terms are used as well. For example, “microbeads” and “beads” are used alternatively. “Sphere” and “spherical particles” are also employed for a large size and rigid morphology.

Coacervation techniques are conventionally divided into “aqueous” and “nonaqueous” coacervation systems. Aqueous coacervation systems are themselves subdivided into “simple” and “complex” coacervations. Simple coacervation involves single polymeric materials, such as cellulose acetate and albumin, while complex coacervation is based on two oppositely charged polymers.

Simple coacervation of chitosan in the production of chitosan beads has been studies by several researchers (Timmy, 2002, Murata, 1996, Kubota, 1993). In general, chitosan is dissolved in a diluent acid such as acetic acid or formic acid. Using a compressed air nozzle, this solution is blown into NaOH, NaOH-methanol, or ethanediamine solution to form coacervate drops. The drops are then filtered and washed with hot and cold water successively. The diameters of droplets can be controlled by varying the exclusion rate of the chitosan solution or nozzle diameter. The porosity and the strength of the beads correspond to the concentration of

chitosan-acid solution, the degree of deacetylation of chitosan, and the type and concentration of coacervation agents used.

Miiyazaki et al. (1996) investigated the suitability of dried chitosan beads as vehicles for the sustained release of the poorly soluble drugs such as indomethacin and papaverine hydrocholoride. The drugs were dispersed in the gel beads and showed zero order release; with 40% of the indomethacin released into pH 7.4 buffer at 24 hours and 100% papaverine hydrocholoride into 0.1N HCl in the same time period. Knapczyk (1996) prepared gel beads from 93% and 66% deacetylated chitosans with lactic acid and found that gel beads prepared from the chitosan, with higher degree of deacetylation, were more stable in combination with drugs than those prepared with less deacetylated chitosan.

Suspension crosslinking technique are widely used in the preparation of polysaccharides-based polymer supports for chromatography and microspheres for biomedical application. These polysaccharides include allyldextran, acrystarch, agarose, and cellulose (Felt, 1998). The process involves the formation of a stable droplet of polymer solution (or melt) suspended in an immiscible liquid, the gradual hardening of the droplet by covalent crosslinking. When the polymer solution contains a dissolved or dispersed substance (i.e., the core material) which has a substantially higher affinity for the droplet phase than for the suspension medium, microcapsules incorporating the core substance can be prepared. This technique can be applied to produce chitosan microspheres/microcapsules, a suspension system with or without the use of any stabilizer. The aqueous phase is composed of a chitosan acetic acid solution while the oil phase can utilize soya oil, tubine oil, paraffin oil or mineral oil.

2.2 Controlled drug delivery systems, DDS

2.2.1 General

The means by which a drug is introduced into the body is almost as important as the drug itself. Drug concentration at the site of action must be maintained at a level that provides maximum therapeutic benefit and minimum toxicity. The pharmaceutical developer must also consider how to transport the drug to the appropriate part of the body and, once there, make it available for use (Baldwin, 1998).

As the name implies, a controlled-release drug delivery system serve two functions:

1. Drug delivery involves the absorption and transport of the drug to a particular part of the body. This may be accomplished intravenously, transdermally, orally, by implantable reservoir, etc.
2. Controlled release governs the rate at which the drug is made available to the effect site once it has delivered.

Traditionally, delivery systems have not incorporated means of controlled release. This means that the concentration of most drug peaks and declines rapidly after each dose and will often be above or below the desired therapeutic range.

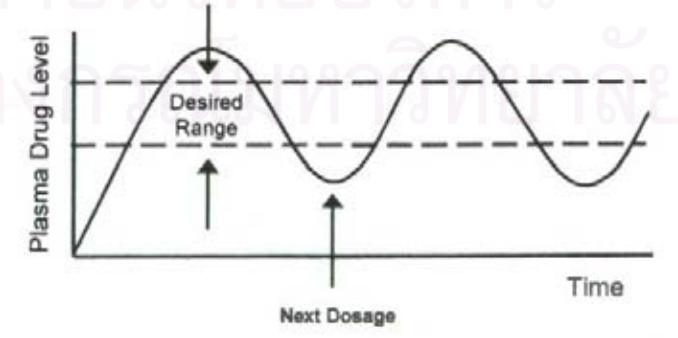

Figure 2.3 Drug levels in the blood with traditional drug dosing.

Sustained release Sustained release is an incremental improvement. It provide prolonged but not uniform release of drug and reduces the need for repeated dosing. Once the maximal level is reached, the amount of drug in the body decrease slowly so it will take longer to drop below the rapeupic range. Sustained release technologies in current use include

i. Complexes
ii. Slowly dissolving coatings
iii. Suspensions
iv. Emulsions
v. Compressed tablets

Release rates are strongly influenced by environmental conditions , release rarely lasts longer than 12 hours; so the benefits are limited.

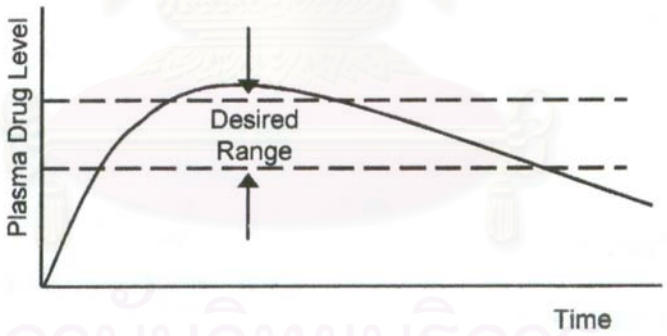

Figure 2.4 Drug levels in the blood with sustained release dosing.

Controlled release This is a sustained advance sustained release. Technologies include

1. Polymers
2. Pumps

Weakly influenced by local environment (fixed release pattern), release can occur over long periods.

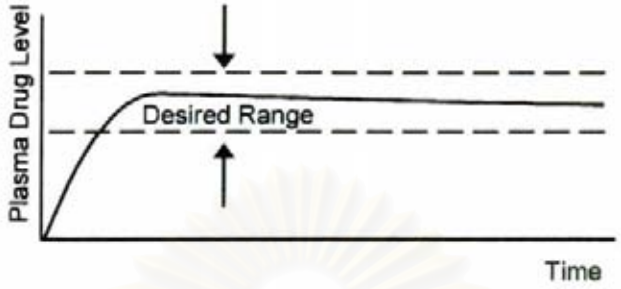

Figure 2.5 Drug levels in the blood with controlled release dosing.

2.2.2 Oral controlled drug delivery

Oral-controlled release drug delivery is a system that provides the continuous delivery of drugs at predictable and reproducible kinetics for a predetermined period throughout the course of gastrointestinal transit (Chien, 1995). The transit time in gastrointestinal tract varies from one person to another and also depends upon the physical properties of the object ingested and the physiological conditions of the alimentary canal (Table 2.3).

Table 2.3 Gastrointestinal tract: physical dimensions and dynamics.

Region	Surface area (m^2)	pH	Transit time	
			Fluid	Solid
Stomach	0.1-0.2	1-1.5	50 min	8 h
Small intestine	100	5.5-7.0	2-6 h	4-9 h
Large intestine	0.5-1	6.5-7.5	2-6 h	3-72 h

2.2.3 Release of drugs from beads/microcapsules

There are three primary mechanisms by which active agents can be released from a delivery system: diffusion, degradation, and swelling followed by diffusion. Any or all of these mechanisms may occur in a give release system. Diffusion occurs when a drug or other active agent passes through the polymer that forms the controlled-release device (Bodmeier, 1989, Gopferich, 1996, Kumar, 2000). The diffusion can occur on a macroscopic scale as through pores in the polymer matrix or on a molecular level, by passing between polymer chains. Examples of diffusion-release systems are shown in Figures 2.8 and 2.9.

In general, to control drug release by using polymer, several factors must be taken into consideration, for examples, types and basic properties of polymer, type of drug and drug controlled-release system. Especially, dosage forms of consumable drugs are ones of the most favorable types, referred to the propagation of drug through the polymer matrix. Drugs are prepared with polymer in form of matrix bead polymer that contains drug confined in bead structure and released by using the propagation of drug through the polymer matrix technique.

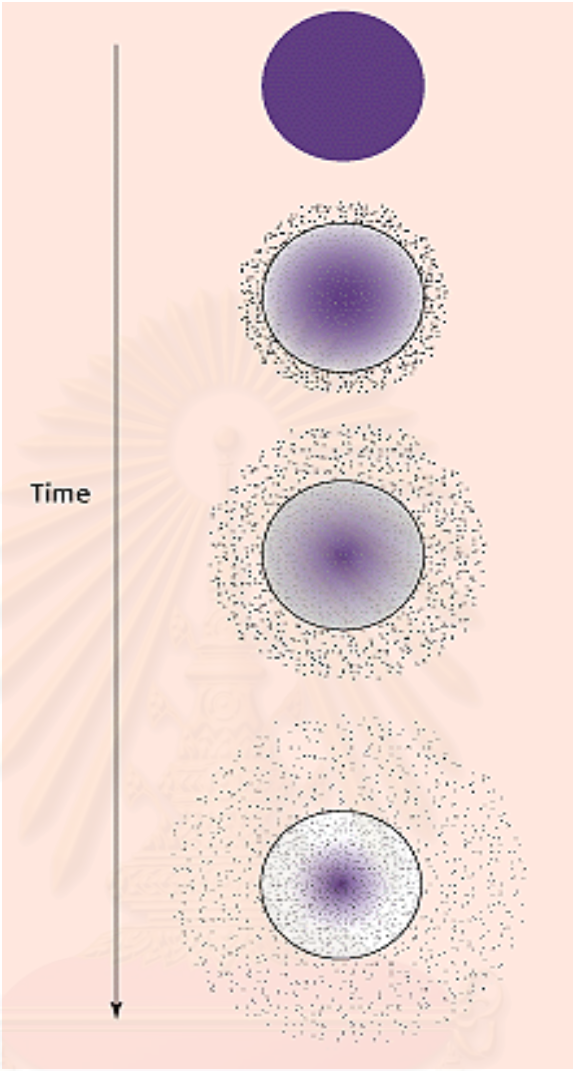

Figure 2.6 Drug delivery from a typical matrix drug delivery system.

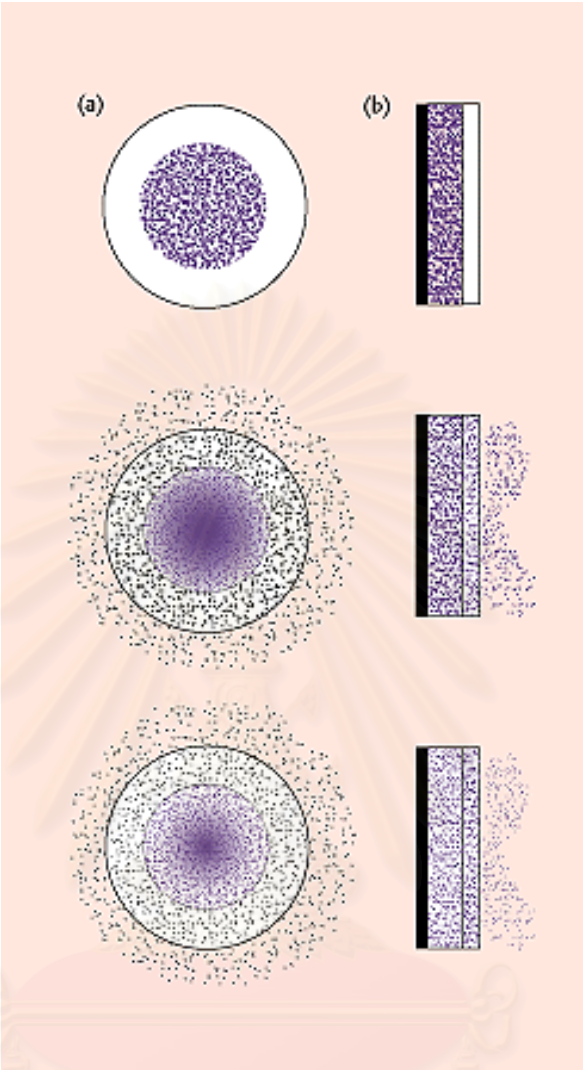

Figure 2.7 Drug delivery from typical reservoir devices :
i. implantable or oral systems; and
ii. transdermal systems

2.3 Applications of polymeric drug delivery systems

Drug delivery system is the preparation of drug in many forms so as to control drug release rate and quantity and to convey drug to the target organs as required (Edlund, 2002, Baldwin, 1998, Okada, 1994). This will give the most effective curing

and reduce side effects. Polymer is a very important factor in this drug delivery system in which it has such three main functions as

1) a substance to control drug release to become slow, steady and consistent delivery in specific quantities,
2) a substance to protect and
3) vehicle of drug to the target organ without pre-emptive drug release or drug decomposition.

This polymer must have important biological properties as followed: biocompatible, biodegradable and becoming metabolite, tissue-related material which is non-toxic to human body, after decomposed.

2.4 Chitosan based on hydrogel properties

Hydrogels are highly swollen, hydrophilic polymer networks that can absorb large amounts of water and drastically increase in volume. Hydrogel is a polymer that is not soluble in water (Lowman, 1999). However, it becomes gel when it is in water because of net structure from intramolecular and intermolecular hydrogen bonding. The swelling behavior of hydrogel occurs when water molecules move into intermolecular hydrogen bonding and destroy some hydrogen bonds so that chains are loosen.

It is well known that the physicochemical properties of the hydrogel depend not only on the molecular structure, the gel structure, and the degree of crosslinking but also on the content and state of water in the hydrogel. Hydrogels have been widely used in controlled release systems (Yang, 2000, Yao, 1995, Brosted, 1991). Recently, hydrogels, which swell and contract in response to external pH, are being explored. The pH sensitive hydrogels have a potential use in site-specific delivery of drugs to

specific regions of GI tract and have been prepared for low molecular weight and protein drug delivery. It is known that the release of drugs from the hydrogels depends on their structure or their chemical properties in response to environmental pH. These polymers, in certain cases, are expected to reside in the body for a longer period and respond local environmental stimuli to modulate drug release. On the other hand, it is some times expected that the polymers are biodegradable to obtain a desirable device to control drug release. Thus, to be able to design hydrogels for a particular application, it is important to know the nature of systems in their environmental conditions to design them in proper situation. Some recent advances in controlled release formulations using gels of chitin and chitosan are presented here.

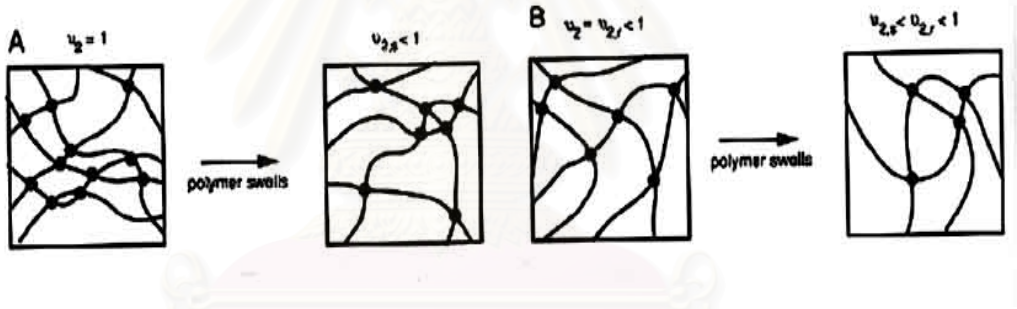

Figure 2.8 Shows swelling behavior of hydrogel.

There are some possibilities that explain molecular structure of chitosan chain and amino and hydroxyl groups that give rise to intramolecular and intermolecular hydrogen bonding. Swelling capability of chitosan is caused by moving of molecules in solution to form intermolecular hydrogen bonding so that chains are loosen and hydrogen bonds are destroyed. Swelling behavior occurs and chitosan becomes gel in solution. From Yao's research, (1995) it suggested that, at high pH, intermolecular hydrogen bonding was formed because of amino group, while at low pH, amino group

would be protonated and became anion so that hydrogen bonds were destroyed and chains were loosen.

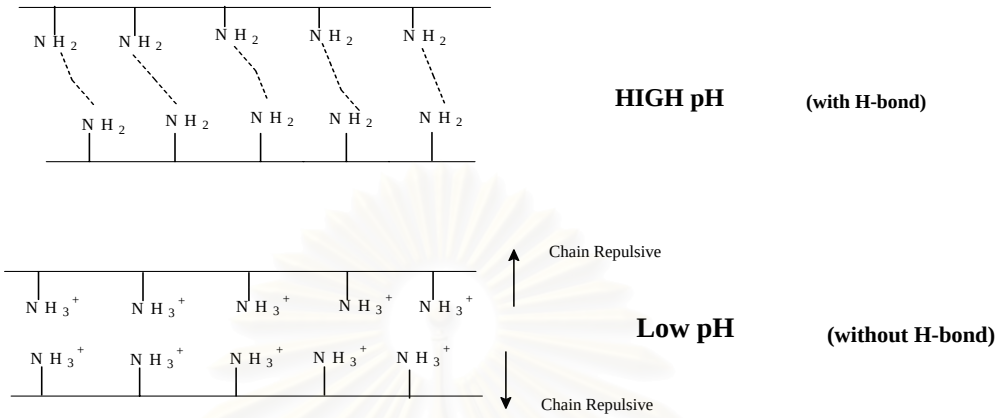

Figure 2.9 Shows chitosan chain under acidic and alkaline condition (Yao, 1995 and Chunharotrit, 1998).

In conclusion, drug release from the insoluble polymer matrix is due primarily to pH change. Drug molecules unable to free diffuse due to insoluble polymer matrix. The following three steps was commonly applied to understand such event: *(i)* water uptake and swelling of the beads, *(ii)* dissolution of drug molecules, and *(iii)* diffusion of drug molecules through the bead.

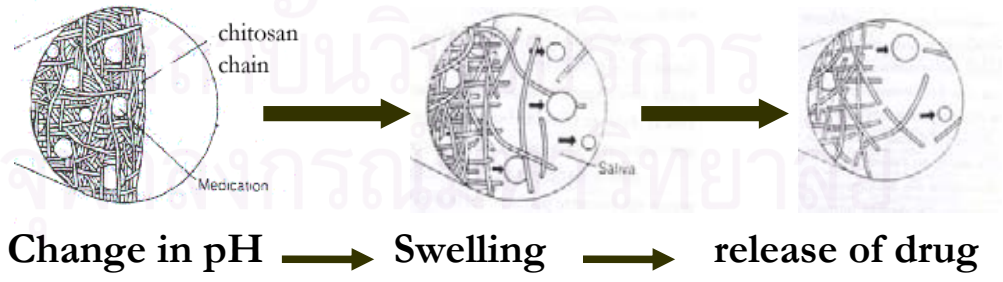

Figure 2.10 Scheme of the possible mechanism of drug release from the chitosan matrices.

2.5 Alginate

Alginic acid, a natural polymer, is a polymeric acid extracted from seaweeds, and is composed of varying proportions of 1-4 linked β-D-mannuonic (M) and α-L-guluronic acids (G). These residues are present in varying proportions depending on the source of the alginic acid. The use of alginate as an immobilizating agent in most applications rests in its ability to form heat-stable strong gels which can develop and set at room temperatures. It is the alginate gel formation with calcium ions which has been of interest in most applications. However, alginate forms gels with most di- and multivalent cations. Monovalent cations and Mg^{2+} ions do not induce gelation while ions like Ba^{2+} and Sr^{2+} will produce stronger alginate gels than Ca^{2+}.

As alginates may form strong complexes with polycations such as chitosan or polypeptides, or synthetic polymers such as polyethyllenimine they may be used to stabilize the gel (Klock, 1997).

2.6 Diclofenac as model drug

Diclofenac, 2-[(2,6-dichlorophenyl) amino]phenylacetic acid (Figure 2.11) is a phenylacetate non-steriodal anti-inflammatory drug (NSAID) (Skoutakis et al. 1988) and it mainly used in the treatment of rheumatoid arthritis and other rheumatoid disorders. It is a good example of adrug that is often prepared as a controlled-release formulation. Diclofenac has numerous solid forms, including the acid and various diclofenac salts. Examples of diclofenac salts include potassium diclofenac dihydrate (Fini et al. 2001), sodium diclofenac tetrahydrate (Fini et al. 2001) and sodium diclofenac pentrahydrate (Muangsin et al. 2002).

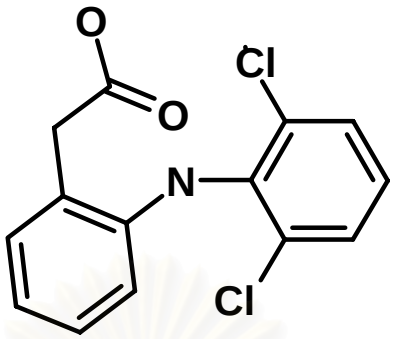

Figure 2.11 The chemical structure of diclofenac.

There have been reports that the physical and chemical properties of diclofenac depend on the acidity of the conditions to which it is exposed. The solubility of diclofenac depends substantially on the pH of the surrounding solution, being lower than 1 mg ml^{-1} in acidic conditions and increasing for pH values above 6.5 (Palomo, 1999, Fini, 1995, Fini, 1992).

2.7 Solvation structure of chitosan by computer simulation

Liquid state, including liquid solutions, plays an essential role in most chemical processes in nature. Many chemical operations, for example, synthesis, mixing, purification and separation are carried out in liquid solution, involving the structure and energetic and dynamic characteristics of solute-solvent interactions at the molecular level. The study of liquid state of matter has a long and rich history, from both theoretical and experimental approaches (Bernal, 1933).

The characteristic of solvation is often used in general to describe the structure of the solution where the geometrical arrangements are significantly different from the bulk structure of the solvent itself. The dynamical stability depends on the

combination of forces acting between homogeneous or heterogeneous molecules of which the solution consists. On one hand, a discrete solvation shell can be based on the solute-solvent interaction which is so strong that the exchange rate is much lower in the first solvation shell than that among solvent molecules. On the other hand, a shell structure can also be detected even when the interaction between solute and solvent is weaker than the solvent-solvent interaction.

Some decades ago, the investigation of solution structure was mainly a domain of spectroscopical methods such as X-ray, neutron diffraction and NMR, etc. They encounter, however, some difficulties to produce data when the sample is very dilute, or when solvent exchange takes place very fast, or when the interaction is so weak that the input energy from the spectroscopic apparatus exceeds that of the interaction which should be measured. In addition, the measurements concern mostly the study of a one-component solvent, while preferential solvation in mixed solvents is acceptably important phenomena, for which theoretical studies are also still quite rare, mostly due to the relatively high computational effort needs for the simulation of multi-component systems.

Quantum chemical investigations, which still have strong limits in the size of molecular system and the related computational time, have been a useful tool for predicting configurations of molecules, stabilization energies, excitation energies, force constants, and other physical data. Although they often produce data in good agreement with experiment, this approach can not reflect all properties of a condensed system with large amounts of particles.

The availability of electronic computers with high processing capacities has changed the situation most favorably within the past twenty years. Numerical calculations for n-electron systems have become feasible at ever increasing levels of

accuracy and complexity. Statistical mechanics has made a remarkable progress with the help of computer technology, and can be applied by simulations of Monte Carlo, MC (Hannongbua, 1992) or molecular dynamics, MD (Pitera, 1998) types. These methods have overcome some limitations of first approaches and made it possible to simulate the statistical and dynamical behaviors of rather large ensembles of molecules based on accurate potentials derived from quantum chemical calculations. Therefore, theoretical investigations of the liquid state and solutions have rapidly developed and numerous studies based on these methods for solution have been published (Tanabe, 1988, Tasaki, 1996, Martins, 2003).

Computer simulation allows not only to evaluate solvation numbers and solute-solvent distances from computed radial distribution functions, but gives also access to data not available from any experimental technique so far, for example, an analysis of the percentual contribution of various coordination numbers to the average solvation number of ions or solvent molecules. The access to the angular distribution of neighbor molecules is also an important means of these methods for the evaluation of structural data in solution.

2.7.1 Monte Carlo simulation

There are many types of calculations that are referred to as Monte Carlo calculations. All Monte Carlo methods are built around some sort of a random sampling, which is simulation is one in which the location, orientation, and perhaps geometry of a molecule or collection of molecules are chosen according to a statistical distribution. For example, many possible conformations of a molecule could be examined by choosing the conformation angles randomly. If enough iterations are

done and the results are weighed by a Boltzmann distribution, this gives a statistically valid result. The steps in a Monte Carlo simulation are as follows:

1. Choose an initial set of atom positions. The same techniques used for molecular dynamics simulations are applicable.
2. Compute the energy for the system.
3. Randomly choose a trial move for the system. This could be moving all atoms, but it more often involves moving one atom or molecule for efficiency reasons.
4. Compute the energy of the system in the new configuration.
5. Decide whether to accept the new configuration. There is an acceptance criteria based on the old and new energies, which will ensure that the results reproduce a Boltzamann distribution. Either keep the new configuration or restore the atoms to their previous positions.
6. Iterate steps 3 through 5 until the system has equilibrated.
7. Continue iterating and collecting data to compute the desired property. The expectation value of any property is its average value (sum divided by the number of iterations summed). This is correct as long as the acceptance criteria in step 5 ensured that the probability of a configuration being accepted is equal to the probability of it being included in a Boltzmann distribution. If one atom is moved at a time, summing configurations into the average every few iterations will prevent the average from over representing some configurations.

There are a few variations on this procedure called importance sampling or biased sampling. These are designed to reduce the number of iterations required to

obtain the given accuracy of results. They involve changes in the details of how steps 3 and 5 are performed.

Monte Carlo simulations require less computer time to execute each interation than a molecular dynamics simulation on the same system. However, Monte Carlo simulations are more limited in that they cannot yield time-dependent information, such as diffusion coefficients or viscosity. As with molecular dynamics, constant NVT simulations are most common, but constant NPT simulations are possible using a coordinated scaling step. Calculations that are not constant. N can be constructed by including probabilities for particle creation and annihilation. These calculations present technical difficulties due to very low probabilities for creation and annihilation, thus requiring very large collections of molecules and long simulation times.

2.7.2 Molecular dynamics simulations

Molecular dynamics calculates the “real” dynamics of the system, from which time averages of properties can be calculated. Sets of atomic positions are derived in sequence by applying Newton’s equations of motion and the state of the system at any future time can be predicted from its current state. The results is a trajectory that specifies how the positions and velocities of the particles in the system vary with time. Newton’s laws of motion can be stated as follows:

1. A body continues to move in a straight line at constant velocity unless a force acts upon it.
2. Force equals the rate of change of momentum
3. To every action there is an equal and opposite reaction.

The trajectory is obtained by solving the differential equations embodied in Newton's second law *(F=ma)*:

$$\frac{d^2 x_i}{dt^2} = \frac{F_{x_i}}{m_i} \qquad (2.1)$$

This equation describes the motion of a particle of mass m_i along one coordinate (*xi*) with Fx_i being the force on the particle in that direction.

2.7.3 Potential force field

Many of the problems that we would like to tackle in molecular modeling are unfortunately too large to be considered by quantum mechanical methods. Quantum mechanics deals with the electrons in a system and the calculations are time-consuming. Force field method (also known as molecular mechanics) ignore the electronic motions and calculate the energy of a system as a function of the nuclear positions only. Molecular mechanics is thus invariably used to perform calculations on systems containing significant numbers of atoms. In some cases, force field can provide answers that are as accurate as event eh highest level quantum mechanical calculations, in a fraction of the computer time. Molecular mechanics cannot of course provide properties that depend upon the electronic distribution in a molecule.

All molecular mechanics works are due to the validity of several assumptions. The first of these is the Born-Oppenheimer approximation, without which it would be impossible to contemplate writing the energy as a function of the nuclear coordinated at all. Molecular mechanics is based upon a rather simple model of the interactions within a system with contributions from processes such as the stretching of bonds, the

opening and closing of angles and the rotations about single bonds. Even when simple functions (e.g. Hooke's law) are used, transferability is a key attribute to a force field, for it enables a set of parameters developed and tested on a relatively small number of cases to be applied to a much wider range of problems. Moreover, parameters developed from data on small molecules can be used to study much larger molecules such as polymers.

2.7.4 Radial distribution functions and integration numbers

From computer simulation, the structure of the solvent can be extracted from the simulation in terms of the atom-atom radial distribution function (RDF), $g_{xy}(r)$, the probability of finding an atom of type *y* in the spherical volume of radius *r* around the central atom of type *x* (Figure 2.12). This function for the N particles system in configuration is obtained with r_{ij} as

$$g(r) = \frac{N(r)}{\rho 4\pi r^2 dr} \qquad (2.2)$$

where N(r) is the average number of particles in the spherical shell of width *dr* at the radial distance *r* from the central particle. ρ is the number density of the system of the pair of the particle in the cubic volume V. Based on the radial distribution function, solvation shells can be derived from the peaks pronounced over the standard level, and the first solvation number is obtained by the integration of the function up to the first minimum (Matteoli, 1995).

The average number of particles within a sphere of a given radius can be determined by

$$n(r) = \rho \int_0^{r_m} g(r) 4\pi r^2 dr \qquad (2.3)$$

where r_m is often chosen as the radial value of the first or second minimum in g(r).

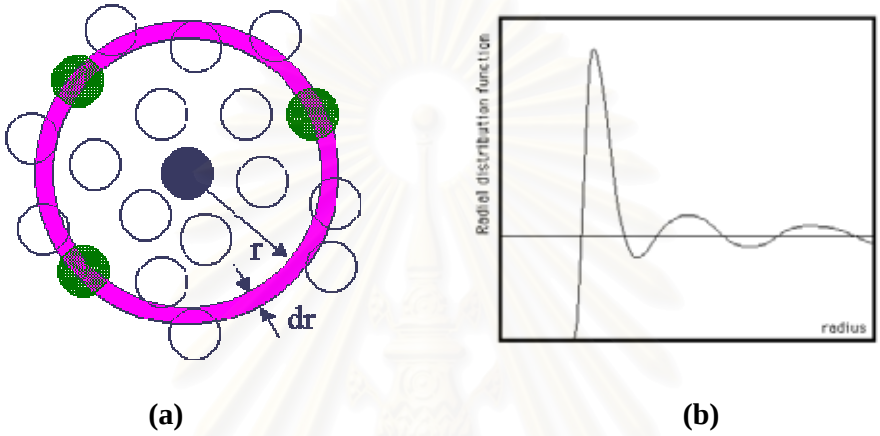

(a) **(b)**

Figure 2.12 The RDF histograms shows counting particles in shells (a) and the RDF plotted as a function of the interatomic separation ***r*** (b).

CHAPTER 3

MATERIALS AND METHODS

3.1 Materials

Chitosan from shrimp shells with low degree of deacetylation (70%DD, LDD) and high degree of deacetylation (91%DD, HDD) were taken from Asian Institute of Technology (AIT) while three different molecular weights of chitosan samples, low (LMW, 150,000 Dalton), medium (MMW, 400,000 Dalton), and high (HMW, 600,000 Dalton) molecular weights, were purchased from Fluka Biochemie, Buchs, Switzerland. Sodium alginate (low viscosity; 1% solution, approximately 250 cps) and diclofenac sodium (DS) were also purchased from Fluka. Other reagents used are in analytical grade.

3.2 Characterization of chitosan samples

3.2.1 Determination of moisture content

Moisture content of sample was determined by drying approximately 1 g of sample in an oven at 105^{o}C, 24 h (Lertsutthiwong, 2000). The weight was determined after cooling in a desiccator. The moisture content was calculated by the following formula:

Moisture content = $\{(W_2-W_3)100\}/(W_2-W_1)$

when W_1 = weight of a crucible after drying at 105 ^oC for 2 h,

W_2 = W_1+weight of initial sample,

W_3 = W_1+weight of sample after drying at 105 ^oC for 24 h

3.2.2 Determination of ash content

Ash content was determined by drying approximately 1 g of sample in an oven at 105 ^oC for 24 h. After cooling in a desicator, this moisture free sample was burned in a muffle furnace at 650^oC for 3 h (Lertsutthiwong, 2000). The ash content was calculated by the following formula:

Ash content (%) = $\{(W_4-W_1)*100\}/(W_3-W_1)$

when W_1 = weight of a crucible after drying at 650 ^oC, 1 h,

W_3 = W_1+weight of sample after oven dry at 105 ^oC, 24 h,

W_4 = W_1+ weight of sample after burning at 650 ^oC, 3 h.

3.2.3 Apparent viscosity by Brookfield DV II+ method

Viscosity, one of the important factors, which determines the quality of chitosan, was measured by using Brookfield viscometer DVII+. To determine the viscosity, chitosan solution was prepared by dissolving chitosan (1% w/v) in acetic acid (1% w/v) by shaking for 24 h at room temperature. Undissolved particles were, then, removed by filtration with nylon cloth. Chitosan solution was kept in water bath at 25±1^oC for 2 h before measuring the viscosity.

3.2.4 Determination of degree of deacetylation

Percentage degree of deacetylation defined as percentage of glucosamine residues in the chitosan sample, was measured by UV-spectrophotometer SPECORD S100. The first derivative UV-Spectrophotometric method reported by Muzzarelli et al., 1985 was used after slight modification for determination of the %DD of chitosan. This method permits a simple and time saving assay of *N*-acetyl glucosamine residues in chitosan leading to increase precision and accuracy. The %DD was determined using the following formula:

$$\%DD = [1-((A/((10W)-204A)+161A)/161)]\ 100$$

when, A = the fraction of *N*-acetyl-D-glucosamine in the sample,
204 = molecular weight of *N*-acetyl-D-glucosamine,
161 = molecular weight of D-glucosamine,
W = weight of sample (g) in 100 ml of 0.01 M of acetic acid.

3.2.5 Determination of molecular weight

The molecular weight was analyzed using Gel Permeation Chromatrography (Hein et al., 2000). Columns used in this method were Waters Ultra-Hydrogel 500, 1000 and 2000 GPC columns. The solvent of 1 L composed of 8.2 g CH_3COONa and 19.03 ml of gracial acetic acid. This solvent was filtrated through a 0.45 μm membrane filter before use. Dextrane (molecular weight, 9,900-2,000,000 Dalton) was used as a standard solution. The sample was prepared by dissolving 0.1% chitosan in the solvent and shaken at 100 rpm for 24 h. It was then filtered with a 0.45 μm membrane filter. The injection volume was 150 μl, temperature of the column was set at 40^{o}C and the flow rate of the solvent was 0.6 ml per min.

Table 3.1 General characteristics of chitosan

Parameter	LDD	HDD	LMW	MMW	HMW
Form	flake	flake	flake	flake	flake
Degree of deacetylation (%DD)	70	91	76	82	79
Molecular size (MW)	$5.6x10^5$	$6.3x10^5$	$1.5x10^5$	$4.0x10^5$	$6.0x10^5$
Moisture content (%)	< 8	< 8	< 5	< 5	< 5
Ash content (%)	< 2	< 2	< 2	< 2	< 2
Protein content (%)	< 2	< 2	< 2	< 2	< 2
Initial viscosity (cps)	59.5 ± 0.07	102.5 ± 0.06	106 ± 2.04	438.23 ± 2.04	504.01 ± 2.04

3.3 Preparation of chitosan beads and microparticles

3.3.1 Preparation of chitosan beads

The cationic form of chitosan solution (2.5% w/v) was prepared by dissolving chitosan in dilute acetic acid (1% v/v) at room temperature and filtering through nylon cloth to remove insoluble parts. The chitosan beads were formed in the coagulation fluid which prepared by dissolving 10% NaOH (w/v) in 50% ethanol (v/v). The chitosan solution (50 ml) was dropped through a 24 gauge blunt ended needle into 400 ml of coagulation fluid under magnetic stirring at 150 rpm (Figure 3.1). The drop flow rate was maintained at 0.1 ml/min controlled by peristaltic pump. The smooth and spherical beads were obtained under continuous stirring in the coagulation fluid for 1 h. The beads were collected after throughly washed, dewatering under ethanol-acetone condition then followed by air-drying. The performance for drug release of chitosan beads were further studied.

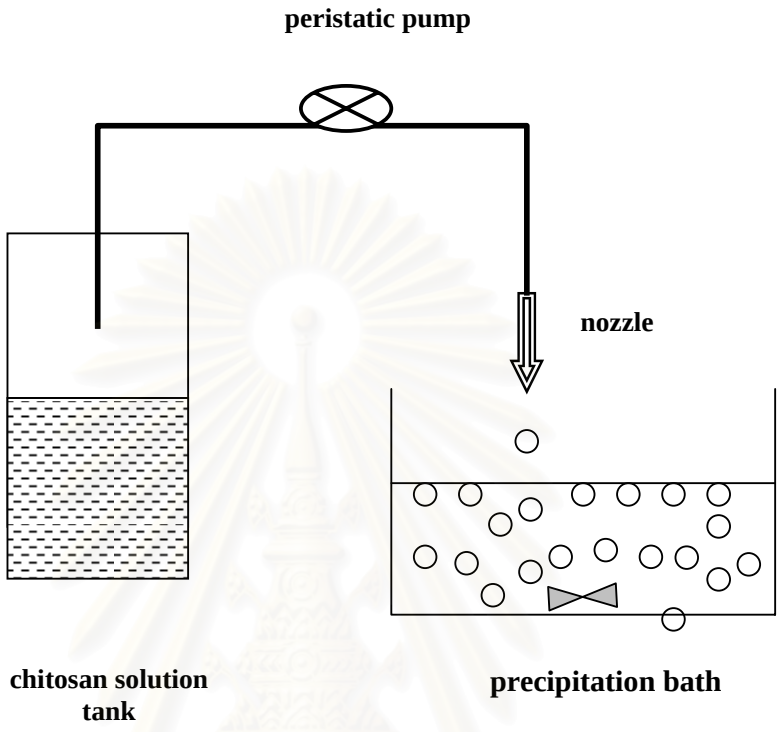

Figure 3.1 Schematic diagram for the preparation of chitosan beads.

3.3.2 Preparation of chitosan microparticles

The chitosan microparticles was prepared by suspension method as previously described by Emir (1999). The modification technique is schematically presented in Figure 3.2. Chitosan solution (2.5% w/v) was prepared by dissolving in dilute acetic acid (1% v/v) at room temperature and filtering through nylon cloth to discard impurities. The 50 ml of chitosan solution was dispersed in 200 ml of mineral oil and petroleum ether (25/35, v/v) as dispersion medium and an emulsifier (Span-80) under mechanical stirring (1500 rpm, Janke & Kunkel IKA RW20) at room temperature. The system was maintained under agitation for 2 h, then add 2 ml of 5% NaOH (w/v)

under the same stirring condition for 1 h. At the end of this period, the chitosan microparticles were collected by vacuum filtration (0.45 μm PFTE membrane filters, Lida, Spain), and thoroughly washing and dewatering under ethanol-acetone condition. Then, the microparticles were dried in an oven at 40^{o}C overnight and kept in a vacuum desiccator for further analysis and uses.

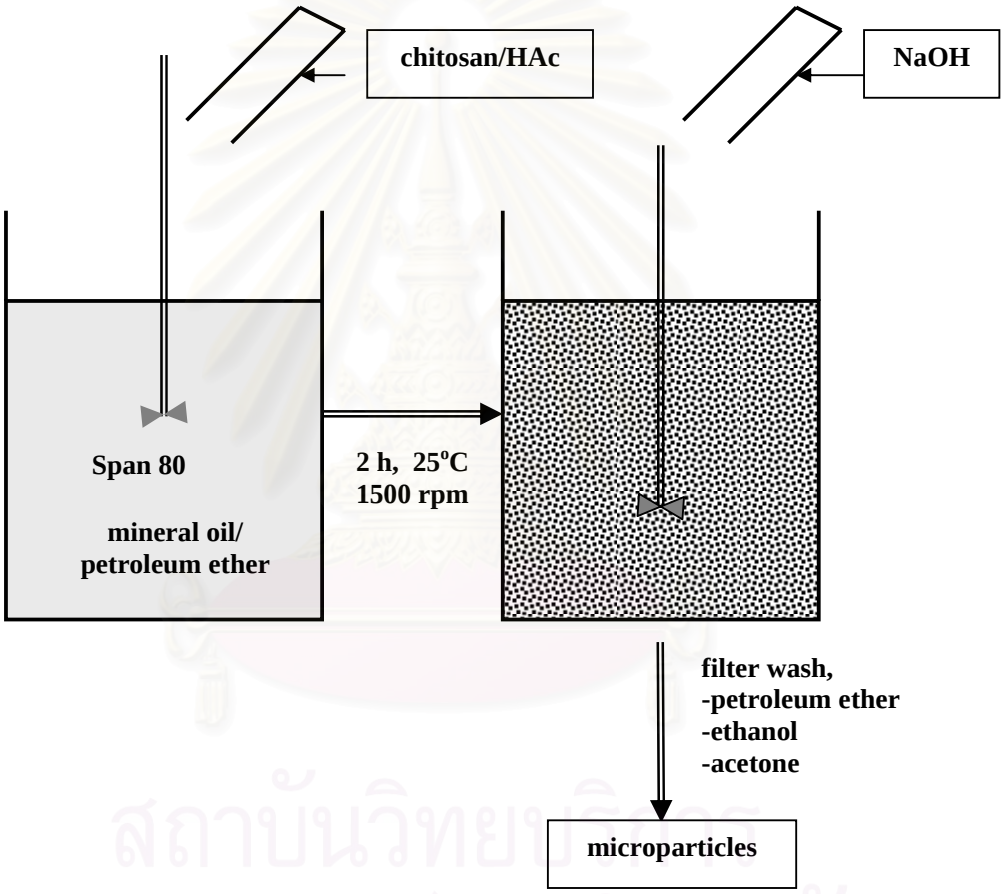

Figure 3.2 Schematic presentation of preparation of chitosan microparticles.

3.4 Morphological characterization of chitosan beads and microparticles

The mean particle size of chitosan bead was directly measured by Scanning Electron Microscope, SEM using approximately 150 beads. The morphology and surface appearance of beads (before and after release) was also examined by SEM. The samples were mounted onto aluminum stubs using double-sided carbon adhesive tape and coated with a gold-palladium target using a Polaron, SC7610, England sputter coater. Coating was achieved at 18 mA for at least 5 mins. Scanning was performed at ambient temperature with beam voltage between 10-20 kV. The DS distribution within the beads was investigated. Energy Dispersive X-ray Spectrometer, EDS analysis using a Philips XL30CP scanning electron microscope with EDS attachment (EDAX, SUTW).

3.5 Swelling measurement

The swelling behavior of dried chitosan beads were determined in a HCl solution (pH 2.0) and phosphate buffer (pH 6.8). The weight of 50 mg of chitosan beads were soaked into 100 ml of the swelling solution at room temperature for 8 hours. The wet weight of the swollen beads was measured by weighing with electronic balance after removing adhering water by filter paper. All experiments were done in triplicate.

The percentage of swelling index of the beads was calculated by the formula:

$$\mathbf{SWI} = \mathbf{\{(W_t - W_o)100\}/ W_o}$$

when SWI = the swelling index,

W_t = final weight of beads,

W_o = initial weight of beads.

3.6 Evaluation of DS released from the chitosan beads/microparticles

3.6.1 Drug loaded chitosan matrices

The 50 mg of beads or microparticles were added into the solution of 25 mg DS in 50 ml of 50% methanol and stirred at room temperature for 24 h. The preparation was air dried until complete.

3.6.2 Determination of drug loading efficiency

The DS content in beads or microparticles were determined by methanol extraction. The 20 mg of bsample was pulverized and incubated in 50 ml of methanol in a 100 with magnetic stirring for 24 h. The suspensions were then centrifuged at 3000 rpm for 30 min. The supernatant solution was assayed for DS contents by spectrophotometer at a wavelength 276 nm. Supernatant from the blank beads or microparticles was used as reference. All samples were analyzed in triplicate.

3.6.3 Drug release studies

The DS release from beads or microparticles was studied by incubating 50 mg of matrix beads in 500 ml of phosphate buffer of pH 6.8 and in a glass apparatus at room temperature under stirred condition at 100 rpm. The drug release assay was done every 1 hour by withdrawing 5 ml of sample and replaced by equal volume of fresh buffer medium to maintain the same value of the system. Samples were filtered (0.2 μm Nylon filters, Whatman, England) and assayed for the drug released by measuring the absorbance value at 276 nm by UV-spectrophotometer (SPECCORD S100). Each experiment was repeated three times.

3.7 Preparation of multiplayer chitosan-alginate beads

The chitosan matrices beads (MMW with DS-loaded) were incubated in the solution of 0.5% sodium alginate for 5 min then transferred to 3% $CaCl_2$ solution as coagulation fluid for the first alginate layer. The obtained chitosan-alginate matrices beads were coated for second wall with two different concentration of chitosan solution (0.5 and 1.0%) followed by 5% NaOH as coagulation fluid. The third wall of the matrices was continuing coated by the same condition of alginate solution. The obtained multiplayer coated beads were further studied for drug release behavior.

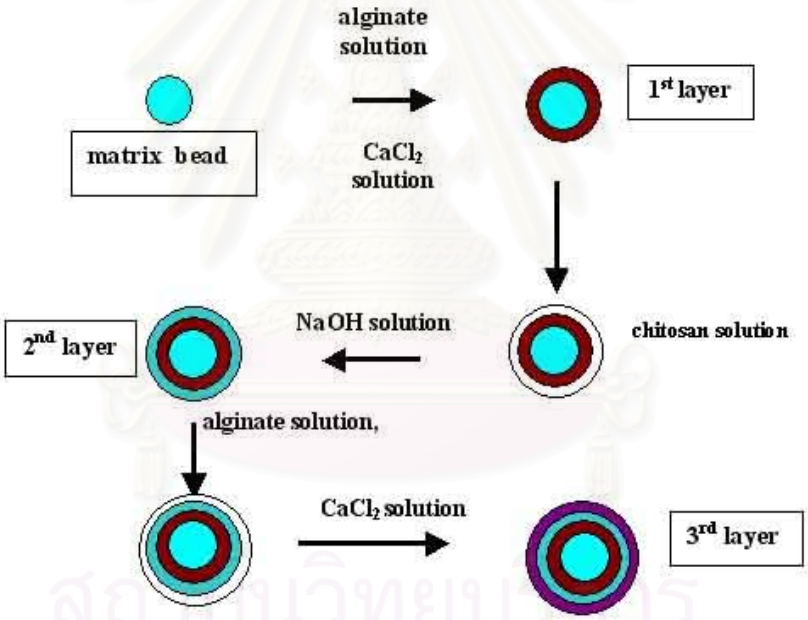

Figure 3.3 Schematic presentation of the preparation of chitosan-alginate beads.

3.8 Statistical analysis:

All values in the text and tables are expressed as mean. The statistically significant difference ($p < 0.05$) was obtained. T- test was then performed using SPSS program version 9.05 for Windows.

3.9 Computer simulations

To seek for more detailed characteristic of the solution in molecular level, computer simulations were performed using Monte Carlo (MC) and Molecular Dynamic (MD) methods for investigation the solvation structure of glucosamine molecule (chitosan monomer) and chitotetraose molecule (chitosan tetramer).

3.9.1 The potential functions

Potential function is the primary data required for the simulations and controlled quality of the simulations. The potential functions used for the study were the *ab initio* fitted function for the small (glucosamine) and the force field function for the big (chitosan tetramer) systems.

3.9.1.1 The developing of glucosamine-water potential

An *ab initio* potential function was newly developed to represent glucosamine-water interaction. Geometry of glucosamine obtained from X-ray crystallography Nakatsuka, S., 1992) was used as starting structure. The missing hydrogen atoms were added and then partial optimization for these atoms was performed using Gaussian 98 program (Frisch, et al., 1998) with double zeta plus polarization (DZP) basis set (Al-Angary, 1993). An experimental geometry of water, i. e., 0.957 Å of O-H bond and 104.5° of H-O-H angle (Benedict, 1997) was employed. The glucosamine and water

molecules were treated as rigid throughout the calculations. To develop the pair potential, the atoms of glucosamine molecule were classified into 12 groups by their atomic net charges obtained from the Mulliken population analysis. Total 4000 single point energies of glucosamine-water dimer were calculated using *ab initio* self-consistent field method with the DZP basis set. The data were fitted to an analytical function of the form:

$$\Delta E(\mathrm{L,W}) = \sum_{i=1}^{25}\sum_{j=1}^{3}\left(-\frac{A_{ij}}{r_{ij}^{6}}+\frac{B_{ij}}{r_{ij}^{12}}+\frac{q_i q_j}{r_{ij}}\right) \qquad (3.1)$$

where, 25 and 3 denote the numbers of atoms of glucosamine (L) and water (W), respectively. A_{ij} and B_{ij} are fitting parameters, r_{ij} is the distance between atom i of water and atom j of glucosamine, and q_i and q_j are the net Mulliken charges of atoms i and j, respectively. The optimal fitted parameters are summarized in Table 3.2.

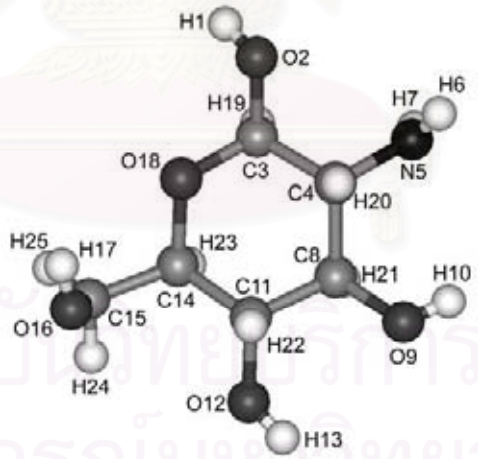

Figure 3.4 Structure of glucosamine with atomic numbering.

Table 3.2 Classification of atoms in glucosamine and water molecules by atomic net charges (see Figure 3.4 for glucosamine structure).

Group	Atom	Charge (a.u.)
Glucosamine		
C^1	C3, C4, C8, C11, C14	0.156
C^2	C15	-0.056
N	N5	-0.597
O^1	O2, O9	-0.494
O^2	O12	-0.542
O^3	O16	-0.547
O^4	O18	-0.485
H^1	H19, H20, H21, H22, H23, H24, H25	0.108
H^2	H6, H7	0.245
H^3	H1, H10	0.289
H^4	H13	0.282
H^5	H17	0.331
Water		
O	O	-0.660
H	H	0.330

3.9.1.2 Force field potential

The standard AMBER force field (Weiner *et al.,* 1984,) is parameterized to small organic constituents of proteins and nucleic acids. Only experimental data were used in parameterization. However, AMBER has been widely used not only for proteins and DNA, but also for many other classes of models, such as polymers and small molecules. For the latter classes of models, various authors have added parameters and extended AMBER in other ways to suit their calculations. The AMBER force field has also been made specifically applicable to polysaccharides. AMBER is used mainly for modeling proteins and nucleic acids. It is generally lower in accuracy and has a limited range of applicability.

The AMBER energy expression contains a minimal number of terms. No cross terms are included. The functional forms of the energy terms used by AMBER are given in this equation ;

$$E_{pot} = \underset{(1)}{\sum_b K_2 (b - b_0)^2} + \underset{(2)}{\sum_\theta H_\theta (\theta - \theta_0)^2} + \underset{(3)}{\sum_\phi \frac{V_n}{2} [1 + \cos(n\phi - \phi_0)]} + \underset{(4)}{\sum \varepsilon [(r^*/r)^{12} - 2(r^*/r)^6]} + \underset{(5)}{\sum q_i q_j / \varepsilon_{ij} r_{ij}} + \underset{(6)}{\sum \left[\frac{C_{ij}}{r_{ij}^{12}} - \frac{D_{ij}}{r_{ij}^{10}} \right]} \quad (3.2)$$

The first three terms in the equation handle the internal coordinates of bonds, angles, and dihedrals. Term 3 is also used to maintain the correct chirality and tetrahedral nature of sp^3 centers in the united-atom representation. (In the united-atom representation, nonpolar hydrogen atoms are not represented explicitly, but are coalesced into the description of the heavy atoms to which they are bonded.) Terms 4 and 5 account for the Van der Waals and electrostatic interactions. The final term, 6, is an optional hydrogen-bond term that augments the electrostatic description of the hydrogen bond. This term adds only about 0.5 kcal mol^{-1} to the hydrogen-bond energy

in AMBER, so the bulk of the hydrogen-bond energy still arises from the dipole-dipole interaction of the donor and acceptor groups.

3. 9.1.3 The advantage and disadvantage of *ab initio* and force field potential

Ab initio is the quantum calculation especially for the complicated system that more accuracy and difficult to develop while the force field is more generalize with low accuracy but have a fast comfortable to applied in very large systems.

In this study, both force field and *ab initio* potential models were used in the simulation of chitosan. Unfortunately, the intramolecular interaction for glucosamine molecule is very difficult to develop. Then, MC simulation where the molecules were kept rigid, was use to investigate precise solvation of glucosamine. While for the force field potential, both intramolecular and intermolecular interactions were included in the function. Therefore, MD simulation which allow the flexibility of molecule, were used to examined the truetural properties of the chitosan tetramer. In addition, the system is too big to perform *ab initio* calculations and, hence, to develop the tetramer-water potential function.

3.9.2 Monte Carlo simulation of glucosamine in aqueous solution

Monte Carlo simulation has been carried out for a glucosamine molecule in aqueous solution at temperature of 298 K and pressure of 1 atm. The system contained 202 rigid molecules, one glucosamine molecule fixed at the center of the cube and 201 water molecules. The volume of periodic box is the summation of volume of 201 water molecules with the density of 1 g/cm^3 and additional space occupied by glucosamine molecule, leading the cube length of 18.26 Å. A spherical cut-off for the site-site interaction potentials was applied at half of this length. The

starting configuration of the water molecules was randomly generated. The Metropolis sampling algorithm was applied. The MCY potential was employed to describe water-water interactions. The simulation was started at 298 K of temperature for 5 million configurations and then the system was heated up to 1000 K to rearrange water positions. After 3 million configurations the system was cooled down to the room temperature. Equilibrium was reached after 34 million configurations at this temperature. Further 16 million configurations were generated and every 500 of them were stored for subsequent analysis.

3.9.3 Molecular dynamic (MD) simulation of monomer and tetramer system

Each of the chitosan unit modeled was simulated at 298 K in a periodic cubic box of 18 Å in length containing 614 and 1043 TIP3P solvent water molecules (Cornell, W.D., 1995), for monomer and tetramer of chitosans, respectively,

The AMBER 7.0 program was used to minimize and perform MD simulation with the *ff99* force field and time step of 2 ps. The systems are observed to reach equilibration after 10 ps. Then the trajectories, after equilibration, were collected every 10 ps for 800 ps simulation time.

All of the trajectories from the simulation are in term of on radial distribution functions, as well as orientation of water molecules around the ligand.

CHAPTER 4

RESULTS AND DISCUSSION

4.1 Chitosan beads characteristics

The polycationic chitosan polymer in acidic aqueous solution dropped into an aqueous solution of sodium hydroxide is known to form gel beads. In this study, smooth, spherical and homogenous gel beads were yielded. Surface morphology and ultrastructural characteristics of all batches were observed by scanning electron microscope: Diclofenac Sodium (DS) as a model drug was embedded into the matrices beads by absorption techniques. Drug content and absorption efficiency of DS-loaded chitosan beads are reported in Table 4.1.

Table 4.1 Size, drug-loaded efficiency, swelling index of chitosan matrix beads

Batch	MW (kDa)	%DD	Mean size (μm)	Drug-loaded efficiency(%)
LDD	560	70	845±4	63.5±2
HDD	630	91	856±6	78.9±4
LMW	150	76	823±2	57.2±2
MMW	400	82	864±4	82.7±1
HMW	600	79	815±5	80.3±2
Microparticles	400	82	37±10	85.2±4
Multiplayer beads (with chitosan concentration at 2nd layer)	400	82		
0.25%chitosan	400	82	819±6	81.6±5
0.5%chitosan	400	82	825±4	82.7±3
1.0%chitosan	400	82	865±5	80.3±2

4.2 Morphology observation of beads

To monitor the shape and the surface structure of the beads before and after DS-loaded, the samples were carried out using scanning electron microscope (SEM). There were no significant differences in varying %DD and molecular weight; therefore, only those of MMW was displayed. Figures 4.1 show SEM micrographs of the external and the cross-section of the beads. The spherical and smooth surface beads were formed (Figure 4.1a). Surface roughness was detected at high magnification (Figure 4.1b).

a

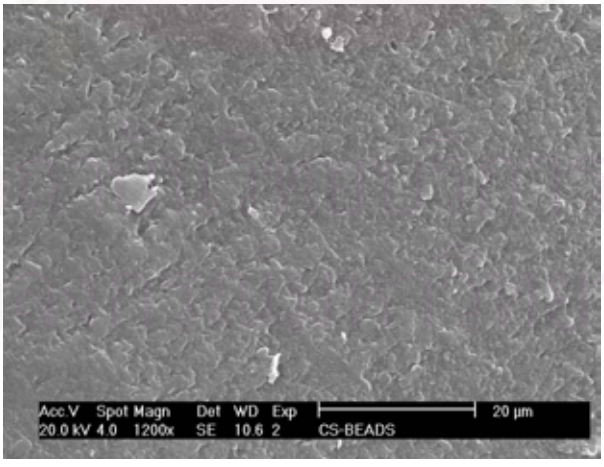

b

Figure 4.1 SEM micrographs of the surface of MMW chitosan beads (a) external and (b) cross-section.

The microparticles was prepared by suspension technique, where chitosan sample of MMW (400,000, 82%DD) was used. The shape and surface morphology of particles were observed by SEM (Figure 4.2). Particle size was analyzed by laser particle size analyzer, Mastersizer-S long bed ver. 2.11. The mean size of the microparticles obtained by this method was 37±10 μm.

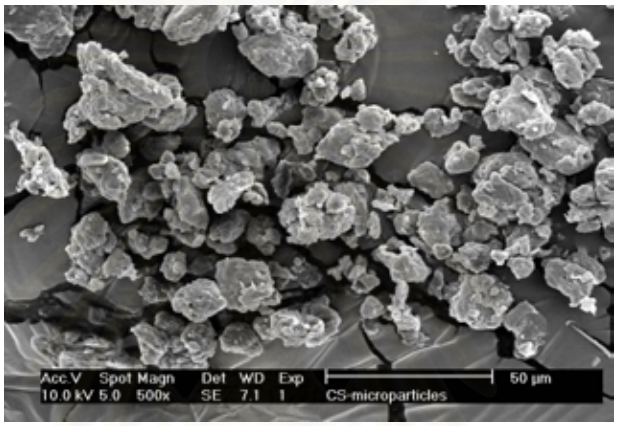

Figure 4.2 SEM-micrograph of chitosan microparticles prepared by suspension technique.

The DS particles that are deposited on the surface of the beads can be measured using Energy disperse spectrophotometer, EDS, analysis. The EDS measurement was done in both of on the surface and inner region of the beads. Figure 4.4 shows the EDS-microanalytical pattern of chitosan beads with and without DS-loading.

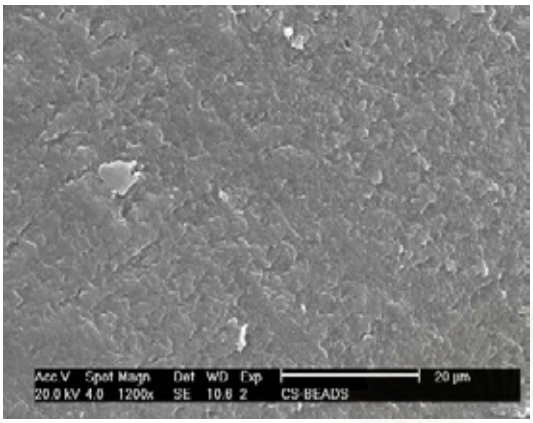

a

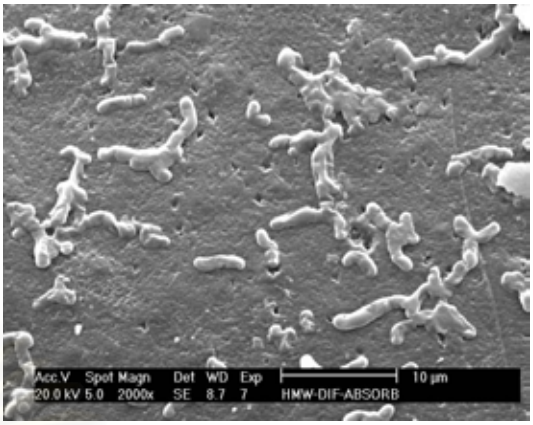

b

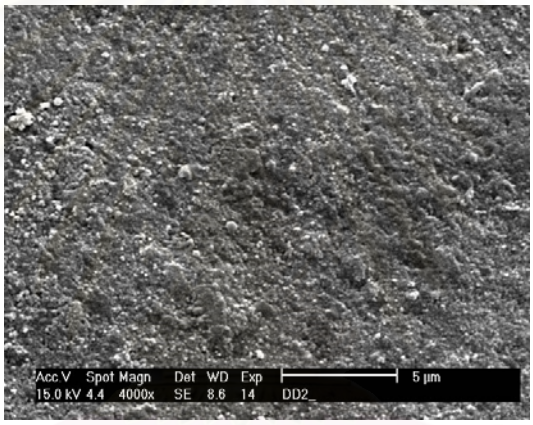

c

Figure 4.3 SEM micrographs on the surface of MMW chitosan beads before (a), and after (b and c) DS-loaded.

From EDS analysis indicated Na and Cl atoms which are the composition in the DS in both of outer (white spot on the surface of beads, Figure 4.3b) and inner regions of the beads (Figure 4.3c). This indicated that the DS molecules were embed in the chitosan beads.

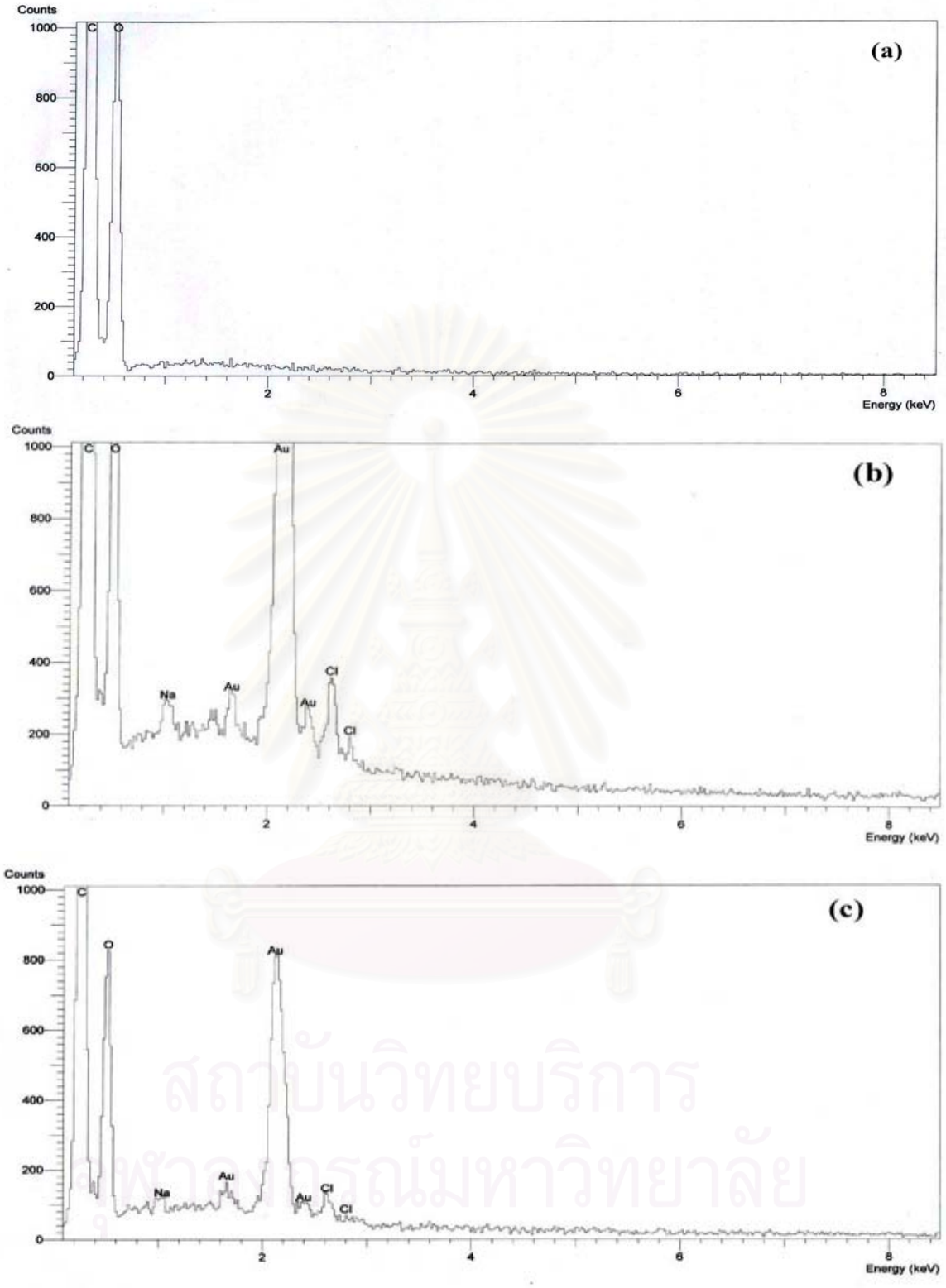

Figure 4.4 EDS-Microanalytical chart of the chitosan bead without DS (a) DS distributs on the surface (b) and in the bead (c).

4.3 Swelling behavior

The swelling index of the chitosan beads in solutions at pH 2.0 and 6.8 is shown in Figure 4.5. The beads exhibit high pH sensitivity. The swelling index of the beads at pH 2.0 is obviously higher than that at pH 6.8. This pH sensitive swelling is due to the transition of beads structure between the collapsed and the expanded rates, which is related to ionization degree of amino groups on chitosan in different pH solutions.

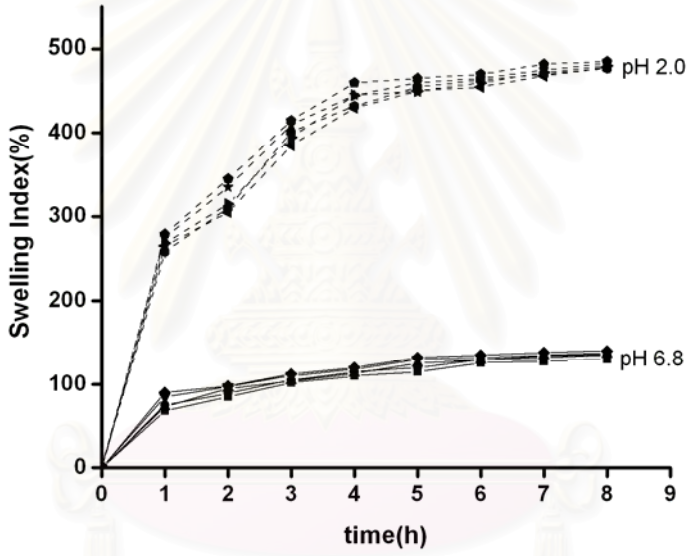

Figure 4.5 Swelling behavior in solution at pH 2.0 and 6.8 of chitosan beads at different degrees of deacetylation (LDD, 70%DD and HDD, 91%DD) and molecular weights (LMW, 150,000, MMW, 400,000 and HMW, 600,000).

4.4 Drug loading efficiency

From Table 4.1, the DS loading efficiency of the beads is in the range 57-82% while that of the microparticles is slightly higher, about 85%. It was found also that drug

adsorption capacity increases with decreasing particle size of chitosan beads. This would relate directly to an increase of surface area of the bead.

Effect of chitosan with different molecular weight (LMW, 150,000, MMW, 400,000, and HMW, 600,000 dalton) on the adsorption capacity was clearly seen in Table 4.1. The decrease in molecular weight of chitosan leads to a reduction in drug loading efficiency. This can be understood by the fact that at high molecular weight, chain entanglement and structural network were enhanced due to an increase of the inter- and intra- molecular contacts, leading directly to the decrease of the bead size and hence the increase of particle surface area.

It is shown also in Table 4.1 that adsorption of DS at 70%DD is lower than that at 91%DD. This can be due to lower density of amine groups on chitosan chain in the 70%DD than the other one at 91%DD. At drug the loading condition (50% methanol), the pH of DS solution less than 6.5 which is approximately the pKa of the amine group, therefore, chitosan in solution carries a positive charge along its backbone. The $–COO^-$ ions in the DS molecules could ionically react with the $–NH^{3+}$ binding site in the chitosan chain by deprotonation.

4.5 DS release studies from the matrices chitosan

It is known that drug release consists of three steps: (i) water uptake and swelling of the beads; (ii) dissolution of DS; and (iii) diffusion of DS molecules through the chitosan gel beads. In this study, release behavior in acidic medium was not taken into consideration due to low solubility of DS in acidic solution. In addition, chitosan bead was found to form gel at low pH media. Therefore, the release profile of DS from

matrices chitosan beads was considered only at phosphate buffer medium similar to SIF (simulated gastric fluids) at pH 6.8.

4.5.1 Effect of degree of deacetylation

DS release profiles from the beads with the two degree of deacetylations were compared in Figure 4.6. The release pattern shows a trend of rapidly increasing for the first 240 mins and thereafter, the release is relatively slow and remaines constant afterward. The % release of DS from the beads during test period (480 mins) were 73.1 and 74.2% for low (LDD) and high (HDD) %DD of chitosan, respectively. The release rate is not significant different which might occur from the low affinity of chitosan and drug at isoelectric point (pH 6.8).

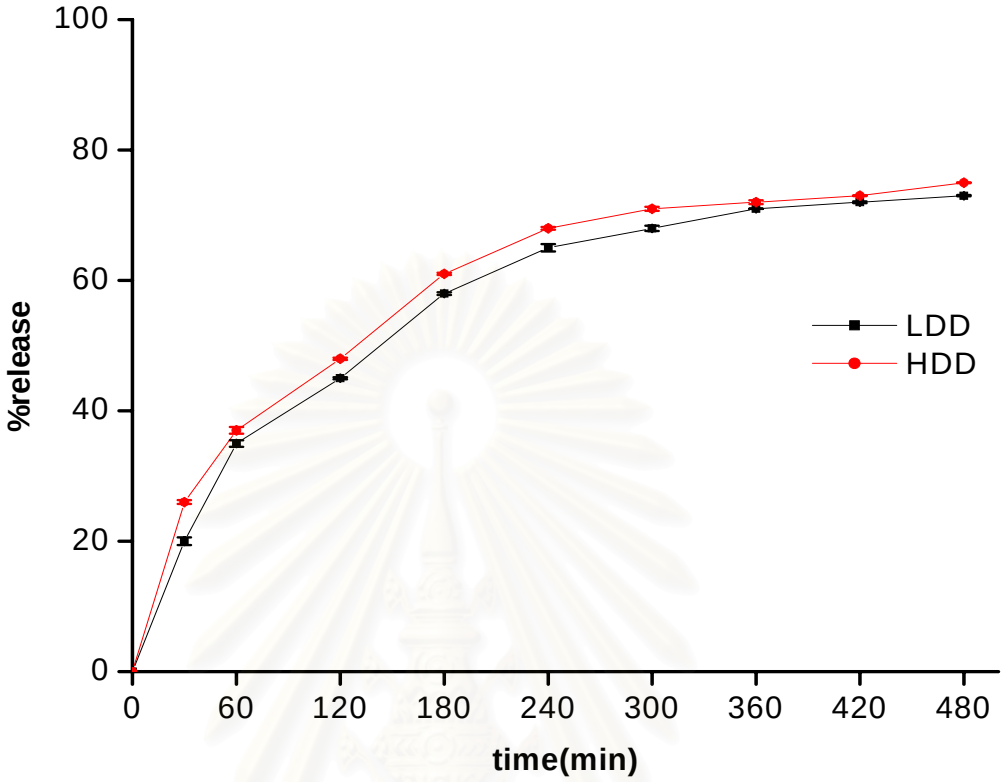

Figure 4.6 The DS release profile for the low (LDD) and high (HDD) degrees of deacetylation of chitosan.

4.5.2 Effect of molecular weight

The DS release profiles of the beads at different molecular weight of chitosan were investigated and shown in Figure 4.7. Similar to effect of the %DD, the release profiles for all plots increase rapidly in the first 240 mins and almost constant after that. However, no significant difference was found via increasing chitosan's molecular weight. This is in contrast to what reported by Genta et al. (1998) where the molecular weight was examined at the very high range, 70,000 to 2,000,000 Dalton.

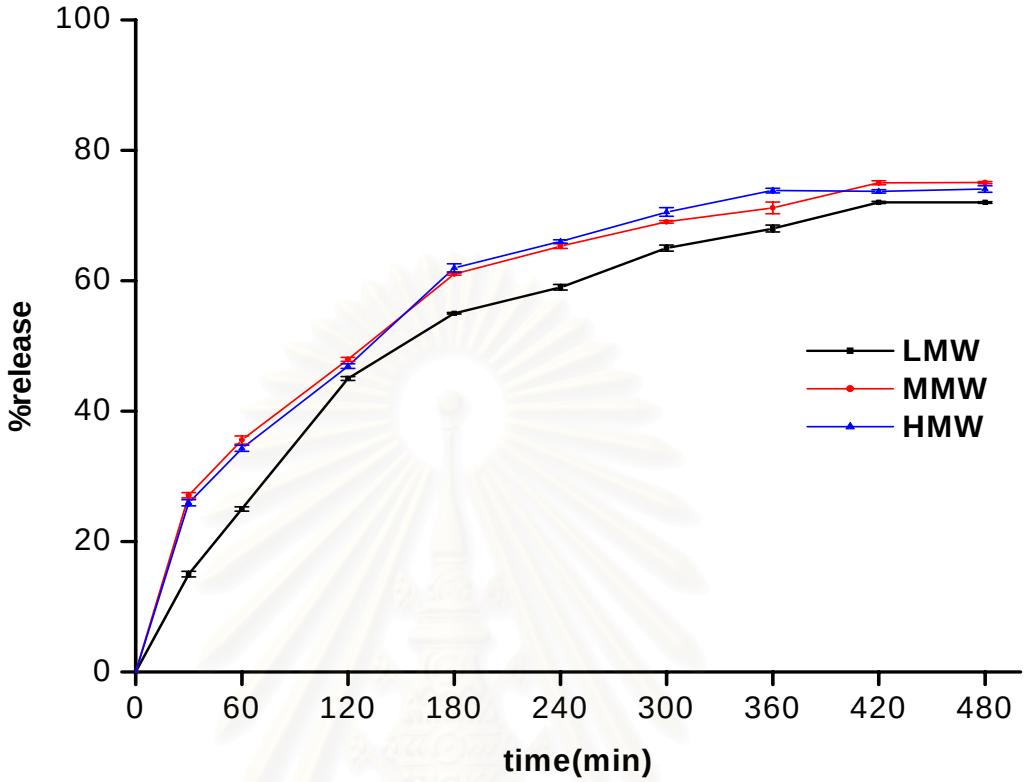

Figure 4.7 The DS release profile for the low (LMW), medium (MMW) and high (HMW) molecular weights of chitosan.

4.5.3 DS release studies from chitosan-alginate multilayer beads

The chitosan-alginate multiplayer coated matrix, alginate/chitosan/alginate, was prepared. The SEM micrograph of the cross-section was shown in Figure 4.8. The black region indicated the coated layer. The mean particles size of the multiplayer beads coated by two concentrations, 0.5% and 1.0%, of chitosan were 825 ± 5 and 865± 4 μm, respectively (Table 4.2). Note that concentration of alginate was kept constant at 0.5 % solution. The shape of chitosan-alginate multiplayer beads was almost spherical. The

swelling behavior of the coated beads were studied in both acidic and basic condition similar to SGF (simulate gastric fluids) and SIF (simulate intestinal fluids), respectively. For the second layer, increase in the concentration of chitosan led to a slight increase in the size of the matrix beads. The multilayered beads showed an increase in particle size, probably due to the coating (Table 4.2). The results show that swelling index of the coated beads after 5 h is less than 100% for both acidic and basic solutions (Table 4.2). This is in good agreement with that reported by Yotsuyanagi et al., 1991.

Table 4.2 Properties of multilayer chitosan-alginate beads with different in concentration of chitosan.

Chitosan conc. (%)	Mean sizes(μm) (±SD)	Swelling Index(%) (incubate for 5 h)	
		0.1N HCl (±SD)	phosphate buffer (±SD)
0.25	816± 5	64 ±0.80	85.9± 0.45
0.5	825 ± 5	64 ±0.50	86.7± 0.30
1.0	865± 4	68± 0.40	95.6± 0.45

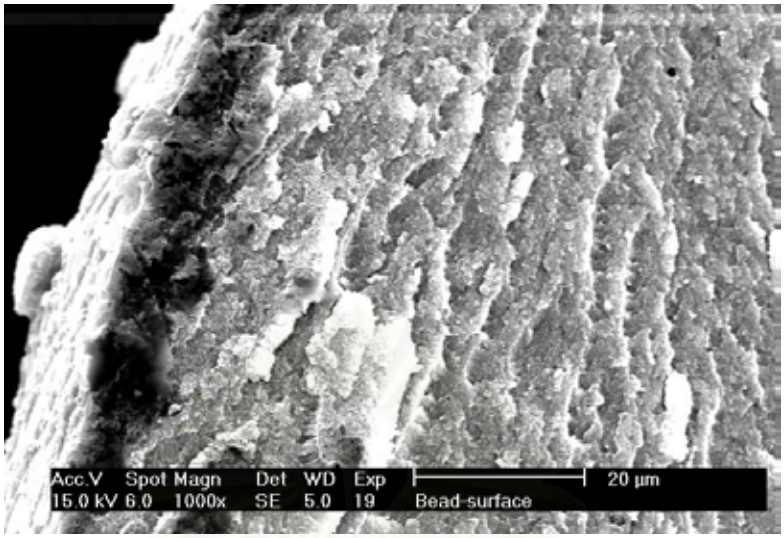

Figure 4.8 SEM-micrograph indicated surface of chitosan-alginate multilayer beads.

Similarly to chitosan beads, chitosan microparticle formed gel and dissolve gradually in acidic medium of pH 2.0. Therefore, DS release study was performed only in phosphate buffer of pH 6.8. The percentage release of DS from the microparticles was plotted as a function of time in Figure 4.9. Those of chitosan beads were, again, given in the same figure for comparison.

The drug release profile from multilayer beads was shown in Figure 4.9, under condition similar to SIF at pH 6.8. From multilayer beads coated with 1.0 % chitosan, no drug release was observed while at 0.25% and 0.5 % chitosan 2nd coated beads, only a small amount of drug was released. These are much lower those of the chitosan beads and microparticles. It can be clearly seen that the percentage of drug release was controlled by the thickness of the coated layers (Table 4.2) and hence, the concentrations

of the chitosan coating solution. It was expected from this data that an idea of coated bead can be further developed to be continuous release drug delivery system.

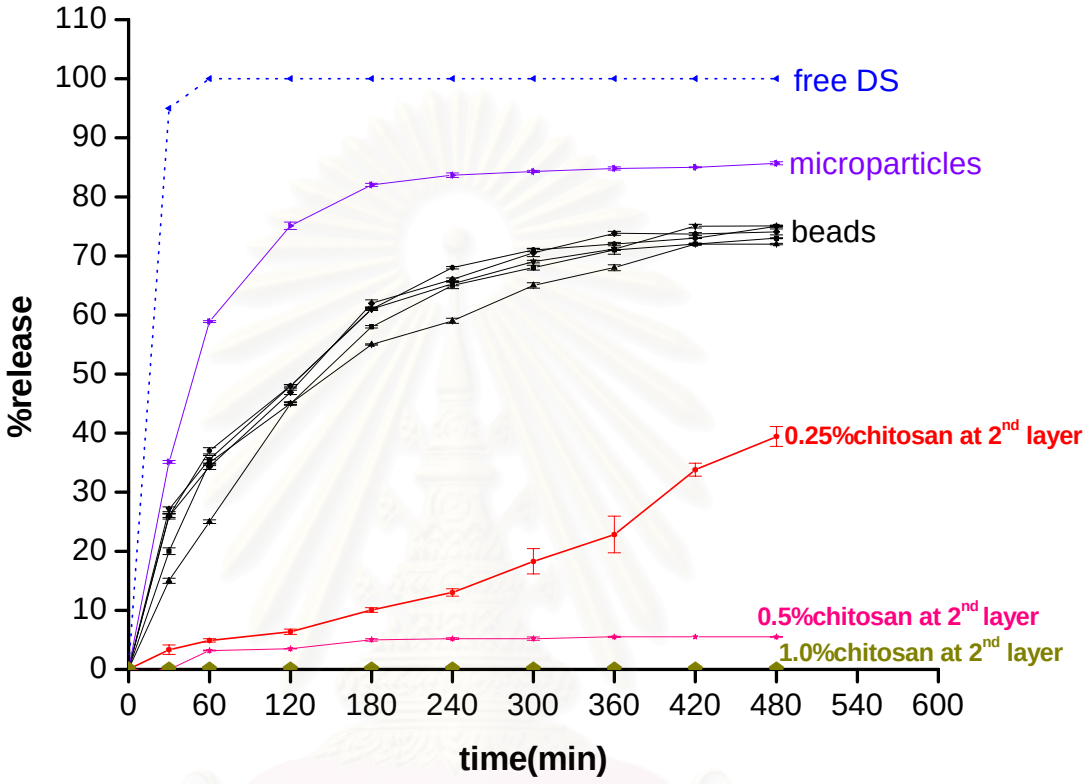

Figure 4. 9 Release profiles of DS from the matrices chitosan at pH 6.8.

4.6 Computer Simulation Results

4.6.1 Validation of *ab initio* glucosamine-water potential function

As it is known that the most important factor indicating quality of the potential function is the correlation between the positions of the energy minima obtained from the quantum chemical calculation and from the analytical function. To examine the quality of the function, stabilization energies of the configurations shown in an inset of Figure 4.10a were then calculated using *ab initio* SCF method (ΔE_{SCF}) and using the function (ΔE_{FIT}). Here, O atom of water molecule is in C3-C14-O18 plane of the ligand and this plane is perpendicular to the plane of H-O-H of water molecule. The distance *r* between O atom of water and center of glucosamine is varied from 3.2 to 9.5 Å. The plot in Figure 4.10a shows that the differences in the position to the minima as well as the interaction energies are almost negligible. The plot approaching zero at the distance of about 7.5 Å justifies that correction of the Culombic interactions beyond the cut-off distance in the computer simulations can be neglected. Further confirmation of the quality of the fit is the comparison of all data points (Fig.4.10b). Perfect agreement would have implied a straight line of unit slope, and the scatter about this line gives a graphical measure of the quality of the fit. The plot indicates a good agreement between both data sets, especially for the attractive regions, which is important for prediction of the simulation results.

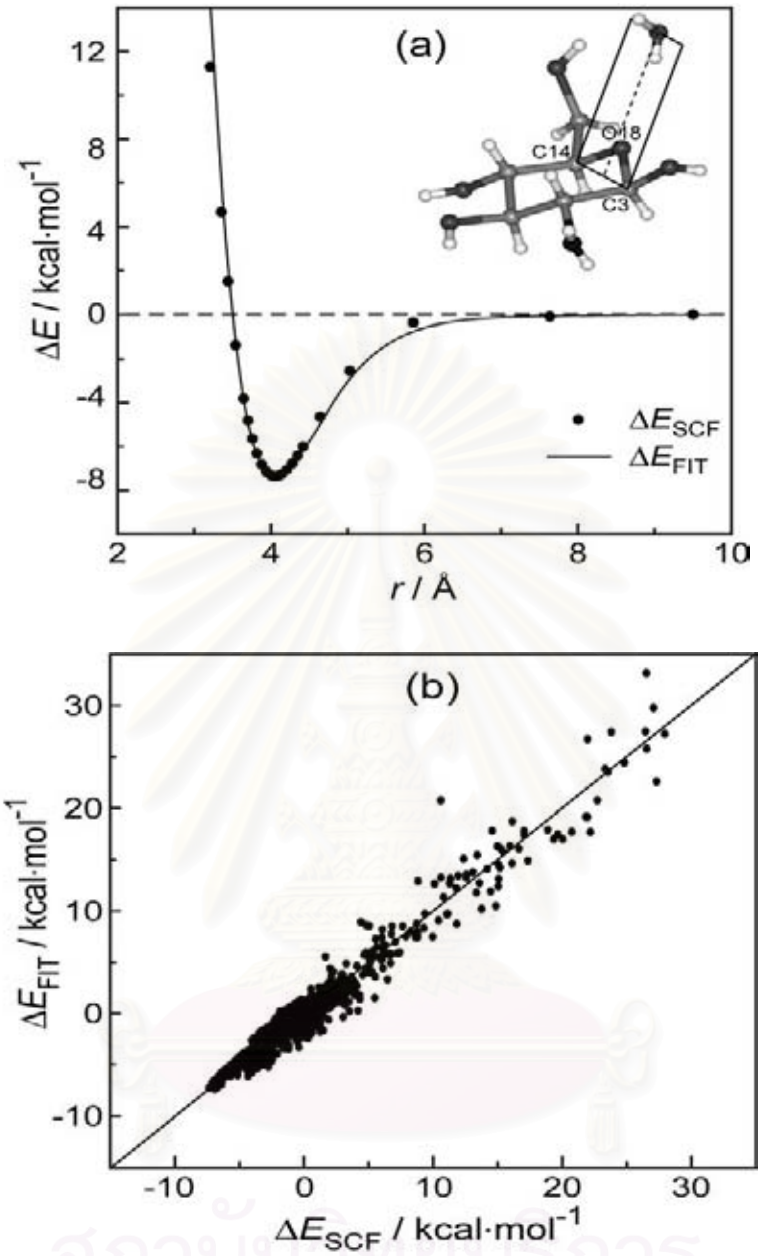

Figure 4.10 Glucosamine-water stabilization energies obtained from *ab initio* self-consistent field calculation (ΔE_{SCF}) and from fitting function (ΔE_{FIT}); (a) 23 values of the dimer configurations given in the inset and (b) the energies of 370 dimer configurations, see text for more details.

4.6.2 Solvation structure of glucosamine from MC simulation

The atom-atom radial distribution functions (RDFs) from nitrogen (N) and oxygen (O) atoms of glucosamine molecule (see Figure 3.4 for glucosamine structure) to water molecules are displayed in Figure 4.11a–f. For all plots, the RDFs to H of water are detected before those to O atom. This indicates preferential orientation of water molecule in which one of its H atom is oriented to point toward N or O atoms of glucosamine. The plots show well defined peaks, except that of O16 atom, centered at about 3 Å (Figure 4.11e).

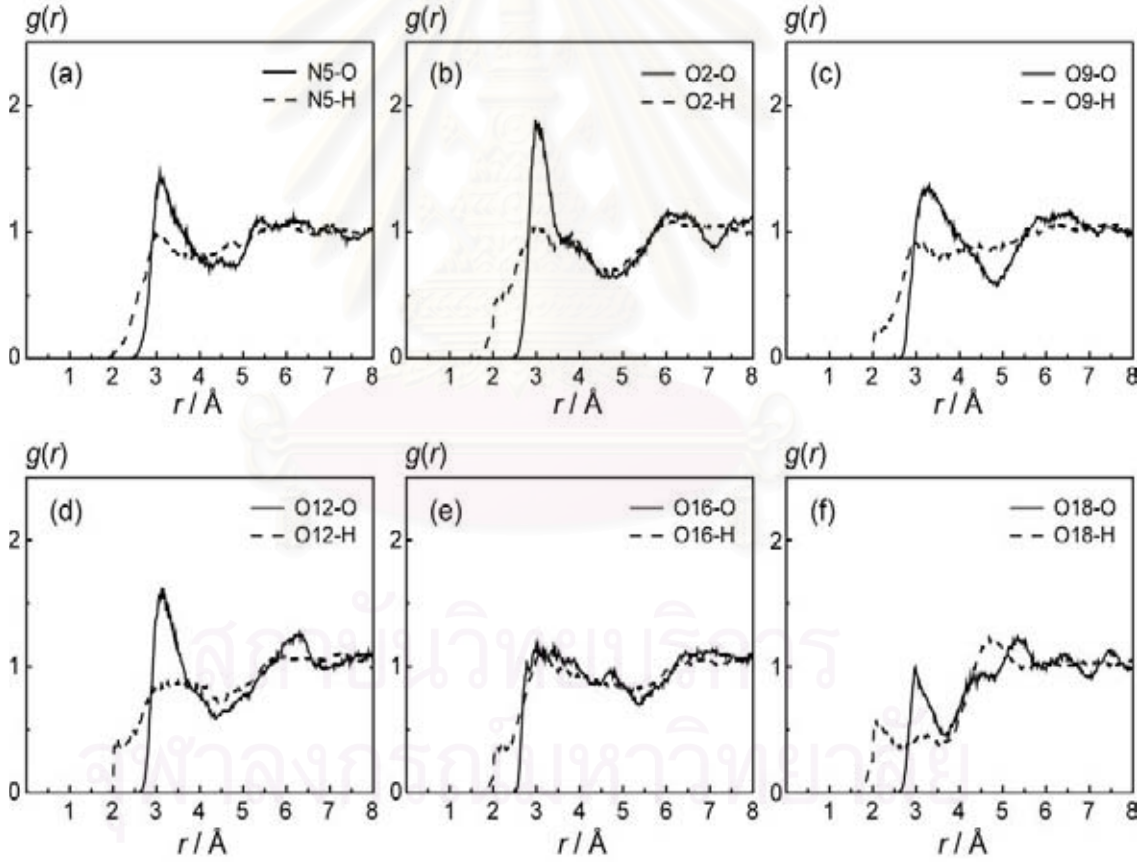

Figure 4.11 Radial distribution functions from O (solid line) and H (dash line) atoms of water to N5, O2, O9, O12, O16 and O18 atoms of glucosamine.

The running integration numbers up to the first minima of the N5-O, O2-O, O9-O, O12-O, and O18-O RDFs are 7.4, 4.7, 11.2, 7.7 and 2.2 water molecules, respectively. As it is commonly agreed that H-bond is established when the distance between donor hydrogen and acceptor oxygen is less than 2.4 Å, the coordination numbers of hydrogen atoms of water molecules are integrated up to 2.4 Å and the obtained values of the N5-H, O2-H, O9-H, O12-H, O16-H and O18-H RDFs are 0.2, 0.8, 0.3, 0.6, 0.5 and 1.0, respectively. This data as well as an appear of the first peak or the hump of the RDFs from N or O atoms of the ligand to H atom of water indicates clearly that water molecules lying under the first peaks the O-O RDF to O atoms at 3 Å form hydrogen bond with glucosamine molecule. The obtained coordinate numbers, which are quite high, do not indicate numbers of hydrogen bonding because of the overlapping of the RDFs. This fact is confirmed by the broaden or splitting of these peaks. More details investigation of number of water molecules as well as their orientation are given in the next paragraph. Note that:

(i) the RDF of O18-H shows very sharp first peak which indicates strong H-bond between water and O18, and

(ii) the difference between the distance to the first maxima of the O18-O and O18-H RDFs which almost equivalent to the O-H bond length of water indicates a formation of linear H-bond.

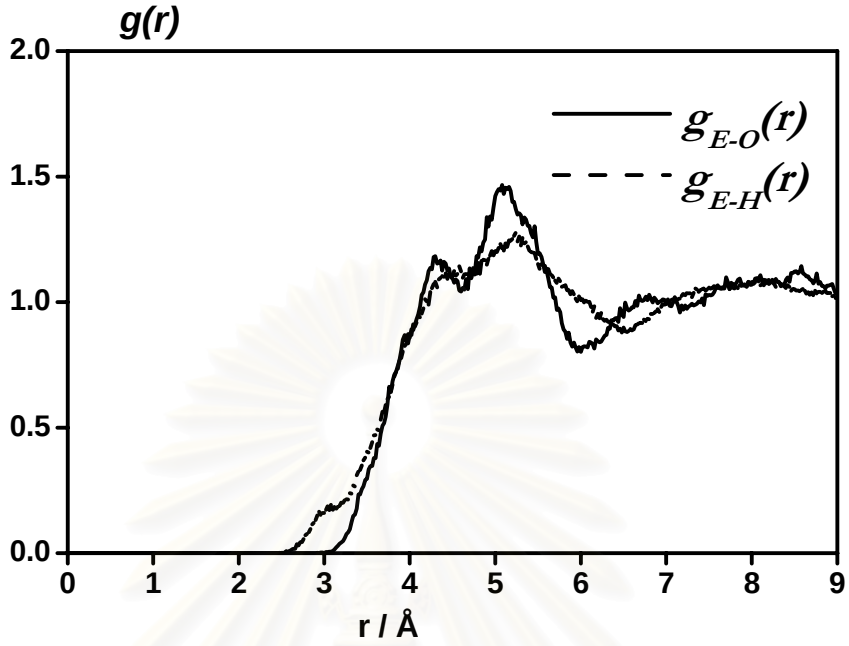

Figure 4.12 Radial distribution functions from O (solid line) and H (dash line) atoms of water to the center of glucosamine for the entire volume.

In Figure 4.12 total radial distribution functions from center of glucosamine for the entire volume (E) to oxygen and hydrogen atoms of water, respectively $g_{E\text{-}O}(r)$ and $g_{E\text{-}H}(r)$, have been calculated. The plot displays 2 peaks, centered at about 4.3 and 5.1 Å. Their running integration numbers, integrated up to the corresponding minima of 4.6 Å and 6.0 Å, are 7 and 26 water molecules, respectively. Due to complexity of the glucosamine molecule, the RDFs between atoms of glucosamine and those of water molecules overlap each other. Therefore, $g_{E\text{-}O}(r)$ and $g_{E\text{-}H}(r)$ plots do not give much information.

4.6.3 Solvation structure of glucosamine from MD simulation

The atom-atom RDFs from nitrogen and oxygen atoms of glucosamine molecule to oxygen and hydrogen atoms of water molecules are displayed in Figure 4.13a-f. The running integration numbers up to the first minima of the N5-O, O2-O, O9-O, O12-O, O16-O and O18-O RDFs are 4.3, 4.0, 3.4, 5.8, 3.9 and 2.0 water molecules, respectively.

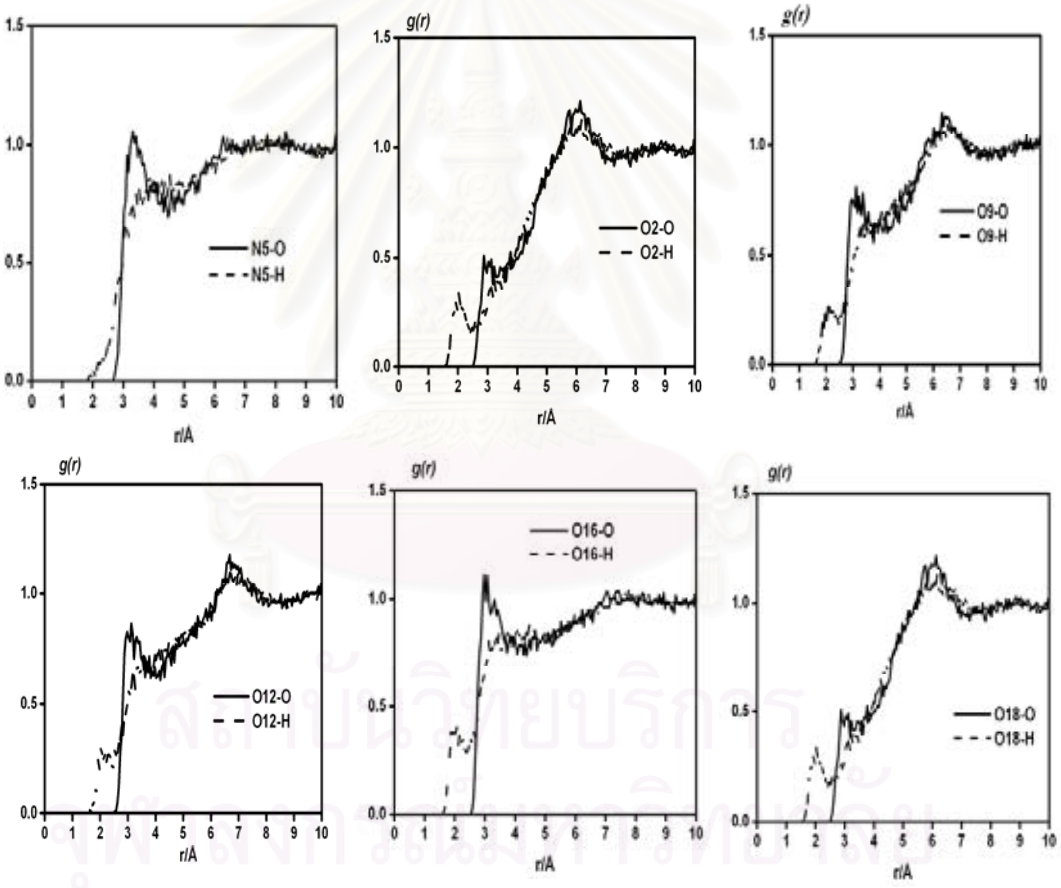

Figure 4.13 Radial distribution functions from O (solid line) and H (dash line) atoms of water to N5, O2, O9, O12, O16 and O18 atoms of glucosamine from MD simulation.

In addition, the RDF from the center of the glucosamine to the oxygen and hydrogen atom of water, $g_{EO}(r)$, and $g_{EH}(r)$ was shown in Figure 4.14.

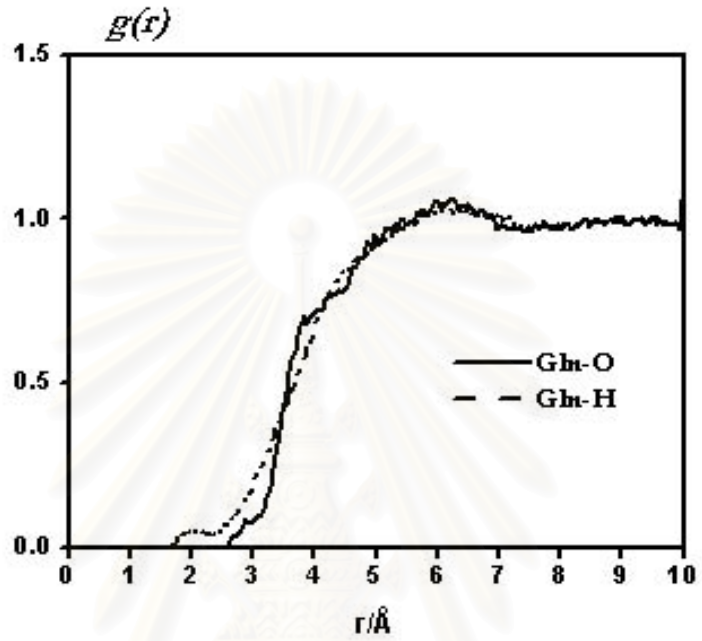

Figure 4.14 Radial distribution functions from O (solid line) and H (dash line) atoms of water to the center of glucosamine for the entire volume (from MD simulation).

It is interesting to note that the pattern of the RDFs to the H and O of water for all plots are similarly to those obtained from the MC simulation. However, the H-RDF peaks obtained from MD simulation is shaper than those of MC simulation. That means that hydrogen bands can be clearly represented. Significant difference takes place on the entire RDFs from the center of glucosamine obtained from MC (Figure 4.12) and MD (Figure 4.14) simulations, especially on the $g_{E-H}(r)$ RDF. The MC RDFs are much pronounce than those of the MD data, indicating a clearer solvation shell of glucosamine. The difference is surely not due to the method used, MC or MD, because both methods

are well established. Therefore, the only source of discrepancy would be due to the quality of the potential function. The force field potential is known to the lost of some specific details of the molecular structure as well as the solution. For their reason, discrepancy was found when the force field potential is used (MD simulation in the study) to represent the interaction between glucosamine and water in which hydrogen bonding could be very important and better represented by *ab initio* fitted potential (employed in the MC simulation).

4.6.4 Solvation structure of chitosan tetramer

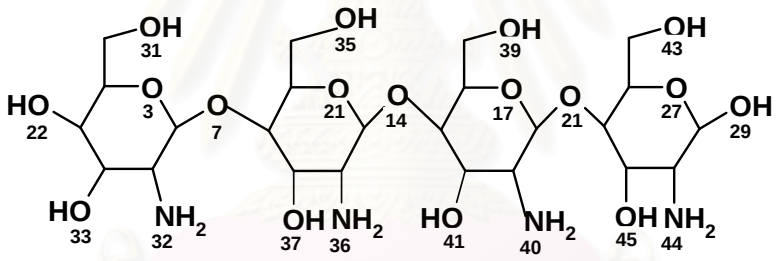

Figure 4.15 Structure of chitosan tetramer with atomic numbering.

The solvation structure of the chitosan tetramer molecule has been investigated by the molecular dynamic simulation using force field potential and Amber 7.1 program. The atom-atom RDFs from nitrogen and oxygen atoms of chitosan tetramer to water molecules are displayed in Figures 4.16-4.21. Characteristics of the RDFs for both glucosamine molecules and chitosan tetramer were evaluated and summarized in Table 4.3.

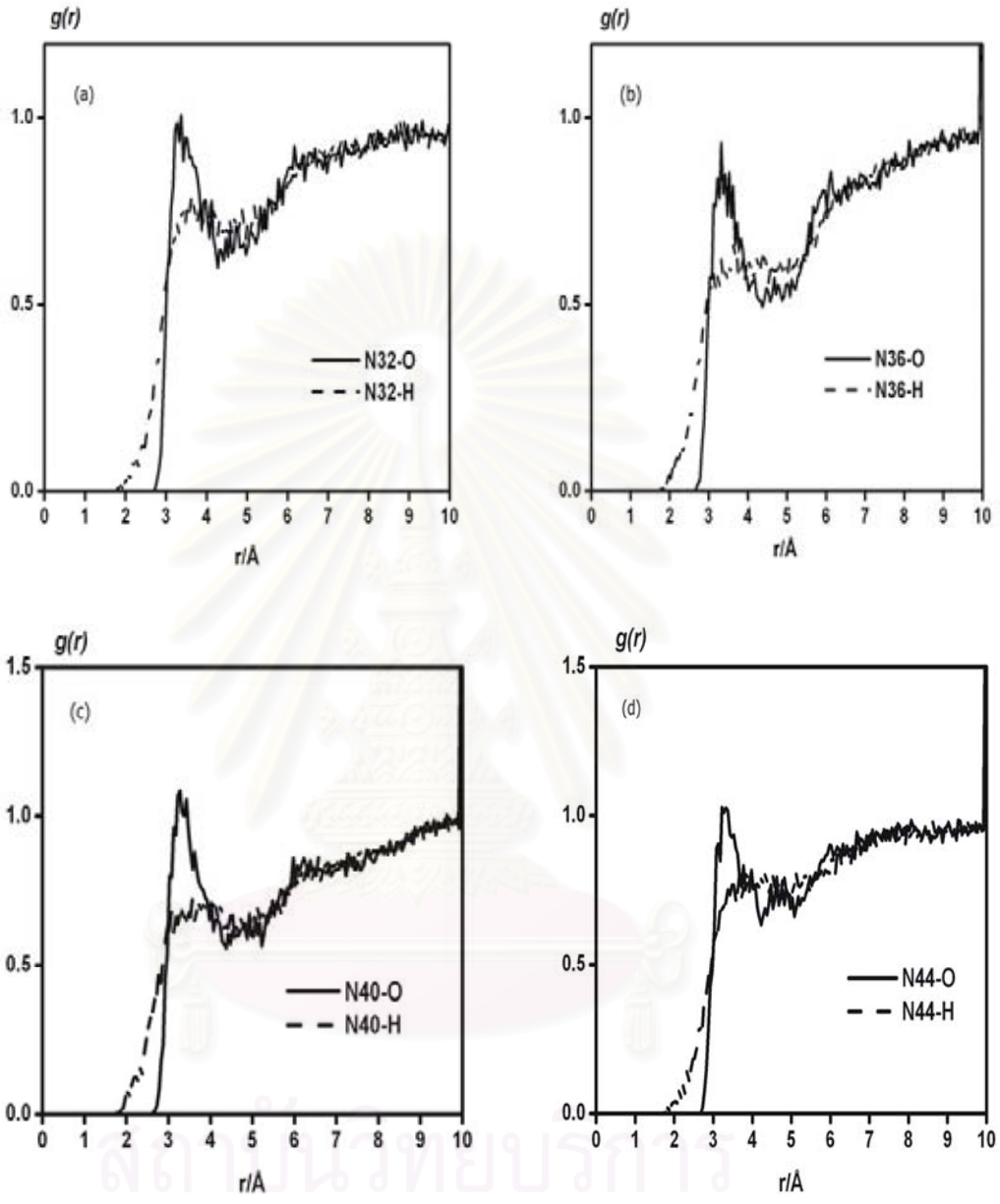

Figure 4.16 Radial distribution functions from O (solid line) and H (dash line) atoms of water to amine group(-NH_2) included N32, N36, N40, and N44 atoms of tetramer.

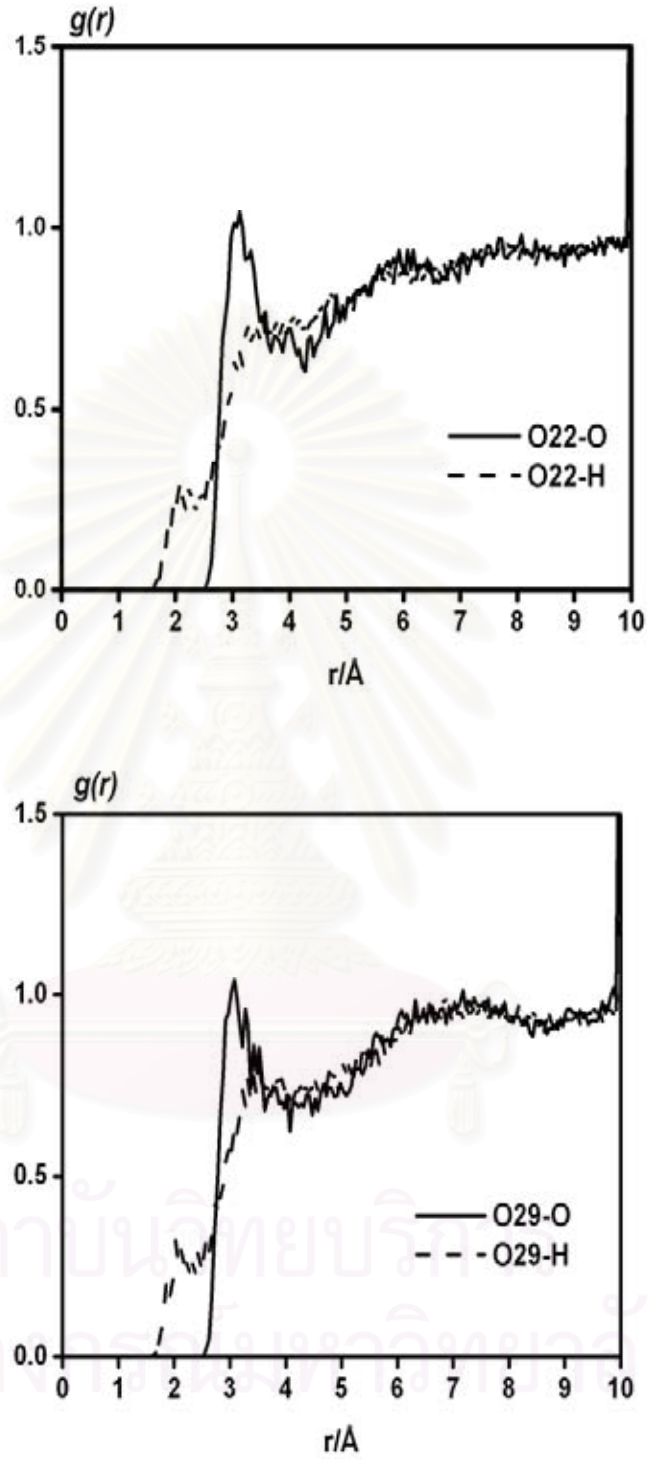

Figure 4.17 Radial distribution functions from O (solid line) and H (dash line) atoms of water to oxygen atom in hydroxyl group at terminal chain of tetramer.

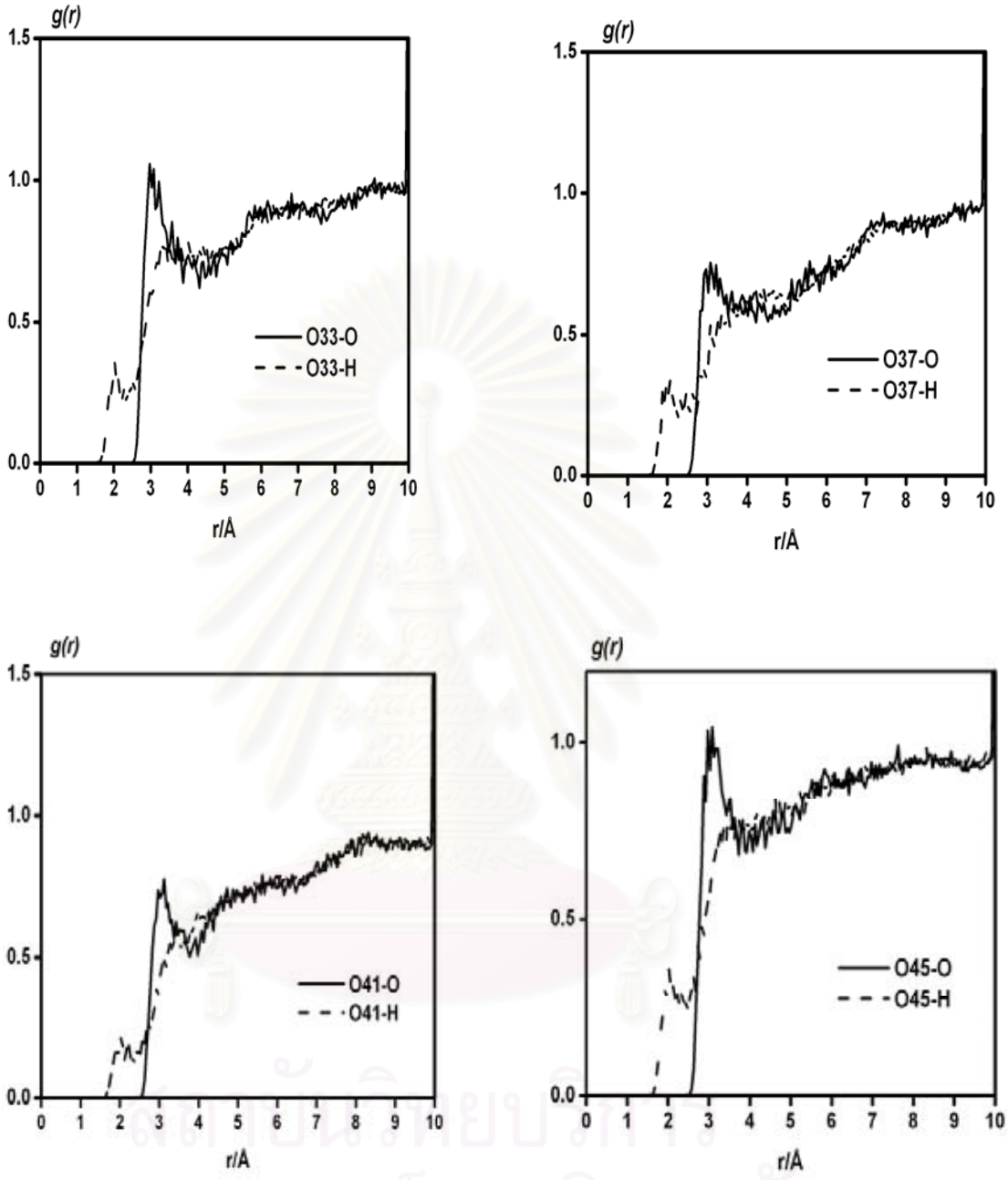

Figure 4.18 Radial distribution functions from O (solid line) and H (dash line) atoms of water to oxygen at hydroxyl group at C-3 in each monomer of tetramer.

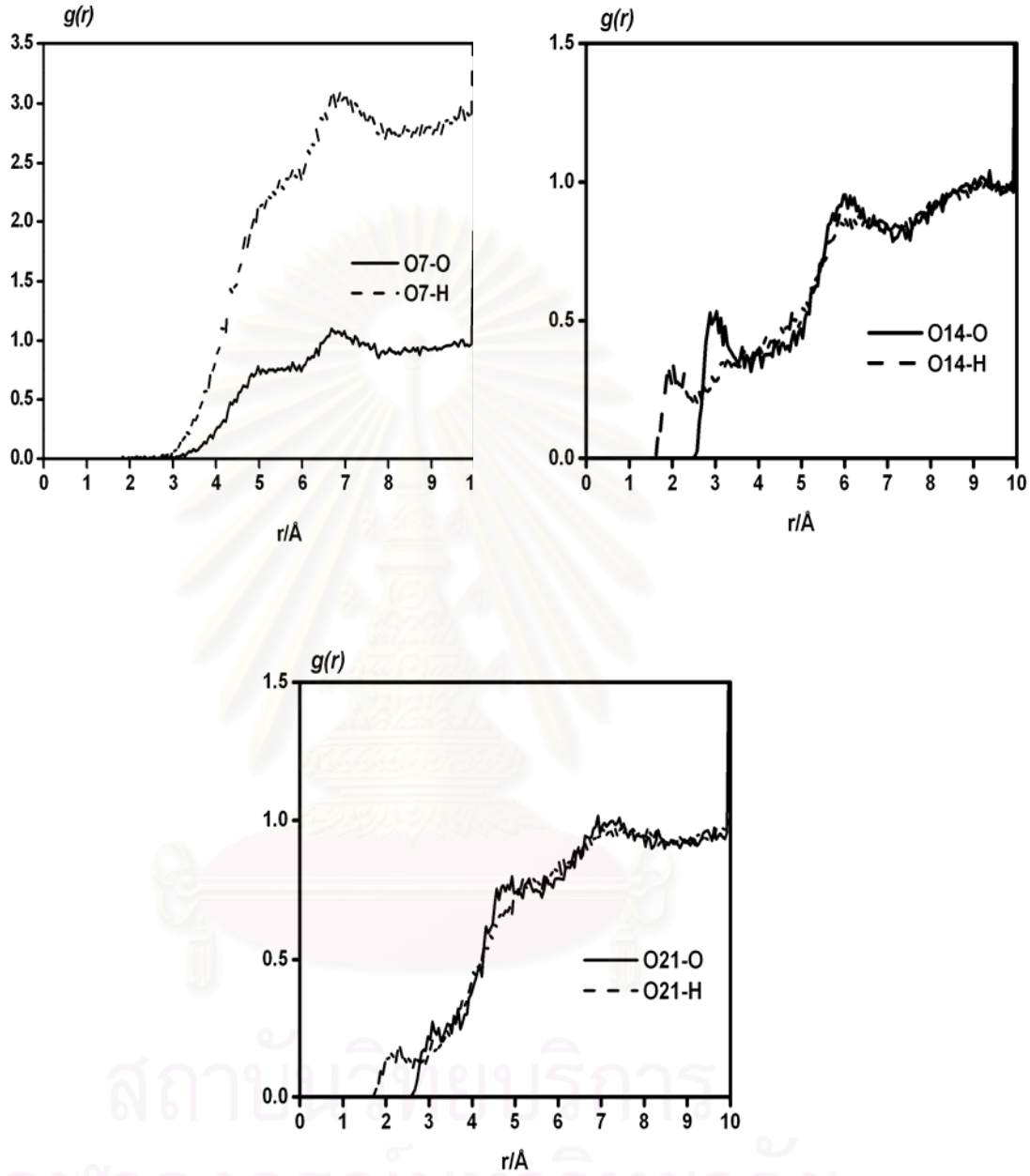

Figure 4.19 Radial distribution functions from O (solid line) and H (dash line) atoms of water to oxygen atom at β-1-4–glycosidic linkage of tetramer.

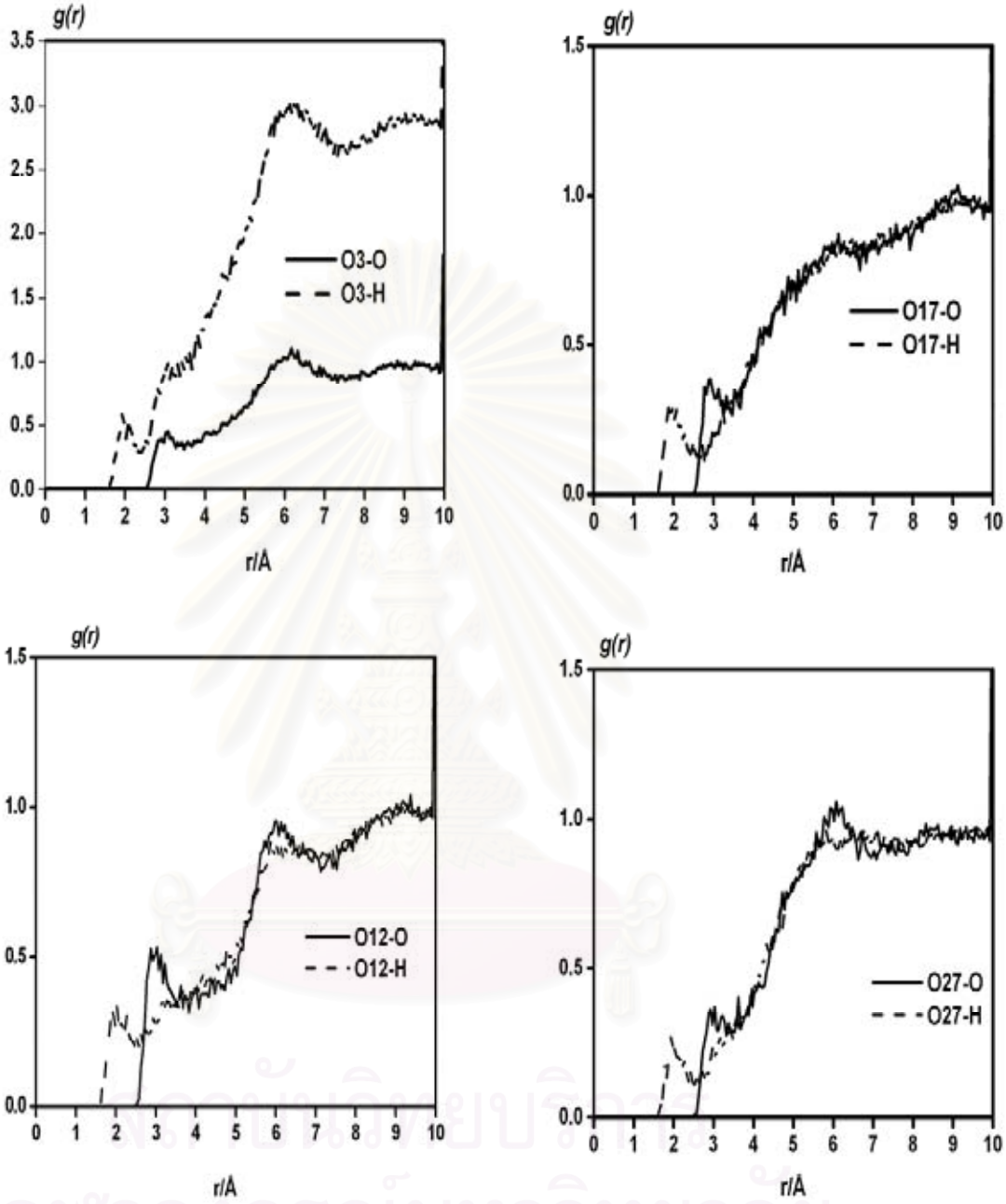

Figure 4.20 Radial distribution functions from O (solid line) and H (dash line) atoms of water to oxygen atom in ring of tetramer.

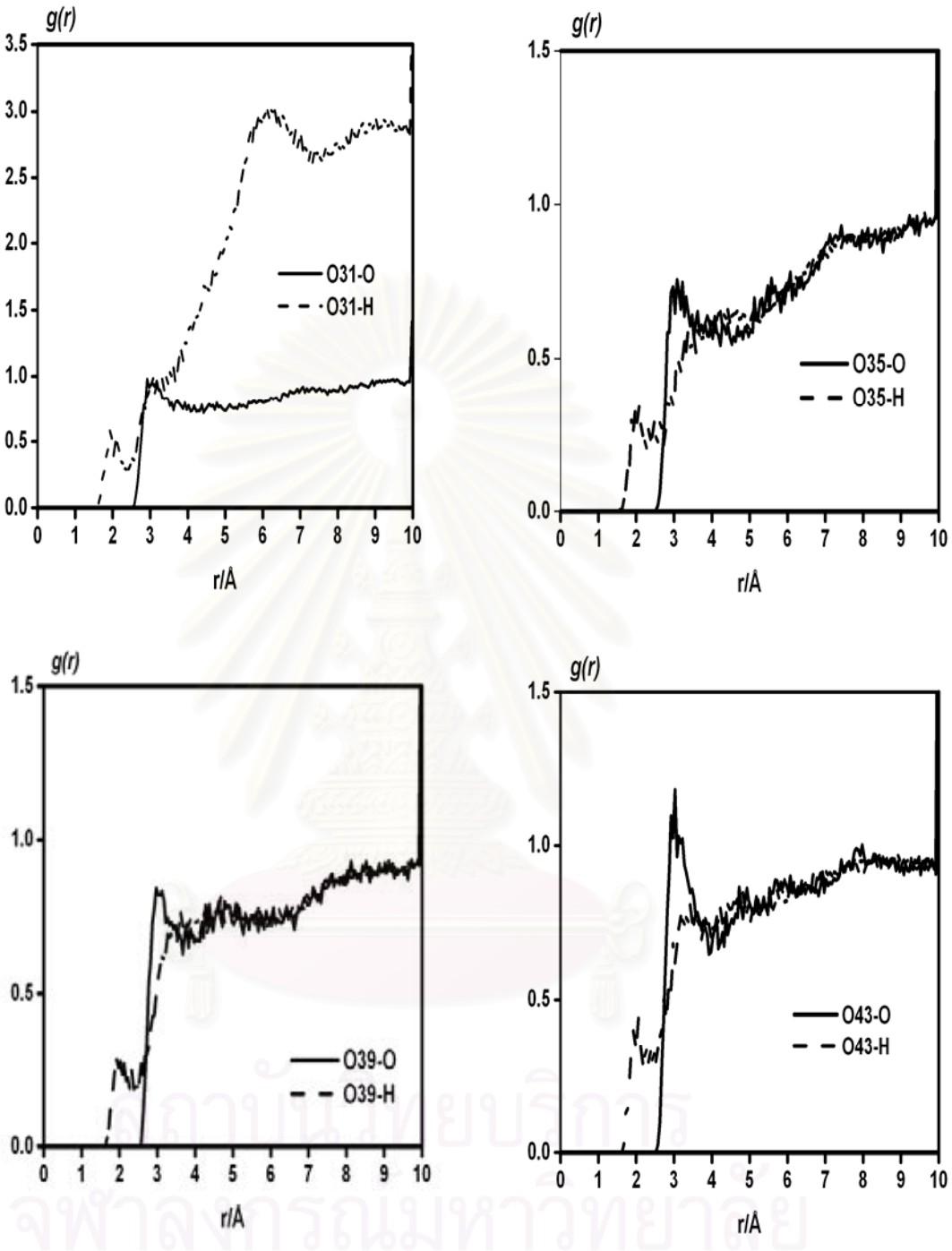

Figure 4.21 Radial distribution functions from O (solid line) and H (dash line) atoms of water to oxygen atom in hydroxyl group at C-6 in each monomer of tetramer.

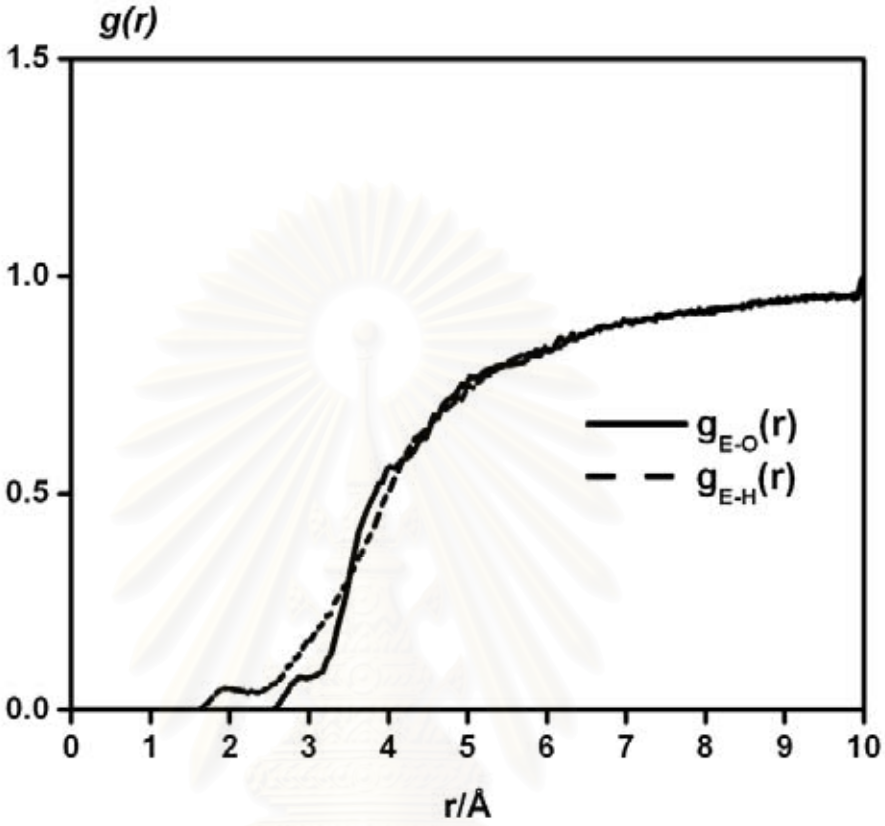

Figure 4.22 Radial distribution functions from O (solid line) and H (dash line) atoms of water to the center of tetramer molecule for the entire volume (from MD simulation).

Table 4.3 The solvation structure for each solvated group in chitosan monomer and tetramer molecule (see Fig. 3.4 and 4.13 for glucosamine and tetramer structure)

Group	Atom	Glucoasmine				Tetramer From MD simulation	
		From MC simulation		From MD simulation			
		r*	n(r)	r*	n(r)	r*	n(r)
$-NH_2$	N5 (gluocosamine)	4.0	7.4	3.8	4.3	-	-
$-NH_2$	N32, N36, N40,N44 (tetramer)	4.0	-	-	-	3.4	6.3
-OH[a]	O2, O12 (glucosamine) O22 and O29 (tetramer)	4.0	6.2	3.8	3.8	3.8	4.5
-OH[b]	O16 (glucosamine) O31, O35, O39, O43 (tetramer)	4.0	4.0	3.8	4.0	3.8	5.3
-OH[c]	O9 (glucosamine) O33, O37, O41, O45 (tetramer)	4.0	11.2	3.8	3.4	4.0	5.0
-O-[d]	O6 (glucosamine) O3,O12,O17,O27 (tetramer)	4.0	2.2	4.0	2.0	4.0	2.2
-O-[e]	O7,O14, O21 (tetramer)	-	-	-	-	4.0	0.8
center of mass	-	4.6	7	4.6	7	4.2	10

[a]*hydroxyl group at terminal,*
[b]*hydroxyl group at C-6 in each monomer of chitosan in the chain*
[c]*hydroxyl group at C-3 in each monomer of chitosan in the chain*
[d]*oxygen atom in the ring*
[e]*oxygen atom at β 1,4-glycosidic linkage*
[*]*radius at first peak, Å*

From the RDF patterns, of both monomer and tetramer appeared at almost the same distance which are about 3.8-4.0 Å. The running integration number indicates that

the salvation at the oxygen atom in the hydroxyl and amine groups is much higher than that at oxygen atom positions at molecular linkage and oxygen atom in the ring. The MD simulation, results the average coordination number of 10 water molecules in the first salvation shells.

CHAPTER 5

CONCLUSION

The present study, simulate the used of chitosan for controlled-release in oral drug delivery system. The effect of various parameter such as %DD, molecular weight and characteristic of the matrices, chitosan beads, microparticles and multilayer beads have been explored. Diclofenac sodium, DS was used as a model drug and chitosan was used as supported polymer. The investigations lead to the

Chitosan beads/microparticles

1. The bead and microparticles were prepared using the gelation and dispersion methods, yield a smooth surface with spherical mean size of 860 and 37 μm, respectively.
2. Swelling index of dry beads was found to increase with the increasing of % DD and molecular weight.
3. highest drug loading efficiency of 83% was observed for medium molecular weight of chitosan (MMW=400,000) while lowest value of 57% was found at low molecular weight (LMW=150,000).
4. The release rate for all type of chitosan increases exponentially for the first 5 h and remain constant afterward.
5. Maximal release from the matrices beads microparticles take place at approximately 75% and 85%, respectively.

Chitosan-alginate multilayer beads

1. The particle shows smooth surface, spherical shape with the size ranging from 825 to 865 μm.

2. Multilayer alginate/chitosan/alginate beads were prepared by giving post-treatment of the matrices with either with alginate, chitosan and alginate, respectively.
3. Swelling index of the multilayer beads increase with the increased concentration of chitosan in coagulation fluid.
4. The release from the multilayer beads is about 5-39% when they are coated by 0.25% and 0.5% chitosan and drug release does not take place when the beads are coated by 1.0% chitosan. This result indicates that the multilayer beads show potential to be used as a delay release in the drug delivery system.

The solvation structure from computer simulation

The solvation structure of chitosan was studied using MC and MD two simulation methods, with the newly and force field potential function, respectively. The results show that both simulations yield almost identical data, in terms of radial distribution functions and integration numbers. Slightly difference was observed when characteristic of hydrogen bond was considered, i.e., the force field potential gives the data with too strong hydrogen bond. This lead to a conclusion that the force field potential, which is much simple and already available in the commercial software, is suitable for the studying of complicated system.

The MD simulation was extended to chitosan tetramer using force field potential. The result show the average condition numbers of 10 water molecules.

Further study

For further study of controlled drug release design for oral application the following recommendations are made:

1. Chitosan-alginate multilayer beads might be further tested in acid condition (mimic as simulated gastric fluid) for disintegration time testing.
2. The matrix need to further study the ratio of entrapment of drug between inner and outer phase for enhancers uptake on drug adsorption.
3. Further research is essential to simulated chitosan-diclofenac interaction to get information of the actual chemistry of interaction between chitosan and drug.
4. These bead systems can be tested with water insoluble drugs of oral drug delivery system.

REFERENCES

1. Alagona, G., Ghio, C., and Kollman, P. A. (1985). Monte Carlo Simulations of the Solvation of the Dimethyl Phosphate Anion. J. Am. Chem. Soc. 107:2229-2238.

2. Alder, B. J., and Wainwight, T. E. (1960). Studied in Molecular Dynamics. II. Behavior of a Small Number of Elastic Spheres. J. Chem. Phys. 33:1439-1451.

3. Amzel, L. M. (2001). Molecular Modeling. Course # 100.705.1

4. Apocella, A., Cappello, B., Delnobile, M.A. larotonda, M.I.. mensiticri, G. and Nicola, L. (1993). Biomaterials. 14:83.

5. Balaji Narasimhan, Nikolaos A. Peppas. (1997). Molecular Analysis of Drug Delivery Systems Controlled by Dissolution of the Polymer Carrier. J. Pharm. Sci. 86, 3 (March).

6. Baldwin, S.P. and Saltzman,W.M.(1998). Materials for protein delivery in tissue engineering. Adv.Drug Deliv. Rev. 33:71-86.

7. Basma, M., Sundara, S., Calgan, D., Vernali, T., and Woods, R.J. (2001). Solvated Ensemble Averaging in the Calculation of Partial Atomic Charges. J. Comput. Chem. 22, 11:1125-1137.

8. Benedict, W. S., Gailar, N., and Plyler, E. K. (1956). Rotation-Vibration Spectra of Deuterated Water Vapour. J. Chem. Phys. 24:1139-1165.

9. Bernal, J.D. and Fowler, R.H. (1933). A theory of water and ionic solution with paricular reference to hydrogen and hydrogel ions. J. Chem. Phys. 1: 515-548.

10. Bodek, K.H. G. and Bak, W. (1999). Ageing phenomena of chitosan and chitosan-diclofenac sodium system detected by low-frequency dielectric spectroscopy. Eur. J. Pharm. Biopharm. 48:141-148.

11. Bodmeir, R., Chen,H. and Pacrataluk. (1989). A novel approach to the oral delivery of micro or nanoparticles. Pharm. Res. 6, 5:413-417.

12. Bonferoni, M. C., Rossi, S., Ferrari, F., Stavik, E., Romero, A.P. and Caramella, C. (2000). Factorial Analysis of the influence of Dissolution Medium on Drug Release From Carrageenan-Diltiazem Complexes. AAPS Pharm. Sci. Tec. 1, 2 (article 15).

13. Bonvin, M. M., and Debertorello, M. M. (1994). In-Vitro Drug-Release from Chitosan Membranes: Study of the Mechanisms of Permeation. Polym. Bull. 32: 69-75.

14. Bravo, S. A., Lamas, M. C., and Salomon. C. J. (2002). In-Vitro Studies of Diclofenac Sodium Controlled-release from Biopolymeric Hydrophilic Matrices. J. Pharm. Pharm. Sci. 5, 3:213-219.

15. Cambridge Crystallographic data center, Cambridge, UK. (www.ccdc.cam.ac.uk).

16. Canto, J., Fernandez, Y., Pons, M., Giralt, E. and Perez, J. J. (1999). Molecular dynamics study of kaliotoxin in water. Int. J. Biol. Macromol. 24:1-9.

17. Cardinal, J. R., Curatolo, W. J., and Ebert, C. D. (1990). Chitosan Compositions for Controlled and Prolonged Release of Macromolecules. U.S.Patent. 4,895,724.

18. Cavalieri, E. F., Chiessi, M., Paci, G. , Paradossi, A., Flaibani, and Cesaro, A. (2001). Conformational Dynamics of Hyaluronan in Solution. 1. A 13C NMR Study of Oligomers. Macromolecules. 34:99-109.

19. Chien, Y.W. (1995). Biopharrmaceutics basis for transmucosal delivery. Pharm. Sci. 4:257-275.

20. Chien., Y.W. (1992). Novel Drug Delivery Systems. vol.1 Second Edition New York.: Marceld EKKER, Basel. Hongkong.

21. Cornell, W.D., et.al. (1995). A second generation force field for the simulation of Proteins, Nucleic acids, and organic molecules. J. Am. Chem. Soc. 117:5179-5197.

22. Cummins, P.L. and Gready, J.E. (1997). Coupled Semi-empirical Molecular Orbital and Molecular Mechanics Model (QM/MM) for Organic Molecules in Aqueous Solution. J. Comput. Chem. 18, 12:1496-1512.

23. Denkbas, E.B., and Odabasi, M. (2000). Chitosan Microspheres and Sponges: Preparation and Characteriaztion. J. Appli. Polym Sci. 76:1637-1643.

24. Deuchi, K., Kanauchi, O., Imasato, Y., and Kobayashi, E. (1994). Decreasing Effect of Chitosan on the Apparent Fat Digestibility by Rats Fed on a High-Fat Diet. Biosci. Biotechnol. Biochem. 58:1613-1616.

25. Dodance, V., and Viliralam, V.D. (1998). Pharmaceutical applications of chitosan. Phram.Sci.Technol.Today. 1:246-253.

26. Dunning, T.H., and Hay, P.J. (1977). Methods of Electronic Structure Theory. vol. 3. New York:Plenum Press.

27. Edlund, V. and Albertsson, A.C. (2002). Degradable polymer microspheres for controlled drug delivery. Adv. Polym. Sci. 157:67-112.

28. Eiselt, P., Yeh, J., Latvala, R.K., Shea, L.D., and Mooney, D.J. (2000). Porous carriers for biomedical applications based on alginate hydrogels. Biomaterials. 21:1921-1927.

29. Felt, O., Buri, P., and Gurny, R. (1998). Chitosan: A Unique Polysaccharide for Drug Delivery. Drug Dev. Ind. Pharm. 24, 11:979-993.

30. Fraternali, V. and Gunsteven, W.F. (1996). An efficient mean solvation force model for use in molecular dynamics simulations of proteins in aqueous solution.. J. Mol. Biol. 256:939-948.

31. Frisch, M.J., Trucks, G.W., Head-Gordon, M., Gill, P.M.W., Wong, M.W., Foresman, J.B., Johnson, B.G., Schlegel, H.B., Robb, M.A., Replogle, E.S., Gomperts, R., Andres, J.L., Raghavachari, K., Binkley, J.S., Gonzalez, C., Martin, R.L., Fox, D.J., Defrees, D.J., Baker, J., Stewart, J.J.P., and Pople, J.A. (1998). Guassian 98, Revision A. Gaussian, Pittsburgh: P.A.

32. Genta, I., Perugini, P., and Pavanetto, F. (1998). Different Molecular Weight Chitosan Microspheres: Influence on Drug Loading and Drug Release. Drug Dev. Ind. Pharm. 24:779-784.

33. Gopferich, A.. (1996). Mechanism of polymers degradation and erosion. Biomaterials. 17:103-114.

34. Gupta, K.C., and Kumar, M.N.V.R. (2000). Drug release behavior of beads and microgranules of chitosan. Biomaterials. 21:1115-1119.

35. Hannongbua, S. (1996). Solvation of 1,4,7,10-Tetraazacyclododecane in Aqueous Solution As Studied by the Monte Carlo Method. J. Phys. Chem. 100:17655-17661.

36. Hannongbua, S. (1997). The role of non additive effects in the first solvation shell of Na^{+} and Mg^{2+} in liquid ammonia: Monte Carlo studies including three-body corrections. J. Chem. Phys. 106:14.

37. Hannongbua, S., and Rode, B. M. (1992). Monte Carlo Simulations of a Magnesium Ion in Liquid Ammonia. Chem. Phys. 162:257-263.

38. Hannongbua, S., Ishida, T., Spohr, E., and Heinzinger, K. (1988). Molecular Dynamics Study of a Lithium Ion in Ammonia. Z. Naturforsch. 43a:572-582

39. Hannongbua, S., Kerdcharoen, T., and Rode, B. M. (1992). Zinc(II) in Liquid Ammonia: Intermolecular Potential Including Three-Body Terms and Monte Carlo Simulation. J. Chem. Phys. 96:6945-6949.

40. Hart, J.P., Pfluger, H.D., Monzingo, A.F., Hollis, T., and Robertus. J.D. (1995). The Refined Crystal Structure of an Endochitinase from Hordeum vulgare L. Seeds at 1.8 A Resolution. J. Mol. Biol. 248:402-413.

41. Hauptmann, S., Mosell, T., Reiling, S., and Brickmann, J.(1996). Molecular dynamics simulations of the bulk phases of 4-cyano-4'-n-pentyloxybiphenyl. Chem. Phys. 208:57-71.

42. Hien, S., Ng, C.H., Chandrkrachang, S., and Steviens, W.F. (2000). A systematic approach to quality assessment system of chitosan. Proceedings of 8th International Chitin and chitosan Conference and 4th Asia pacific chitin and chitosan symposium. Yamaguchi, Japan:Edited by Iragami, T. Kurita, K. and Fukamizp. T:332-335.

43. Illum, L. (1998). Chitosan and its use as a pharmaceutical Excipient. Pharm. Res. 15, 9:1326-1331.

44. Jameela, S.R., and Jayakrishnan, A. (1995). Glutaraldehyde cross-linked chitosan microspheres as a long acting biodegradable drug delivery vehicle: studies on the in vitro release of mitoxantrone and in vivo degradation of microspheres in rat muscle. Biomaterials. 16:769-775.

42. Klock, G., Pleffermann, A., Ryser, C., Grohn, P., Kulttler, B., Hahn, H., and Zimmermann, U. (1997). Biocompatibility of manuonics acid-rich alginated. Biomaterials. 100:707-13.

43. Koseva, N., Manolova, N., Markova, N., Radoucheva,T., and Rashkov, I. (1999). Chitosan gel beads as drug carriers. Polym. Bull. 43:101-107.

44. Kubota, N. (1993). Molecular Weight Dependence of the Properties of Chitosan and Chitosan Hydrogel for Use in Sustained-Release Drug. Bull. Chem. Soc. Jpn. 66:1807-1812.

45. Kumar, M.N.V.R., (1999). Chitin and Chitosan fibers : A review,. Bull. Mater. Sci. 22:905.

46. Kurita, K. (1998). Chemistry and application of chitin and chitosan. Polym. Degrad. Stabil. 59:117-120.

47. Kyper, L., Ashton, D., Merz, K.M., and Kollman, P.A. (1991). J. Phys. Chem. 95:6661-6666.

48. Lert suttthiwong, P., Stevens, W.F., and Chandrkrachang, S. (2000). Improve paper quality using chitosan. Proceedings of 1st Thailand materials Science and technology Conference, Bangkok, Thailand. 361-363.

49. Majeti, N. V., Kumar, M.N.V.R., (2000). A review of chitin and chitosan applications. React. Funct. Polym. 46:1-27.

50. Marit, W., Kjell, A., Varum, M., Smidsrod, O. (1993). Solution properties of chitosans: conformation and chain stiffness of chitosans with different degrees of N-acetylation. Carbohydr. Polym. 22:193-201.

51. Martins, L. R., and Skaf, M.S. (2003). Computer simulations of the solvation dynamics of Coumarin 153 in dimethylsulfoxide. Chem. Phys. Lett. 370:683-689.

52. Matteoli, E. and Mansoori, G.A. (1995). A simple expression for radial distribution functions of pure fluids and mixtures. J. Chem. Phys. 103, 11:4672-4677.

53. Matteoli, E., and Mansoori, G.A. (1995). A simple expression for radial distribution functions of pure fluids and mixtures. J. Chem. Phys. 103, 11:15.

54. Matthew, I.R., Browne, R.M., Frame, J.W., and Millar, B.G. (1995). Subperiosteal behavior of alginate and cellulose wound dressing materials. Biomaterials. 16, 4:275-278.

55. Metropolis, N., Rosenbluth, A.W., Rosenbluth, M.N., Teller, A.H., and Teller, E. (1953). Equation of State Calculation by Computing Machines. J. Chem. Phys. 21, 6:1087-1092.

56. Mitani, T., Nakalima, S. I.E., and Ishii, H. (1995). Effects of ionic strength on the adsorption of heavy metal by swollen chitosan beads. J. Environ. Sci. Health Part. A. 30:669-674.

57. Miyazaki, A., Kawasaki, N., Serizawa, I., and Doi, K., (1996). Pharmaceutical Application of chitosan: Drug release from oral mucosal adhesive films of chitosan and alginate. The proceeding of 2nd Asia pacific symposium, Eds.Stevens, W.F., Rao, M.S., and Chandrakrachang, S. November 21-23, 1996, Asian Institute of technology, Bangkok Thailand. 22-25.

58. Mohr, M., Marx, D., Parrinello, M., and Zipse, H. (2000). Solvation of Radical Cations in Water--Reactive or Unreactive Solvation. Chem. Eur. J. 6, 21:4009-4015.

59. Muangsin, N., Prajaubsook, M., Chaichit, N., Sirilerdmukul, K., and Hannongbua. S. (2002). Crytal Structure of a Unique Sodium Distorted Linkage in Diclofenac Sodium Pentahydrate. Anal. Sci. 18:967-968.

60. Mulliken, R.S. (1955). Electronic Population Analysis on LCAO-MO Molecular Wave Functions I. J. Chem. Phys. 23:1833-1846.

61. Murata, Y., Miyamoto, E., and Kawashima, S. (1996). Additive effect of chondroitin sulfate and chitosan on drug release from calcium-induced alginate gel beads. J. Control. Release. 38:101-108.

62. Muzzarelli, R.A..A., and Rocchetti, R. (1985). Determination of the Degree of Acetylation of Chitosans by First Derivative ultraviolet spectrophotometry. Carbohydr. Polym. 5:461-472.

63. Newton, M.D. (1995). Molecular Theory of Solvation Processes in dipolar and non-dipolar solvents. J. Mol. Liq. 65, 66:7-14.

64. Noble, L., Gray, A.I., Sadiq, L., and Uchegbu. I.F. (1999). A non-covalently cross-linked chitosan based hydrogel. Int. J. Pharm. 192:173-182.

65. Okada, H. et.al. (1994). Drug delivery using biodegradable microspheres. J. Control. Release. 121:121-129.

66. Park, T.G. (1999). Temperature modulated protein release from pH/temperature-sensitive hydrogels. Biomaterials. 20:517-521.

67. Pitera, J., and Kollman, P. (1998). Graphical visualization of mean hydration from molecular dynamics simulations. J. Mol. Graph. 15:355-358.

68. Ramesh, D.V., Medlicott, N., Razzak, M.,and Tucker, I.G., (2002). Microencasulation of FITC-BSA into Poly (e-Caprolactone) by a water-in-oil-in-oil solvent evaporation technique. Trends Biomater. Artif. Organs. 15:31-36.

69. Ravindra, R., Krovvidi, D.R., and Khan, A.A. (1998). Solubility parameter of chitin and chitosan. Carbohydr. Polym. 36:121-127.

70. Rorrer G.L., Hsein T-Y., and Way J.D. (1993). Synthesis of porous-magnetic chitosan beads for removal of cadmium Ions from waste water. Ind.Eng.Chem.Res. 32:2170-2178.

71. Senel, S., Ikinci, G., Kas, S., Yousefi-Rad, A., Sargon, M.F., and Hincal, A.A. (2000). Chitosan films and hydrogels of chlorhexidine gluconate for oral mucosal delivery. Int. J. Pharm. 193:197-203.

72. Sharan, R., Rubas, W., Kolling, W.M., and Ghandehari, H. (2001). Molecular Modeling of Arginine-Glycine-Aspartic Acid (RGD) Analogs: Relevance to Transepithelial Transport. J Pharm. Pharm. Sci. 4, 1:32-41.

73. Shepherd, R., Reader, S., and Falshaw, A. (1997). Chitosan functional properties. Glycoconjugate J. 14:535-542.

74. Shigehiro, H. (1996) Chitin biotechnology applications. Biotechnol. Annu. Rev. 2:237-258.

75. Shigehiro, H. (1999). Chitin and chitosan as novel biotechnological materials. Polym. Int. 48:732-734.

76. Shu, X.Z., and Zhu, K.J. (2000). A novel approach to prepare tripolyphosphate/chitosan complex beads for controlled release drug delivery. Int. J. Pharm. 201:51-58.

77. Smidsrod, O., and Brack, S.G. (1990). Alginate as immobilization matrix for cells. Trends Biotechnol. 8, 3: 71-78.

78. Smith, K.L., and Herbig, S.M.(1992). Controlled release in Membrane Handbook edited by W.S.W Ho and Sirkar, K.K. 915-935.

79. Sudipto K.De, Aluru, N.R., Member, IE EE, Johnson, B., Crone, W.C., Beebe, D. IEEE, J.M., and Moore., J. (2002). Equilibrium Swelling and Kinetics of pH-Responsive Hydrogels: Models, Experiments, and Simulations. J. Microelectromech. Syst. 11, 5 (October).

80. Tanabe, Y., and Rode, B.M. (1988). Monte Carlo Simulation of an 18.45 mol % Aqueous Ammonia Solution. J. Chem. Soc. Faraday. Trans. II . 84:679-692.

81. Tarici, N., Ermis, D. (1997). Sustained release characteristics and pharmacokinetic parameters of ketoprofen suppositories using chitosan. Int. J. Pharm. 147:71-77.

82. Tasaki, K. (1996). Poly(oxyethylene)—Water Interactions: A Molecular Dynamics Study. J. Am. Chem. Soc. 118:8459-8469.

83. Timmy, S.A., Victor, S.P. Sharma, C.P., and Kumari, J.V. (2002). Betacyclodextrin complexed insulin loaded alginate microspheres- oral delivery system. Trends Biomater. Artif. Organs. 15, 2:48-53.

84. Udomsub, S., and Hannongbua, S. (1997). Solvation of a Macrocyclic Compound in a Water-Ammonia Mixture: Monte Carlo Simulations. J. Chem. Soc.-Faraday Trans. 93:3045-3052.

85. Yao, K.D., Peng, T., Yin, Y.J. Xu, M.X., Mattheus, F. and Goosen, A. (1995). Microcapsules/Microspheres Related to chitosan. Macromol. Chem. Phys. C35, 1:155-180.

Appendix A
(Experimental part)

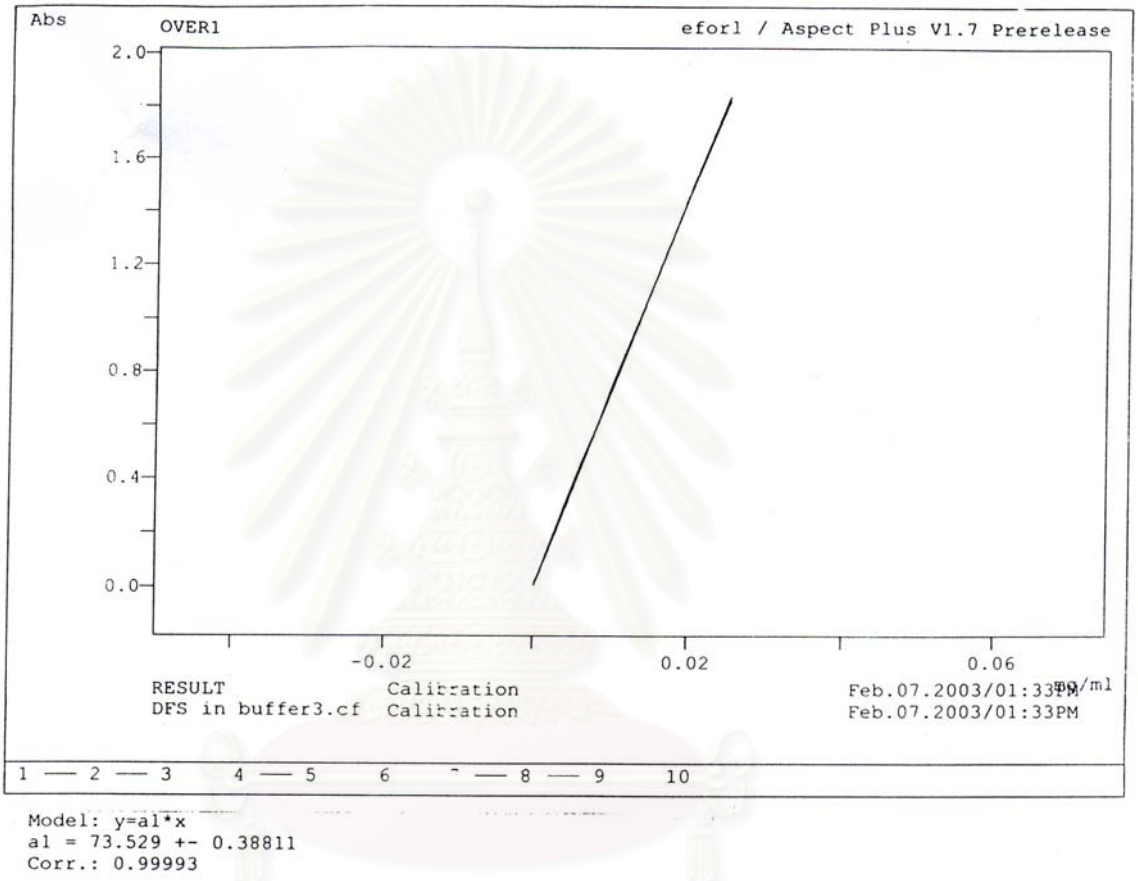

Calibration curve of N-Glucosamine for DIF-release determination (in phosphate buffer pH6.8)

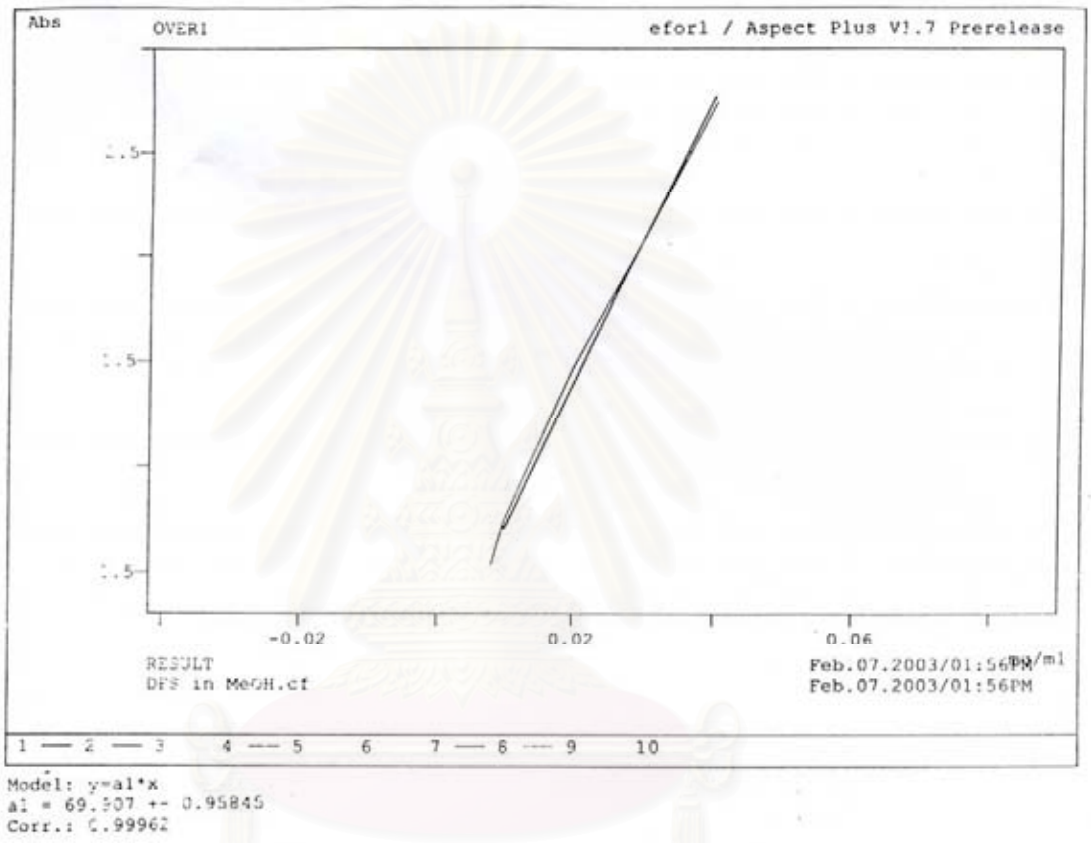

Calibration curve of N-Glucosamine for DIF-loaded efficiency determination (in 50% Methanol)

Analysis Result

Sample Details

Sample ID: MICROGRANULE CTS
Sample File: KRISANA
Sample Path: A:\
Sample Notes: Wet Analysis System
Dispersing medium : water
Tested by Pranee Tethgaluk

Run Number: 6
Record Number: 6

Measured: 20 Feb 2004 10:09PM
Analysed: 20 Feb 2004 10:09PM
Result Source: Analysed

System Details

Range Lens: 300RF mm
Presentation: 3OHD
Analysis Model: Polydisperse
Modifications: Active --

Beam Length: 2.40 mm
[Particle R.I. = (1.5295, 0.1000); Dispersant R.I. = 1.3330]
Killed Data Channels: Low 0; High 2

Sampler: MS17

Obscuration: 8.3 %
Residual: 0.490 %

Result Statistics

Distribution Type: Volume
Mean Diameters:
D [4, 3] = 36.27 um

Concentration = 0.0144 %Vol
D (v, 0.1) = 7.08 um
D [3, 2] = 12.07 um

Density = 1.000 g / cub. cm
D (v, 0.5) = 31.44 um
Span = 1.915E+00

Specific S.A. = 0.4971 sq. m / g
D (v, 0.9) = 67.29 um
Uniformity = 5.954E-01

Size_Low (um)	In %	Size_High (um)	Under%	Size_Low (um)	In %	Size_High (um)	Under%
0.05	0.00	0.06	0.00	6.63	1.28	7.72	10.76
0.06	0.00	0.07	0.00	7.72	1.57	9.00	12.33
0.07	0.00	0.08	0.00	9.00	1.96	10.48	14.30
0.08	0.00	0.09	0.00	10.48	2.47	12.21	16.76
0.09	0.00	0.11	0.00	12.21	3.10	14.22	19.86
0.11	0.00	0.13	0.00	14.22	3.86	16.57	23.72
0.13	0.00	0.15	0.00	16.57	4.74	19.31	28.47
0.15	0.00	0.17	0.00	19.31	5.70	22.49	34.17
0.17	0.00	0.20	0.00	22.49	6.68	26.20	40.85
0.20	0.00	0.23	0.00	26.20	7.60	30.53	48.44
0.23	0.00	0.27	0.00	30.53	8.41	35.56	56.85
0.27	0.00	0.31	0.00	35.56	9.12	41.43	65.97
0.31	0.00	0.36	0.00	41.43	8.83	48.27	74.80
0.36	0.00	0.42	0.00	48.27	7.87	56.23	82.67
0.42	0.11	0.49	0.11	56.23	6.39	65.51	89.05
0.49	0.12	0.58	0.23	65.51	4.67	76.32	93.73
0.58	0.15	0.67	0.38	76.32	3.05	88.91	96.78
0.67	0.19	0.78	0.57	88.91	1.76	103.58	98.54
0.78	0.26	0.91	0.83	103.58	0.88	120.67	99.42
0.91	0.34	1.06	1.17	120.67	0.39	140.58	99.81
1.06	0.43	1.24	1.60	140.58	0.19	163.77	100.00
1.24	0.52	1.44	2.12	163.77	0.00	190.80	100.00
1.44	0.59	1.68	2.72	190.80	0.00	222.38	100.00
1.68	0.64	1.95	3.36	222.38	0.00	258.95	100.00
1.95	0.66	2.28	4.02	258.95	0.00	301.68	100.00
2.28	0.66	2.65	4.69	301.68	0.00	351.46	100.00
2.65	0.66	3.09	5.35	351.46	0.00	409.45	100.00
3.09	0.68	3.60	6.02	409.45	0.00	477.01	100.00
3.60	0.71	4.19	6.74	477.01	0.00	555.71	100.00
4.19	0.79	4.88	7.52	555.71	0.00	647.41	100.00
4.88	0.90	5.69	8.42	647.41	0.00	754.23	100.00
5.69	1.06	6.63	9.48	754.23	0.00	878.67	100.00

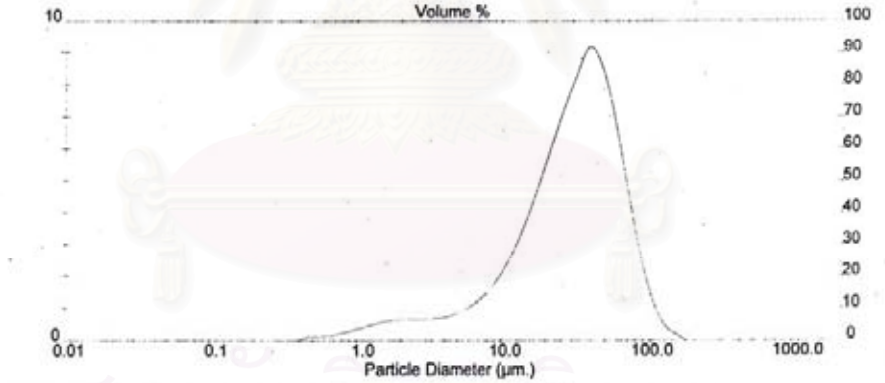

Malvern Instruments Ltd.
Malvern, UK
Tel:0684 892456 Fax:0684 892789

Mastersizer S long bed Ver. 2.11
Serial Number: 32734-89

p. 14
20 Feb 04 10:09

The mean particle size of chitosan microparticles

Amount of diclofenac sodium releasing from the matrix chitosan

chitosan CODE	buffer pH6.8					
	time(min)	%release1	%release2	%release3	Mean(%)	S.D.
LDD	0	0.00	0.00	0.00	0.00	0.00
	30	20.00	21.00	20.00	20.33	0.58
	60	35.00	36.00	35.50	35.50	0.50
	120	45.10	45.20	45.40	45.23	0.15
	180	58.20	57.90	58.30	58.13	0.21
	240	65.00	65.20	66.05	65.42	0.56
	300	68.00	68.71	68.05	68.25	0.40
	360	71.00	70.95	71.02	70.99	0.04
	420	72.00	71.80	72.01	71.94	0.12
	480	73.00	73.10	73.20	73.10	0.10

chitosan CODE	buffer pH6.8					
	time(min)	%release1	%release2	%release3	Mean(%)	S.D.
HDD	0	0.00	0.00	0.00	0.00	0.00
	30	26.00	25.50	26.05	25.85	0.30
	60	37.00	38.05	37.50	37.52	0.53
	120	48.20	48.50	48.50	48.40	0.17
	180	61.20	61.50	61.20	61.30	0.17
	240	68.25	68.25	67.90	68.13	0.20
	300	71.00	70.50	71.05	70.85	0.30
	360	72.00	72.50	72.50	72.33	0.29
	420	73.10	73.20	73.20	73.17	0.06
	480	74.20	74.30	74.20	74.23	0.06

chitosan CODE	buffer pH6.8					
	time(min)	%release1	%release2	%release3	Mean(%)	S.D.
LMW	0	0.00	0.00	0.00	0.00	0.00
	30	15.20	16.05	15.50	15.58	0.43
	60	25.10	24.60	25.20	24.97	0.32
	120	45.10	44.60	45.10	44.93	0.29
	180	55.00	55.20	55.20	55.13	0.12
	240	59.10	59.90	59.20	59.40	0.44
	300	65.20	64.90	65.80	65.30	0.46
	360	68.20	67.30	68.20	67.90	0.52
	420	72.10	72.30	72.00	72.13	0.15
	480	72.50	72.30	72.50	72.43	0.12

chitosan CODE	buffer pH6.8					
	time(min)	%release1	%release2	%release3	Mean(%)	S.D.
MMW	0	0.00	0.00	0.00	0.00	0.00
	30	27.10	26.70	27.50	27.10	0.40
	60	35.20	36.30	35.20	35.57	0.64
	120	48.00	47.60	48.20	47.93	0.31
	180	61.20	60.90	60.90	61.00	0.17
	240	65.00	65.20	65.70	65.30	0.36
	300	69.10	69.20	68.80	69.03	0.21
	360	71.10	70.30	72.10	71.17	0.90
	420	74.70	75.10	75.30	75.03	0.31
	480	75.80	75.50	75.50	75.60	0.17

chitosan CODE	buffer pH6.8					
	time(min)	%release1	%release2	%release3	Mean(%)	S.D.
HMW	0	0.00	0.00	0.00	0.00	0.00
	30	26.10	25.40	26.30	25.93	0.47
	60	34.20	33.90	34.80	34.30	0.46
	120	47.10	46.50	47.10	46.90	0.35
	180	62.10	61.30	62.50	61.97	0.61
	240	66.00	65.80	66.30	66.03	0.25
	300	70.20	70.10	71.30	70.53	0.67
	360	73.80	74.20	73.50	73.83	0.35
	420	74.00	73.60	73.50	73.70	0.26
	480	74.20	74.50	73.50	74.07	0.51

chitosan CODE	buffer pH6.8					
	time(min)	%release1	%release2	%release3	Mean(%)	S.D.
microparticles	0	0	0	0	0	0
	30	35.25	34.85	35.3	35.13	0.25
	60	58.87	59.05	58.75	58.89	0.15
	120	74.45	75.68	75.2	75.11	0.62
	180	82.22	81.75	82.15	82.04	0.25
	240	83.3	83.67	84.05	83.67	0.38
	300	84.34	84.45	84.1	84.30	0.18
	360	84.5	85.01	84.89	84.80	0.27
	420	85.01	85.05	84.95	85.00	0.05
	480	85.5	85.98	85.56	85.68	0.26

chitosan CODE	buffer pH6.8					
	time(min)	%release1	%release2	%release3	Mean (%)	S.D.
Multilayer-coated (with 0.25%chitosan at 2nd layer)	0	0.00	0.00	0.00	0.00	0.00
	30	2.50	3.40	4.10	3.33	0.80
	60	4.90	5.20	4.62	4.90	0.30
	120	6.40	5.90	6.80	6.37	0.45
	180	9.70	10.00	10.50	10.07	0.40
	240	12.50	13.70	12.90	13.03	0.61
	300	15.90	18.80	20.10	18.30	2.16
	360	25.40	23.70	19.40	22.83	3.09
	420	34.90	33.80	32.70	33.80	1.10
	480	37.60	39.80	40.90	39.43	1.68

chitosan CODE	buffer pH6.8					
	time(min)	%release1	%release2	%release3	Mean (%)	S.D.
Multilayer-coated (with 0.5%chitosan at 2nd layer)	0	0.00	0.00	0.00	0.00	0.00
	30	0.00	0.00	0.00	0.00	0.00
	60	3.20	3.12	3.30	3.20	0.09
	120	3.50	3.46	3.45	3.50	0.03
	180	4.90	4.80	5.20	5.00	0.21
	240	5.23	5.10	5.40	5.20	0.15
	300	5.20	5.60	5.05	5.20	0.28
	360	5.50	5.40	5.60	5.50	0.10
	420	5.50	5.50	5.50	5.50	0.00
	480	5.50	5.50	5.60	5.50	0.06

Statistic analysis

For molecular weight

G	47.6	660.04444	10
H	52.6	620.93333	10
I	53.4	678.71111	10

F = 0.15125
p = 0.86036

At the 0.05 level,
the means are NOT significantly different.

For %DD

Data	Mean	Variance	N
B	50.7	634.67778	10
D	53.1	630.76667	10

t = 0.21335
p = 0.83345

At the 0.05 level,
the two means are NOT significantly different.

For chitosan concentration at 2nd multiplayer layer

Data	Mean	Variance	N
P	15.20667	176.45699	10
R	3.86	4.81378	10

t = 3.04927
p = 0.01381

At the 0.05 level,
the two means are significantly different.

Appendix B
(Computer modeling part)

Force Field preparation – extension to AMBER90 parameters

The following table presents new values that were found for atom types important for **glucosamine molecule**.

Bond Stretching parameters:
Atom Types
remark goes here
MASS

OH	16.000	0.465 same as oh
HO	1.008	0.135 same as ho
CT	12.010	0.878 same as c3
H2	1.008	0.135 same as hc
OS	16.000	0.465 same as os
H1	1.008	0.135 same as hc
NT	14.010	0.530 same as n3
H	1.008	0.161 same as hn

BOND

OH-HO	553.20	0.960	same as ho-oh
OH-CT	315.00	1.430	same as c3-oh
CT-H2	341.90	1.089	same as c3-hc
CT-OS	300.50	1.440	same as c3-os
CT-CT	307.60	1.530	same as c3-c3
CT-H1	341.90	1.089	same as c3-hc
CT-NT	320.60	1.470	same as c3-n3
NT-H	434.10	1.010	same as hn-n3

ANGLE

OH-CT-H2	50.000	109.500	same as hc-c3-oh
OH-CT-OS	71.707	110.855	Calculated with empirical approach
OH-CT-CT	67.700	109.540	same as c3-c3-oh
HO-OH-CT	46.700	109.400	same as c3-oh-ho
CT-OS-CT	61.700	114.830	same as c3-os-c3
CT-CT-CT	40.000	109.500	same as c3-c3-c3
CT-CT-H1	46.500	109.990	same as c3-c3-hc
CT-CT-NT	66.100	110.950	same as c3-c3-n3
H2-CT-OS	50.000	109.500	same as hc-c3-os
H2-CT-CT	46.500	109.990	same as c3-c3-hc
OS-CT-CT	67.800	108.800	same as c3-c3-os
OS-CT-H1	50.000	109.500	same as hc-c3-os
OH-CT-H1	50.000	109.500	same as hc-c3-oh
H1-CT-H1	35.000	109.500	same as hc-c3-hc
CT-NT-H	47.500	108.220	same as c3-n3-hn
H1-CT-NT	50.000	109.500	same as hc-c3-n3
H -NT-H	40.400	113.640	same as hn-n3-hn

DIHE

OH-CT-OS-CT	1	0.383	0.000	3.000 same as X -c3-os-X
OH-CT-CT-CT	1	0.156	0.000	3.000 same as X -c3-c3-X
OH-CT-CT-H1	1	0.156	0.000	3.000 same as X -c3-c3-X
OH-CT-CT-NT	1	0.156	0.000	3.000 same as X -c3-c3-X
HO-OH-CT-H2	1	0.167	0.000	3.000 same as X -c3-oh-X
HO-OH-CT-OS	1	0.167	0.000	3.000 same as X -c3-oh-X
HO-OH-CT-CT	1	0.167	0.000	3.000 same as X -c3-oh-X
CT-OS-CT-CT	1	0.383	0.000	3.000 same as X -c3-os-X
CT-OS-CT-H1	1	0.383	0.000	3.000 same as X -c3-os-X
CT-CT-CT-CT	1	0.156	0.000	3.000 same as X -c3-c3-X
CT-CT-CT-H1	1	0.156	0.000	3.000 same as X -c3-c3-X
CT-CT-NT-H	1	0.300	0.000	3.000 same as X -c3-n3-X
H2-CT-OS-CT	1	0.383	0.000	3.000 same as X -c3-os-X
H2-CT-CT-CT	1	0.156	0.000	3.000 same as X -c3-c3-X
H2-CT-CT-H1	1	0.156	0.000	3.000 same as X -c3-c3-X
H2-CT-CT-NT	1	0.156	0.000	3.000 same as X -c3-c3-X
OS-CT-CT-CT	1	0.156	0.000	3.000 same as X -c3-c3-X
OS-CT-CT-H1	1	0.156	0.000	3.000 same as X -c3-c3-X
OS-CT-CT-NT	1	0.156	0.000	3.000 same as X -c3-c3-X
OS-CT-CT-OH	1	0.156	0.000	3.000 same as X -c3-c3-X
HO-OH-CT-H1	1	0.167	0.000	3.000 same as X -c3-oh-X
H1-CT-CT-H1	1	0.156	0.000	3.000 same as X -c3-c3-X
CT-CT-CT-NT	1	0.156	0.000	3.000 same as X -c3-c3-X
OH-CT-CT-OH	1	0.156	0.000	3.000 same as X -c3-c3-X
H1-CT-CT-NT	1	0.156	0.000	3.000 same as X -c3-c3-X
H1-CT-NT-H	1	0.300	0.000	3.000 same as X -c3-n3-X

IMPROPER

NONBON

OH	1.7210	0.2104	same as oh
HO	0.0000	0.0000	same as ho
CT	1.9080	0.1094	same as c3
H2	1.4870	0.0157	same as hc
OS	1.6837	0.1700	same as os
H1	1.4870	0.0157	same as hc
NT	1.8240	0.1700	same as n3
H	0.6000	0.0157	same as hn

Force Field preparation – extension to AMBER90 parameters

The following table presents new values that were found for atom types important for **tetramer molecule.**

Bond Stretching parameters:
Atom Types
remark goes here
MASS

OH 16.000	0.465	same as oh
HO 1.008	0.135	same as ho
CT 12.010	0.878	same as c3
H1 1.008	0.135	same as hc
OS 16.000	0.465	same as os
NT 14.010	0.530	same as n3
H 1.008	0.161	same as hn
H2 1.008	0.135	same as hc

BOND

OH-HO	553.20	0.960	same as ho-oh
OH-CT	315.00	1.430	same as c3-oh
CT-H1	341.90	1.089	same as c3-hc
CT-CT	307.60	1.530	same as c3-c3
CT-OS	300.50	1.440	same as c3-os
CT-NT	320.60	1.470	same as c3-n3
NT-H	434.10	1.010	same as hn-n3
CT-H2	341.90	1.089	same as c3-hc

OH-CT-H1	50.000	109.500	same as hc-c3-oh
OH-CT-CT	67.700	109.540	same as c3-c3-oh
HO-OH-CT	46.700	109.400	same as c3-oh-ho
CT-CT-OS	67.800	108.800	same as c3-c3-os
CT-CT-H1	46.500	109.990	same as c3-c3-hc
CT-CT-CT	40.000	109.500	same as c3-c3-c3
H1-CT-H1	35.000	109.500	same as hc-c3-hc
CT-OS-CT	61.700	114.830	same as c3-os-c3
OS-CT-H1	50.000	109.500	same as hc-c3-os
OS-CT-H2	50.000	109.500	same as hc-c3-os
OS-CT-OS	71.500	110.620	same as os-c3-os
CT-CT-NT	66.100	110.950	same as c3-c3-n3
CT-NT-H	47.500	108.220	same as c3-n3-hn
CT-CT-H2	46.500	109.990	same as c3-c3-hc
NT-CT-H1	50.000	109.500	same as hc-c3-n3
H -NT-H	40.400	113.640	same as hn-n3-hn

DIHE

OH-CT-CT-OS	1	0.156	0.000	3.000	same as X -c3-c3-X
OH-CT-CT-H1	1	0.156	0.000	3.000	same as X -c3-c3-X
OH-CT-CT-CT	1	0.156	0.000	3.000	same as X -c3-c3-X
HO-OH-CT-H1	1	0.167	0.000	3.000	same as X -c3-oh-X
HO-OH-CT-CT	1	0.167	0.000	3.000	same as X -c3-oh-X
CT-CT-OS-CT	1	0.383	0.000	3.000	same as X -c3-os-X
CT-CT-CT-H1	1	0.156	0.000	3.000	same as X -c3-c3-X
CT-CT-CT-CT	1	0.156	0.000	3.000	same as X -c3-c3-X
H1-CT-CT-OS	1	0.156	0.000	3.000	same as X -c3-c3-X

H1-CT-CT-H1	1	0.156	0.000	3.000 same as X -c3-c3-X
CT-OS-CT-H2	1	0.383	0.000	3.000 same as X -c3-os-X
CT-OS-CT-OS	1	0.383	0.000	3.000 same as X -c3-os-X
OS-CT-CT-CT	1	0.156	0.000	3.000 same as X -c3-c3-X
OS-CT-CT-NT	1	0.156	0.000	3.000 same as X -c3-c3-X
H1-CT-OS-CT	1	0.383	0.000	3.000 same as X -c3-os-X
CT-CT-CT-NT	1	0.156	0.000	3.000 same as X -c3-c3-X
OH-CT-CT-OH	1	0.156	0.000	3.000 same as X -c3-c3-X
CT-CT-NT-H	1	0.300	0.000	3.000 same as X -c3-n3-X
CT-CT-CT-H2	1	0.156	0.000	3.000 same as X -c3-c3-X
OH-CT-CT-NT	1	0.156	0.000	3.000 same as X -c3-c3-X
H1-CT-CT-NT	1	0.156	0.000	3.000 same as X -c3-c3-X
NT-CT-CT-H2	1	0.156	0.000	3.000 same as X -c3-c3-X
H -NT-CT-H1	1	0.300	0.000	3.000 same as X -c3-n3-X
H1-CT-CT-H2	1	0.156	0.000	3.000 same as X -c3-c3-X
OS-CT-CT-OS	1	0.156	0.000	3.000 same as X -c3-c3-X

IMPROPER

NONBON

OH	1.7210	0.2104	same as oh
HO	0.0000	0.0000	same as ho
CT	1.9080	0.1094	same as c3
H1	1.4870	0.0157	same as hc
OS	1.6837	0.1700	same as os
NT	1.8240	0.1700	same as n3
H	0.6000	0.0157	same as hn
H2	1.4870	0.0157	same as hc

File Format PDB of monomer molecule

```
ATOM      1  C1  UNK     1      -2.275  -0.521   0.265  1.00  0.00
ATOM      2  C2  UNK     1      -1.585   0.854   0.602  1.00  0.00
ATOM      3  O3  UNK     1      -0.271   0.736   1.224  1.00  0.00
ATOM      4  C4  UNK     1       0.759  -0.050   0.559  1.00  0.00
ATOM      5  C5  UNK     1      -1.383  -1.537  -0.537  1.00  0.00
ATOM      6  O6  UNK     1       1.530   0.789  -0.325  1.00  0.00
ATOM      7  O7  UNK     1      -3.518  -0.322  -0.433  1.00  0.00
ATOM      8  O8  UNK     1      -1.656  -1.394  -1.952  1.00  0.00
ATOM      9  C9  UNK     1      -1.705   1.935  -0.556  1.00  0.00
ATOM     10  O10 UNK     1      -0.805   2.920  -1.145  1.00  0.00
ATOM     11  C11 UNK     1       0.178  -1.300  -0.229  1.00  0.00
ATOM     12  N12 UNK     1      -0.156  -2.051   1.042  1.00  0.00
ATOM     13  H13 UNK     1      -2.521  -0.997   1.221  1.00  0.00
ATOM     14  H14 UNK     1      -2.214   1.244   1.420  1.00  0.00
ATOM     15  H15 UNK     1       1.467  -0.394   1.322  1.00  0.00
ATOM     16  H16 UNK     1      -1.706  -2.558  -0.293  1.00  0.00
ATOM     17  H17 UNK     1       1.928   1.485   0.240  1.00  0.00
ATOM     18  H18 UNK     1      -4.097   0.190   0.171  1.00  0.00
ATOM     19  H19 UNK     1      -1.151  -2.105  -2.401  1.00  0.00
ATOM     20  H20 UNK     1      -1.584   2.635   0.294  1.00  0.00
ATOM     21  H21 UNK     1      -1.016   1.267  -1.088  1.00  0.00
ATOM     22  H22 UNK     1       0.059   2.895  -0.674  1.00  0.00
ATOM     23  H23 UNK     1      -0.138  -0.465  -0.860  1.00  0.00
ATOM     24  H24 UNK     1      -0.340  -1.484   1.871  1.00  0.00
ATOM     25  H25 UNK     1       0.641  -2.656   1.259  1.00  0.00
TER
END
```

File Format PDB of tetramer molecule

```
ATOM      1  C1  UNK     1      -8.711  -1.244   0.955  1.00  0.00
ATOM      2  C2  UNK     1      -8.250   0.244   1.026  1.00  0.00
ATOM      3  O3  UNK     1      -6.826   0.469   0.935  1.00  0.00
ATOM      4  C4  UNK     1      -5.977  -0.691   1.045  1.00  0.00
ATOM      5  C5  UNK     1      -7.872  -2.190   1.866  1.00  0.00
ATOM      6  C6  UNK     1      -6.457  -1.621   2.194  1.00  0.00
ATOM      7  O7  UNK     1      -4.623  -0.265   1.311  1.00  0.00
ATOM      8  C8  UNK     1      -4.068   0.546   0.252  1.00  0.00
ATOM      9  C9  UNK     1      -2.770   1.239   0.753  1.00  0.00
ATOM     10  C10 UNK     1      -1.653   0.173   0.929  1.00  0.00
ATOM     11  C11 UNK     1      -1.417  -0.609  -0.396  1.00  0.00
ATOM     12  O12 UNK     1      -3.833  -0.175  -0.977  1.00  0.00
ATOM     13  C13 UNK     1      -2.766  -1.151  -0.963  1.00  0.00
ATOM     14  O14 UNK     1      -0.804   0.225  -1.408  1.00  0.00
ATOM     15  C15 UNK     1       0.624   0.033  -1.552  1.00  0.00
ATOM     16  C16 UNK     1       1.242   1.364  -2.092  1.00  0.00
ATOM     17  O17 UNK     1       2.430   1.167  -2.896  1.00  0.00
ATOM     18  C18 UNK     1       3.269   0.073  -2.473  1.00  0.00
ATOM     19  C19 UNK     1       0.977  -1.096  -2.567  1.00  0.00
ATOM     20  C20 UNK     1       2.524  -1.286  -2.631  1.00  0.00
ATOM     21  O21 UNK     1       3.709   0.284  -1.115  1.00  0.00
ATOM     22  O22 UNK     1      -8.745  -1.713  -0.408  1.00  0.00
ATOM     23  C23 UNK     1       5.138   0.375  -0.944  1.00  0.00
ATOM     24  C24 UNK     1       5.672   1.807  -1.256  1.00  0.00
ATOM     25  C25 UNK     1       7.181   1.927  -0.873  1.00  0.00
ATOM     26  C26 UNK     1       7.518   1.145   0.435  1.00  0.00
ATOM     27  O27 UNK     1       5.357  -0.042   0.425  1.00  0.00
ATOM     28  C28 UNK     1       6.214   0.810   1.212  1.00  0.00
ATOM     29  O29 UNK     1       8.403   1.919   1.262  1.00  0.00
ATOM     30  C30 UNK     1      -8.775   0.936   2.315  1.00  0.00
ATOM     31  O31 UNK     1      -8.440   2.331   2.284  1.00  0.00
ATOM     32  N1  UNK     1      -5.501  -2.733   2.416  1.00  0.00
ATOM     33  O32 UNK     1      -8.610  -2.414   3.082  1.00  0.00
ATOM     34  C33 UNK     1      -3.173  -2.494  -0.299  1.00  0.00
ATOM     35  O34 UNK     1      -4.379  -2.991  -0.895  1.00  0.00
ATOM     36  N2  UNK     1      -2.364   2.309  -0.190  1.00  0.00
ATOM     37  O35 UNK     1      -0.451   0.801   1.404  1.00  0.00
ATOM     38  C36 UNK     1       1.497   2.394  -0.956  1.00  0.00
ATOM     39  O37 UNK     1       1.947   3.653  -1.479  1.00  0.00
ATOM     40  N3  UNK     1       3.046  -2.275  -1.654  1.00  0.00
ATOM     41  O38 UNK     1       0.356  -2.355  -2.265  1.00  0.00
ATOM     42  C39 UNK     1       6.480   0.097   2.567  1.00  0.00
ATOM     43  O40 UNK     1       7.048  -1.211   2.402  1.00  0.00
ATOM     44  N4  UNK     1       5.423   2.213  -2.660  1.00  0.00
ATOM     45  O41 UNK     1       8.059   1.506  -1.934  1.00  0.00
ATOM     46  H1  UNK     1      -9.753  -1.291   1.290  1.00  0.00
ATOM     47  H2  UNK     1      -8.709   0.767   0.181  1.00  0.00
ATOM     48  H3  UNK     1      -5.988  -1.247   0.107  1.00  0.00
ATOM     49  H4  UNK     1      -7.767  -3.148   1.348  1.00  0.00
ATOM     50  H5  UNK     1      -6.514  -1.027   3.111  1.00  0.00
ATOM     51  H6  UNK     1      -4.782   1.343   0.023  1.00  0.00
ATOM     52  H7  UNK     1      -2.975   1.695   1.727  1.00  0.00
ATOM     53  H8  UNK     1      -1.980  -0.535   1.697  1.00  0.00
ATOM     54  H9  UNK     1      -0.773  -1.464  -0.176  1.00  0.00
```

```
ATOM     55  H10 UNK     1      -2.592  -1.392  -2.018  1.00  0.00
ATOM     56  H11 UNK     1       1.077  -0.199  -0.587  1.00  0.00
ATOM     57  H12 UNK     1       0.506   1.816  -2.767  1.00  0.00
ATOM     58  H13 UNK     1       4.124   0.042  -3.153  1.00  0.00
ATOM     59  H14 UNK     1       0.637  -0.783  -3.560  1.00  0.00
ATOM     60  H15 UNK     1       2.757  -1.672  -3.630  1.00  0.00
ATOM     61  H16 UNK     1      -7.838  -1.667  -0.770  1.00  0.00
ATOM     62  H17 UNK     1       5.643  -0.355  -1.582  1.00  0.00
ATOM     63  H18 UNK     1       5.109   2.506  -0.629  1.00  0.00
ATOM     64  H19 UNK     1       7.381   2.990  -0.701  1.00  0.00
ATOM     65  H20 UNK     1       8.012   0.205   0.175  1.00  0.00
ATOM     66  H21 UNK     1       5.686   1.741   1.438  1.00  0.00
ATOM     67  H22 UNK     1       9.243   2.005   0.762  1.00  0.00
ATOM     68  H23 UNK     1      -9.860   0.832   2.373  1.00  0.00
ATOM     69  H24 UNK     1      -8.327   0.479   3.199  1.00  0.00
ATOM     70  H25 UNK     1      -8.805   2.711   3.112  1.00  0.00
ATOM     71  H26 UNK     1      -5.864  -3.327   3.165  1.00  0.00
ATOM     72  H27 UNK     1      -4.630  -2.334   2.776  1.00  0.00
ATOM     73  H28 UNK     1      -8.150  -3.132   3.564  1.00  0.00
ATOM     74  H29 UNK     1      -3.315  -2.363   0.773  1.00  0.00
ATOM     75  H30 UNK     1      -2.378  -3.227  -0.457  1.00  0.00
ATOM     76  H31 UNK     1      -4.573  -3.839  -0.441  1.00  0.00
ATOM     77  H32 UNK     1      -3.142   2.967  -0.282  1.00  0.00
ATOM     78  H33 UNK     1      -1.603   2.836   0.243  1.00  0.00
ATOM     79  H34 UNK     1       0.162   0.075   1.646  1.00  0.00
ATOM     80  H35 UNK     1       0.564   2.573  -0.422  1.00  0.00
ATOM     81  H36 UNK     1       2.230   2.014  -0.243  1.00  0.00
ATOM     82  H37 UNK     1       2.838   3.497  -1.857  1.00  0.00
ATOM     83  H38 UNK     1       2.675  -2.058  -0.726  1.00  0.00
ATOM     84  H39 UNK     1       2.695  -3.201  -1.908  1.00  0.00
ATOM     85  H40 UNK     1      -0.573  -2.285  -2.567  1.00  0.00
ATOM     86  H41 UNK     1       5.525  -0.017   3.086  1.00  0.00
ATOM     87  H42 UNK     1       7.134   0.707   3.194  1.00  0.00
ATOM     88  H43 UNK     1       7.973  -1.080   2.107  1.00  0.00
ATOM     89  H44 UNK     1       5.960   1.612  -3.288  1.00  0.00
ATOM     90  H45 UNK     1       5.768   3.167  -2.786  1.00  0.00
ATOM     91  H46 UNK     1       7.885   0.555  -2.096  1.00  0.00
END
```

VITAE

Ms Krisana Siraeartmukul was born in Nakornprathom, Thailand, on January, 18, 1968. She received in Bachelor of Education degree majoring in Chemistry in 1989 and Master of Science degree majoring in Biochemistry in 1992 from Srinakarinwirot University. She started as a Ph.D. student with a major in Materials Science, Chulalongkorn University in June 1999 and completed the program in April 2004.